CREATION RESEARCH SOCIETY

QUARTERLY

Volume 59 Summer 2022 Number 1

- WILLISTON BASIN — PART III: COAL AND OIL
- DESIGN REVEALED BY THE SPECTRAL "IR LEDGE"
- MAMMALIAN MEGAFAUNA BONE BEDS OF NORTH AMERICA
- THE "DOLOMITE PROBLEM" SOLVED BY THE FLOOD
- PANORAMA OF SCIENCE — ROCK WRENS
- LATENT HEAT COULD SOLVE ACCELERATED NUCLEAR DECAY'S HEAT PROBLEM, PART 1

Creation Research Society Quarterly

Volume 59
Number 1
Summer 2022

Articles

Departments

Haec Credimus

For in six days the Lord made heaven and earth, the sea, and all that in them is, and rested on the seventh.—Exodus 20:11

Creation Research Society Quarterly

Volume 59
Number 1
Summer 2022

Cover by Michael E. Erkel, Afton, Virginia

Design services by Cindy Blandon, cblandon@aol.com

The *Creation Research Society Quarterly* is published by the Creation Research Society, 1 W. Firestorm Way #145, Glendale, AZ 85306, and it is indexed in the *Christian Periodical Index* and the *Zoological Record*.

Send papers on all subjects to the Editor: CRSQeditor@creationresearch.org or to Tim Clarey, 1806 Royal Lane, Dallas, TX 75229.

Send book reviews to the Book Review Editor: Mary Beth De Repentigny, Book Review Editor, marybethd4@gmail.com.

ISSN 0092-9166

Printed in the United States of America

Creation Research Society Quarterly 2022 59:4–13

Mammalian Megafauna Bone Beds of North America: Agate Fossil Beds National Monument and Cita Canyon, Texas

Don McClenagan*

Abstract

Important mammalian megafauna bone beds are located in Nebraska's Agate Fossil Beds National Monument (Agate Fossil Beds) and Cita Canyon, Texas. Similarities between these two sites are the predominance of broken and disarticulated skeletons, evidence of rapid burial, and similar sedimentary environments. The two bone beds discussed herein are interpreted as post-Flood because they appear to have been deposited in rocks that were carved into older receding phase layers. A hill about 1.5 miles (3 km) east of and at about the same stratigraphic level as the Agate Fossil Beds has yielded over 100 mummified carcasses of *Stenomylus* (gazelle-like camelids), apparently buried and suffocated by a sand/dust storm. Based on the site description, water did not create this deposit or alter it, indicating that the *Stenomylus* camelids perished after the Flood.

Key Words: mammal, megafauna, Stenomylus, Cita Canyon, Palo Duro Canyon, Agate Fossil Beds, loess

Introduction

The timing and depositional mechanisms of mammalian megafauna bone beds in North America is not well understood. This paper discusses Agate Fossil Beds National Monument in Nebraska (Agate Fossil Beds) and Cita Canyon in Texas.

Agate Fossil Beds National Monument was originally a ranch in northwest Nebraska owned by James Cook. Native Americans of that area, the Lakota Sioux, called the fossil localities A'bekiyia Wama'kaskan s'e, meaning "Animal Bones Brutally Scattered About" (Graham, 2009). Cook made the first recorded fossil find in 1885. Over the next several decades, the site was investigated by scientists including Edward Cope of Philadelphia, Othniel Marsh of Yale University, and Olaf Peterson from the Carnegie Museum of Pittsburgh (USDI, 1980).

The fossil beds mostly comprise two main sites, University and Carnegie

* Don McClenagan, PhD, Smithers, BC, don@mcclenagan.net
Accepted for publication January 21, 2022

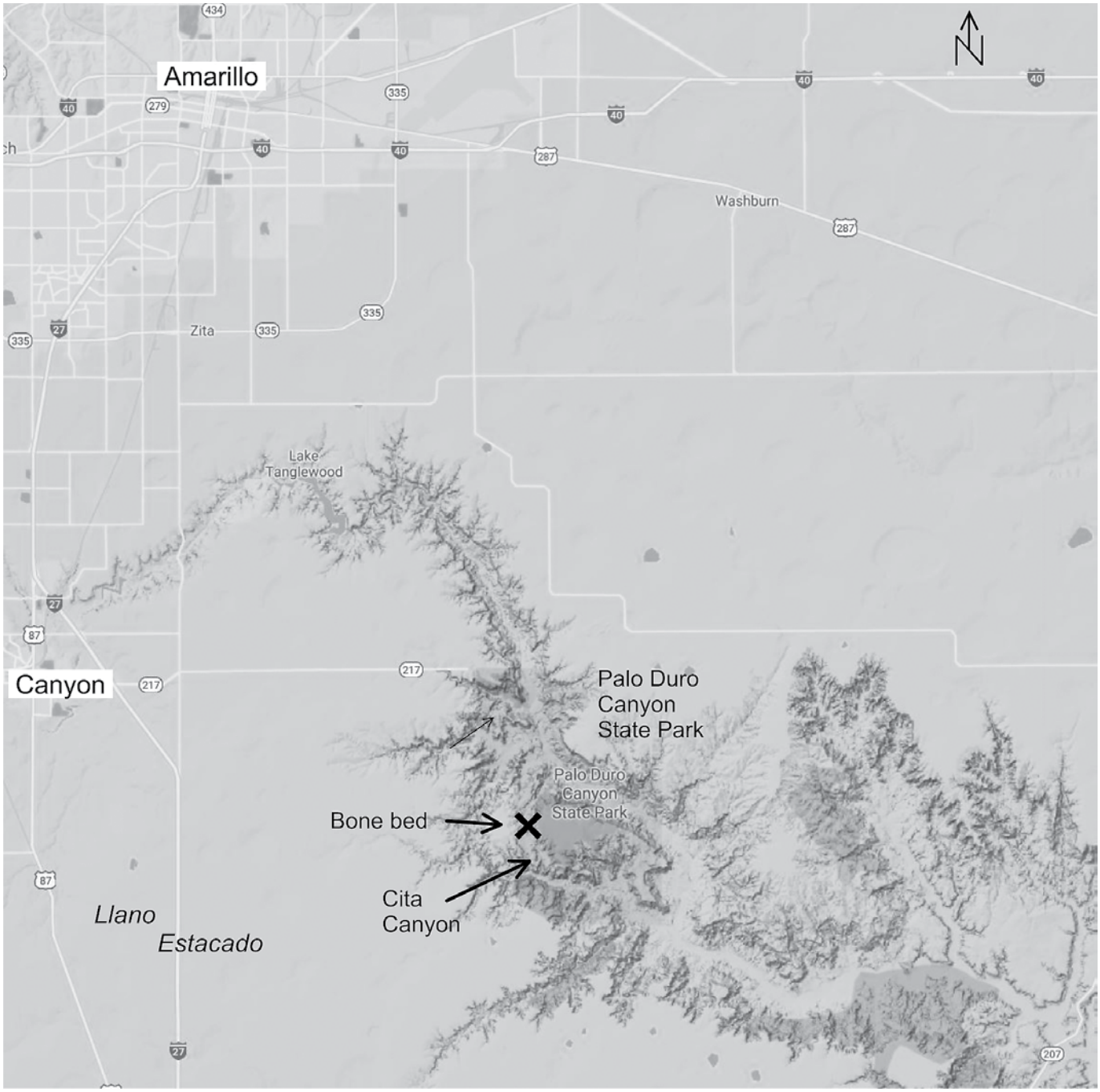

Figure 1. Map showing Palo Duro Canyon State Park in the Texas Panhandle. Palo Duro Canyon is a large erosional entrenchment in the Llano Estacado, an extremely flat area of the southern High Plains. Mammalian fossils are found at a number of locations in the Texas Panhandle where water has cut into the surface of the plains. Base map from Google Maps.

Hills (called the Fossil Hills), and two other important sites, Bear Dog Hill and an unnamed hill about 1.5 miles (2.4 km) east of the Fossil Hills that entombs mummified camelids (*Stenomylus*). The hills overlook the Niobrara River. The beds have produced thousands of fossil bones and teeth (Hunt, 1984).

North Cita Canyon is a tributary of Palo Duro Canyon, the head of which is 12 miles (19 km) east of Canyon, Texas, and 15 miles (24 km) southeast of Ama-

rillo (Figure 1). The canyon is 600–800 feet (180–240 m) deep along Palo Duro Creek. Palo Duro Canyon is a deep erosional cut into the eastern escarpment of the Llano Estacado (Staked Plains), a southern subregion of the High Plains. The head of the canyon is Palo Duro Canyon State Park, Texas. Tributary canyons include Timbercreek, Big and Little Sunday, North and South Cita, and Tule Canyons. The Cita Canyon bone bed is located at the head of North Cita Canyon where a narrow elevated upland plain landbridge separates the North Cita Canyon drainage from Palo Duro Canyon proper (Schultz, 2001).

Fossils of prehistoric animals in the Texas Panhandle were first recorded by E.D. Cope in 1892. Since his phytosaur find, many vertebrate fossils, predominantly mammals, have been found along the eastern High Plains escarpment and along the Canadian River north of the canyon. The Cita Canyon bone bed site was discovered by Floyd V. Studer of Amarillo in the 1930s (Schultz, 2001). Numerous other fossil deposits have been found in the Texas Panhandle (Johnston and Savage, 1955).

Stratigraphy and Sedimentary Context

Both fossil sites discussed here are located in the Great Plains of North America. The Great Plains is a vast area of low relief stretching from Texas northwards into Canada. One of the last continental-scale sedimentary units laid down by the Flood in North America is called the Ogallala Formation. As the Floodwaters ran off North America, the sheet flow that created the planar upper surface of the Ogallala Formation became concentrated into channels. Channelized erosion left erosional remnants. After this erosion, fluvial deposition occurred in channels and basins eroded into the Ogallala Formation. The fossil bone beds of both Agate Fossil Beds and Cita Canyon are part of deposits that infill erosional depressions cut into the Ogallala Formation. As such, both bone beds represent deposition sometime *after* the primary Flood runoff at the end of the Deluge.

The fossils at Agate Fossil Beds occur in the Miocene Harrison Formation and the overlying Upper Harrison (also called the Anderson Ranch Formation or the Marsland Formation) (USDI, 1980; Hunt, 1984; Graham, 2009). The name, Agate Fossil Beds, is due to abundant agates that occur at or near the surface immediately atop the Upper Harrison. The Harrison includes fine-grained, cross-bedded, horizontally-layered, and massive sandstones. The Upper Harrison Formation is about 295 ft. (90 m) thick, and includes calcareous volcanic tuff, fine- to very fine-grained sandstone, some calcareous, capped by dense limestone mud. Local pebble conglomerates occur. The Upper Harrison is interpreted as flood plain and channel deposits. The Fossil Hills bone beds occur in lenses along the bottoms of channels cut into the Upper Harrison (Graham, 2009). Since these channels were eroded into the Upper Harrison, the bone beds were deposited sometime later than the primary deposition of the Upper Harrison. Locally, a silica-cemented land surface is found at or near the top of the Upper Harrison. Sands and silts of the Harrison Formation are pyroclastic (Graham, 2009). Microscopic analyses of the sands in the Harrison beds show approximately equal parts of angular quartz crystals, feldspar, and volcanic glass (Hunt, 1984). In some cases, volcanic glass is fused to quartz crystals.

Palo Duro Canyon exposes Paleozoic, Mesozoic, and Cenozoic strata (Figure 2). Three unconformities are conventionally placed between the Quartermaster and Tecovas, the Tecovas and the Trujillo, and the Trujillo and Ogallala Formations. Beds above and below each unconformity are essentially parallel, so each is more accurately a disconformity (Hood and Underwood, 2001). Many uniformitarian geologists believe millions of years are represented by these unconformities. For example, the time represented by the contact between the Trujillo (upper Triassic dated about 210,000,000 years) and the Ogallala (about 5,000,000 years in the North Cita Canyon exposure) is 205,000,000 years.

The interpretation of these bed contacts as representing enormous expanses of missing time is not supported by the observed bed relationships; there is little or no evidence of erosion in the underlying surface at these contacts. It is difficult or impossible to imagine a plausible reason why the underlying surface at each of these contacts would be perfectly level after millions of years of weathering. Each unconformity more likely represents a short period of time since the exposed surface of each underlying bed is essentially horizontal and shows no significant erosion and surface roughening. Several papers comment on the missing time in the Texas Panhandle in particular (Reed, 2002) and the sedimentary record in general (Reed and Oard, 2017; Reed and Oard, 2018).

The Cita Canyon bone bed is found in the Ogallala Formation. The bone bed sediments infill a basin cut into the upper surface of the Ogallala (Johnston and Savage, 1955; Schultz, 2001). In other words, the Cita Canyon bed was not deposited at the same time as the Ogallala, but after it. The Ogallala is a vast complex of fluvial sands, silts, gravels, and caliche that extends from western Nebraska to the Edwards Plateau in Texas (Schultz, 2001), and serves as the principal aquifer of the High Plains. Ogallala sediments are thought by uniformitarian scientists to have been deposited by streams or rivers originating from the eastern Rocky Mountains as a vast alluvial blanket atop the undulating pre-Ogallala surface (Hood and Underwood, 2001). In contrast, some Flood geologists have suggested that the Ogallala was the result of late Flood

Figure 2. Stylized stratigraphic column showing the major units exposed at Palo Duro Canyon. Not to scale.

sheet flow as the waters were receding off the continents (Clarey, 2018). Channel sands and floodplain clays contain mammalian megafauna fossils at many sites in the Texas Panhandle. In Palo Duro Canyon, the Ogallala is only 20–40 ft. (6–12 m) thick, far thinner than the 400–500 ft. (122–152 m) at the Canadian River. It forms the canyon rim at some locations.

The general stratigraphy at the Cita Canyon fossil site contains both fossiliferous and non-fossil-bearing layers (Figure 3). Fossils are found in friable sandstone, unconsolidated sand, or calcareous sandstone. The total fossil-bearing thickness is about 30 ft. (9 m).

Field Visit to North Cita Canyon

Field exploration in Spring of 2019 located the fossil bone deposits (Figures 4 and 5). The beds were friable and appeared susceptible to erosion by rain events. A harder red shale/siltstone layer underlying the fossil-bearing units is probably the upper surface of the red Trujillo Formation (Triassic). Fossil bone fragments are scattered on this surface (Figures 6 and 7). I infer that these bones originated from the light-colored units in Figure 5, and were either moved by rain events or displaced by fossil collecting.

The North Cita Canyon fossils were deposited in a basin eroded into the Ogallala Formation (Johnston and Savage, 1955; Schultz, 2001). The basin was elongate, about 3–4 miles from east to west and 1.5–2 miles from north to south (Locality Map 1 in Johnston and Savage, 1955; Schultz 2001). It extended from the south edge of Big Sunday Canyon, across the head of Little Sunday Canyon, to the north side of North Cita Canyon (Figure 4). Subsequent headward erosion of North Cita Canyon cut into the basin and exposed the fossil bed. The interpretation of the deposit as fluvial basin fill is supported by the occurrence of ubiquitous rip-up clasts of caliche, probably from the High Plains caprock, and scattered quartzite in the fossil-bearing beds (Johnston and Savage, 1955). Fossil-bearing sediments are apparently alluvial deposits in a basin carved into the pre-existing Ogallala Formation. An interesting side point is that Johnston and Savage (1955) noted the fossil-bearing units have normal magnetic polarity; whereas, overlying units have reversed polarity.

Fossils

Fossils at the Cita Canyon site in Texas occur in friable sandstones or sands, but also in sandy gravel at the base of the fossil-bearing units. Some sandstone is calcareous. The fossil matrix indicates fossil deposition in moving water. The most abundant megafauna fossils at the Cita Canyon site are horse bones, including hundreds of teeth, jaws, and leg bones, representing two types, a large zebra-like horse and a smaller, less-abundant 3-toed horse. Bones from several camel types, ranging from the

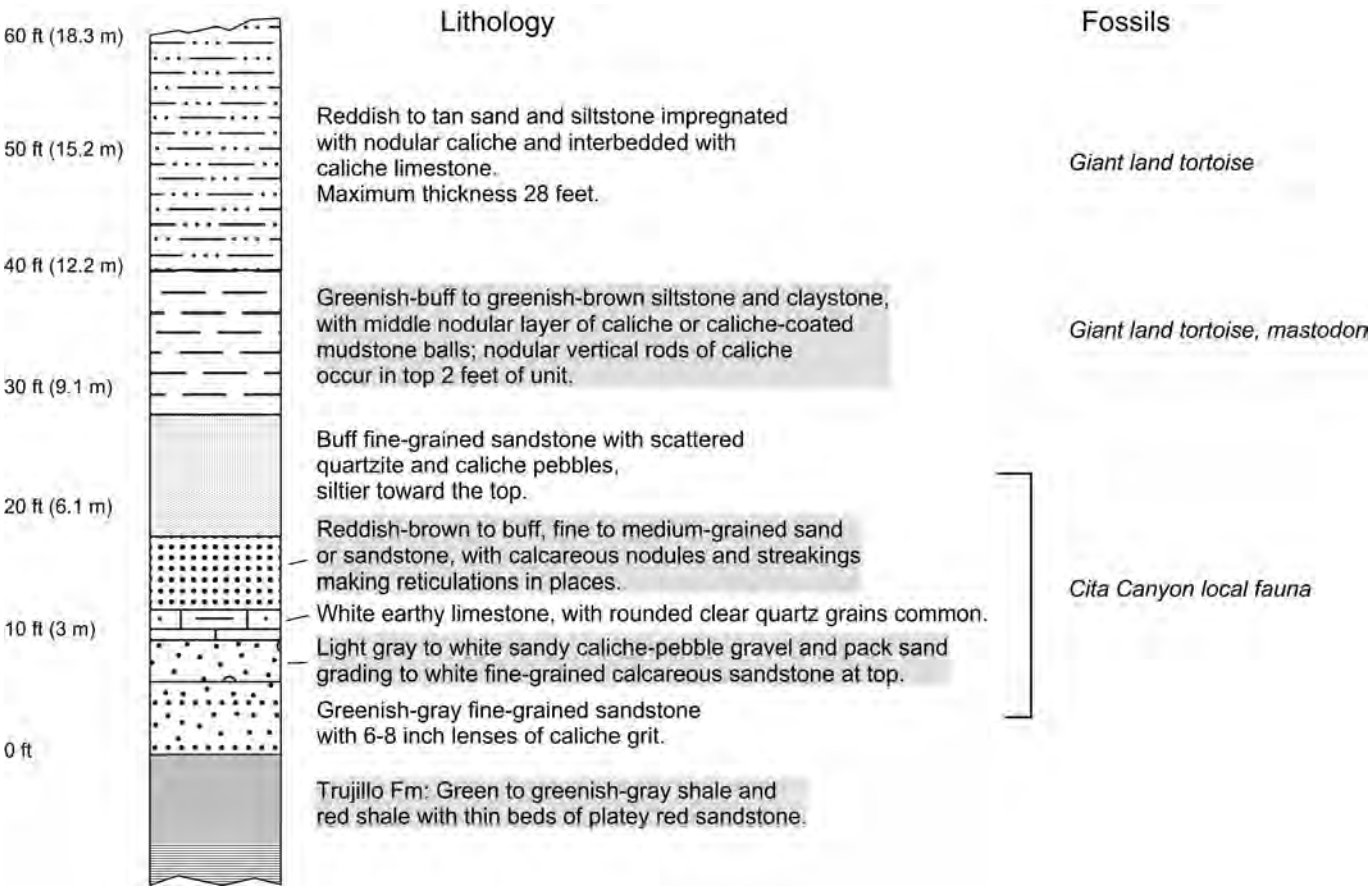

Figure 3. North Cita Canyon strata at bone bed location. Figure redrawn and modified from Figure 3 of Johnston and Savage (1955).

size of a modern dromedary to llama-sized, are also found. Other megafauna include deer, pronghorn, peccary, giant ground sloth, and giant armadillo. Carnivores comprise a small percentage of finds, including saber-toothed cat, puma (or cheetah), coyote, bone-crushing dog, and short-faced bear (Johnston and Savage, 1955; Schultz, 2001). An upper sedimentary unit at the site has yielded mastodon and bison.

Other fossils of interest include sand cat, racoon, rabbit/hare, badger, lynx, giant land tortoise, turkey, and ibis. Tortoises, about 5.0 ft. (1.5 m) long and 3.0 ft. (1.0 m) high, were identified by the recovery of several large shells, a skeleton, and an egg (Schultz, 2001). Mammal megafauna found at other sites in the Texas Panhandle and in similar stratigraphic context includes Columbian mammoth and dire wolf. The mammal types found at the Cita Canyon site are also found at other sites in the Texas Panhandle (Johnston and Savage, 1955).

Most of the bones at the Nebraska site are from three mammals. The most abundant mammalian fossils come from a small rhinoceros called *Menoceras* meaning "crescent horned" (USDI, 1980; Hunt, 1984; Graham, 2009). It stood about 3.0 ft. (1.0 m) tall. Males had two, side-by-side horns on the tip of the snout. Females were hornless. Thousands of bones, representing hundreds of individuals, have been recovered. The next most common fossil is the chalicothere *Moropus*. The chalicothere is a large claw-footed browser thought to be related to horses, rhinos, and tapirs, standing about 8.0 ft. (2.4 m) high at the shoulder. Bones from 50–75 individuals have been found concentrated in one area of the quarry (Hunt, 1984; Graham, 2009). Graham (2009, p. 3) comments: "Remarkably, *Moropus* had toes that were tipped with claws instead of hooves, an anatomical feature difficult to explain in an ungulate." I presume that Graham thought this remarkable and difficult to explain because *Moropus* is considered to be an evolutionary ancestor of the horse.

The third most common mammal bones are from the huge entelodont called "terrible pig" or "hell pig" (Figure 8). These animals ranged from 330 lb. (150 kg) to 2,000 lbs. (900 kg) and were several times the size of modern pigs. The skulls typically measure 3.0 ft. (1.0 m) in length (Hunt, 1984). Two almost complete skeletons of these mammals have been recovered from Agate Fossil Beds.

Other minor mammal fossils at Agate Fossil Beds come from oreodont (sheep-sized, cud-chewing herbivore), saber-toothed cat, carnivorous bear dog, small horse, *Paleocastor* (a land beaver), small camels, 4-horned pronghorn antelope, and deer. Due to its unusual occurrence, an important deposit of the gazelle-like camelid, *Stenomylus*, was found about 1.5 miles (2.4 km) east of the Fossil Hills.

Descriptions of fossil occurrence

Based on the 2019 reconnaissance of the Cita Canyon site discussed above, the Cita Canyon fossil bones were not lithified. All the observed fossils were broken pieces of bone or antler (Figures 6 and 7). I examined a number of the bones. They were light and porous. Many of the fossils that were recovered from the site during fossil excavations in the early- to mid- 1900s were bone fragments and teeth (Johnston and Savage, 1955), although some more complete skeletal parts and skulls were recovered [see Figure 5 in Schultz (2001)]. I am not aware of any complete, articulated skeletons recovered from the Cita Canyon site.

The main bone beds at Agate Fossil Beds are in University and Carnegie Hills, in the upper Harrison formation. The bones are encased and packed in fine-grained sand, sometimes lithified, and calcareous silts and volcanic ash (USDI, 1980; Hunt, 1984; Graham, 2009). The silts are interpreted as loess.

Bone concentration in the principle fossil-bearing strata exceeds 100 bones

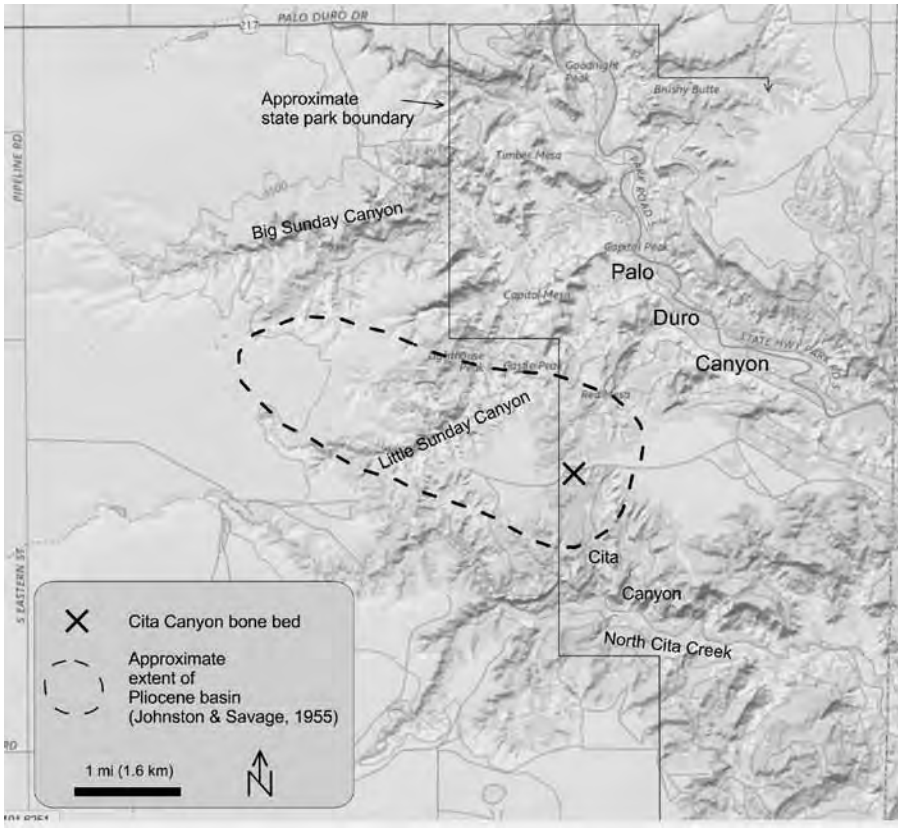

Figure 4. Location of Cita Canyon bone bed in Palo Duro Canyon State Park. Erosion into the outlined basin exposed the bone bed. Base map from: https://viewer.nationalmap.gov/basic/.

Figure 5. View northeast at the Cita Canyon bone bed. Red surface in foreground is Triassic Trujillo Formation. Lighter strata (background) are fossil-bearing Pliocene sediments. Bone shards in Figures 6 and 7 rest on Trujillo red beds but originated from the overlying sediments. Photograph by author.

Figure 6. Bone shard on red Trujillo bed. Note sediment pedestal beneath fossil formed by erosion of red bed. Fossil specimen is about 6 in. (15 cm) long. Photograph by author.

Figure 7. Multiple fossil fragments on Trujillo at base of fossil-bearing sediments. Whitish objects are bone and antler pieces. Fossils came to rest here after either slumping/erosion of fossil-bearing sediments or from previous fossil collecting (circa 1930s). Photograph by author.

per square meter. One sandstone block, about 5.5 ft. by 8 ft. (1.7 m by 2.4 m), containing 22 skulls and an uncounted number of skeletons, is now at the American Museum of Natural History in New York (Graham, 2009). A similar block is on display at the Agate Fossil Beds National Monument Visitor Center (Figure 9).

The principle fossil-bearing strata is a "tangled mat" (USDI, 1980) about 1.5 ft. (0.5 m) thick (USDI, 1980; Hunt, 1984). In some parts of the quarry, the bones are so abundant a man could walk on bones without touching the underlying sediment (Hunt, 1984). Hunt refers to the deposit as a "logjam" of individual bones, and rhino bones are described as being piled "like a gigantic mass of jackstraws" (USDI, 1980). It is noteworthy that the bones are completely jumbled, but are not badly broken or abraded and show little evidence of water erosion (Figure 10). This is remarkable as the deposit is dated conventionally as being about 21,000,000 years old. Almost all of the bones are disarticulated, but rare partial or complete skeletons do occur (Hunt,

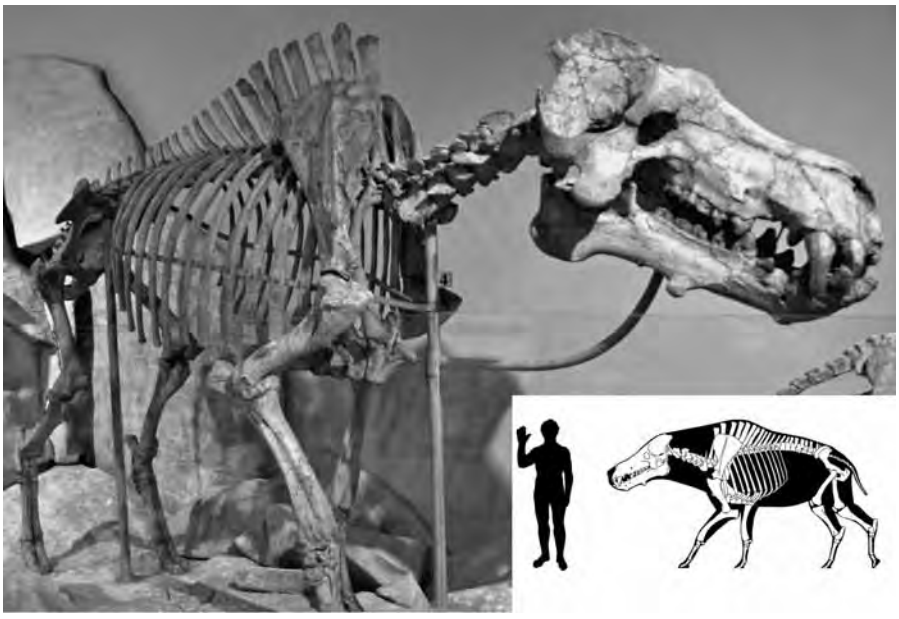

Figure 8. Complete skeleton of 'Terrible' or 'Hell' Pig recovered from Agate Fossil Beds in Nebraska. Skeleton photo by James St. John, https://commons.wikimedia.org/w/index.php?curid=57469214. Inset drawing by Deviant Art user bLAZZE92: https://blazze92.deviantart.com.

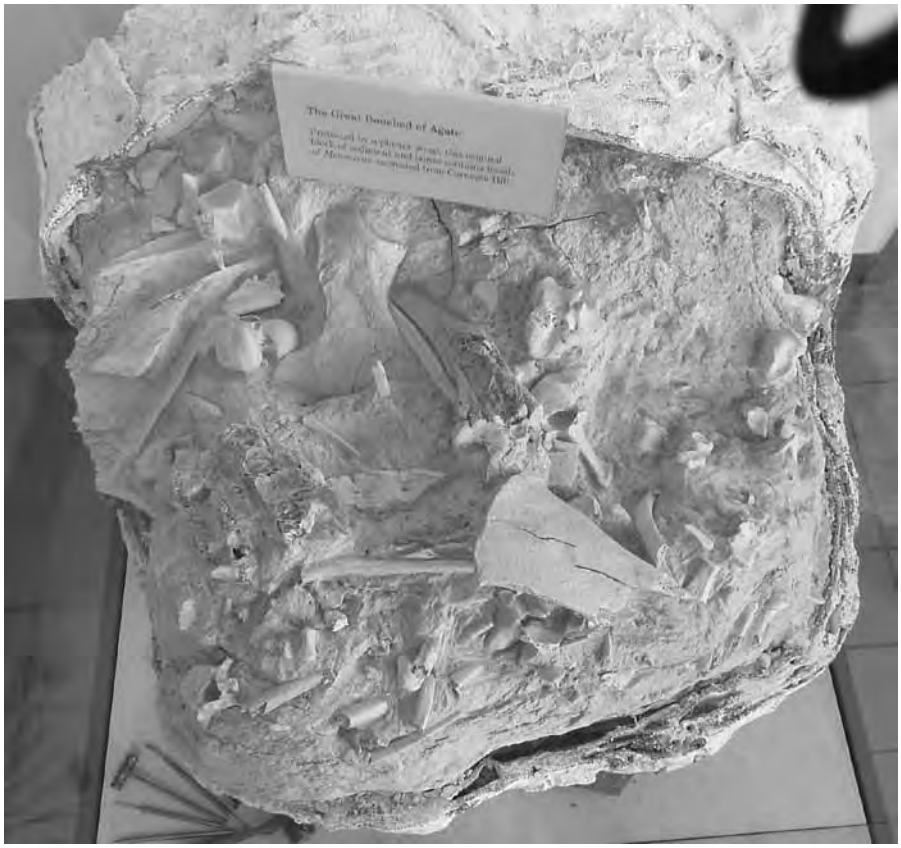

Figure 9. Block of bones, partially protected by a plaster wrap, from Carnegie Hill, Agate Fossil Beds National Monument. The bones are from the small rhinoceros, *Menoceras*. Display at the Agate Fossil Beds Visitor Center. The bones do not appear and are not reported as being lithified, and are easily recognizable as bones. They are dated conventionally as being about 21,000,000 years old.

1984). Whole bones of the three main animal types are common. In contrast, whole bones of other mammals are rare, these rare mammals being represented by isolated teeth, jaw fragments, and occasional bones. The Agate Fossil Bed bones are, apparently, not lithified. The excavation and survey methods of Hunt et al. (2018, p. 34) state that "Fragile bones were hardened with the preservative resin Glyptal." Lithified bones would not require stabilization.

A *Stenomylus* (small gazelle-camel) bone bed was discovered in a hill about 1.5 miles east of Fossil Hills. There is no public access to this site. Significantly, the fossils are dessicated, mummified carcasses of over 100 individuals. Stratigraphically, they are located in the lower Harrison Formation, although it is unclear whether they are in a channel or basin eroded into the Harrison. The gazelle-like camels are frequently found with the heads pulled sharply back in the familiar death pose of many dinosaurs. The carcasses are buried in windblown silt or sand, i.e. loess (USDI, 1980). Graham (2009, p. 3) remarks that "the demise of these animals remains a mystery." It is remarkable that, even though these animals are conventionally dated as at least 21,000,000 years old, they are preserved as mummies at a relatively shallow depth. It is more likely that these *Stenomylus* fossils are a few thousand years old.

There is disagreement in the literature about the "death pose" in which many dinosaurs and these Nebraskan gazelle-camels are found. A number of authors have propounded the idea that this fossil skeletal configuration, called "opisthotonic posture," is due to rigor mortis, desiccation, and/or contraction of tendons and ligaments. A study reported in *Paleobiology* maintains otherwise. Instead, Faux and Padian (2007) conclude that this common fossil posture is due to muscle spasms at death. These death throes are associated with asphyxiation and other causes (Faux and Padian, 2007).

Discussion

Key features of the Cita Canyon site in Texas are:

- Hundreds of mammalian megafauna fossils recovered from the site.
- Fossils found in a basin excavated into the Ogallala Formation.

The Cita Canyon fossil-bearing sediments were deposited in a basin carved into the Ogallala Formation. It is important to distinguish between fossils located in situ in Ogallala beds and fossils located in a basin carved into the Ogallala. If the fossils were deposited at the same time as the Ogallala Formation, and since the Ogallala was probably a late Flood deposit, then the fossils would be Deluge deposits. However, if deposited in a later basin (Schultz, 2001), then the fossils can be interpreted as post-Flood. I prefer the post-Flood interpretation.

Key features of the Agate Fossil Beds in Nebraska are:

- Disarticulated bones of hundreds of individuals, mainly small pig-sized rhinoceroses, occur as a thick, jumbled mass in fluvial channels cut into pyroclastic sandstone.
- Many individuals of the strange chalicothere are found.

Figure 10. Exhibit at Agate Fossil Beds National Monument Visitor Center. The bones in the exhibit are most likely replicas intended to show the original appearance of the bone bed deposits when excavated.

- Two of the best skeletons ever found of the large entelodont known as "terrible pig" were found at the site.
- A deposit of articulated, mummified, gazelle-sized camels was found nearby. These camelids were often found in the typical dinosaur death pose. The camelids were probably buried and suffocated by a catastrophic sand/dust storm.
- Nearby, the phenomenon interpreted as the corkscrew burrow of an extinct land beaver was found.
- The fossil-bearing strata are capped by limestone mud and, locally, by a silica-cemented surface containing agates.

The main bone beds were found in a channel incised in the Ogallala Formation. The Ogallala likely formed late in the Flood (Clarey, 2018). The channel could have formed from late-Flood runoff or sometime after the Flood. The Fossil Hills deposits are associated with volcanic pyroclastic debris, alluvial channel fill, and windblown loess.

Akridge and Froede (2005) interpreted the mammalian megafauna found at Ashfall Fossil Beds State Historical Park, Nebraska (Ashfall Fossil Beds), as post-Flood deposits. These fossil beds are about 300 miles (483 km) east of Agate Fossil Beds, and include articulated remains of rhinoceroses, camels, horses, and deer. The remains are buried in volcanic ash deduced to have originated in the Late Miocene from a volcanic center located in southern Idaho. Agate Fossil Beds could also have been affected by a plume of volcanic material from that same volcanic center since Agate Fossil Beds lies between Idaho and Ashfall Fossil Beds. The Ashfall Fossil Beds are in the Cap Rock member of the Ash Hollow Formation, which is part of the Ogallala Group. The fossil-bearing Harrison and Upper Harrison Formations of the Agate Fossil Beds are also in the upper part of the Ogallala Group.

I interpret the Agate Fossil Beds as post-Flood. The mechanisms of catastrophe resulting in the bone bed deposit included volcanism, flooding, and windstorms. The nearby site of mummified camelids supports this idea. The camelids are buried in loess, not alluvial sediments, and are articulated mummies, unlikely to have formed during a flood. Also, the camelids show no evidence of being altered after burial by later flooding. The camelids are found in the Lower Harrison Formation, and the bones of Fossil Hills are found in the Upper Harrison. If the camelids were deposited after the Flood, then the Agate Fossil Beds were also post-Flood deposits.

Summary

There are similarities between Agate Fossil Beds and Cita Canyon fossil beds. The great majority of fossils found at both sites are dismembered skeletons and broken bones, explained most easily as resulting from transport and deposition by water. For example, at Agate Fossil Beds, the dense concentration of bones (Figures 9 and 10) would probably *not* result from *in place* death, disarticulation, bone mixing, *bone concentration*, and quick burial of hundreds of individuals. Rather, concentration by water of many already-dead carcasses is more likely.

The striking exception to the more common disarticulated state of the fossils at both sites is the *Stenomylus* bone bed near Agate Fossil Beds, in which over 100 mummified carcasses of the small gazelle-like camelid have been found (Graham, 2009). These animals obviously perished at the bone bed location, possibly by asphyxiation from a massive dust/sand storm that buried and smothered them.

Agate Fossil Beds bones are found in lenses at the base of channels cut into

the Upper Harrison, a member of the Ogallala Formation. The Cita Canyon site was a fluvial deposit into a basin eroded into this same region-spanning Ogallala Formation and later exposed by the erosion of Palo Duro Canyon and/or its tributaries. The deposit of mummified gazelle-like camels near the Fossil Hills in Agate Fossil Beds National Monument is an exception to the pattern of fluvial deposition.

Excellent bone preservation and high fossil concentrations at Agate Fossil Beds indicate rapid burial. If the fossil deposits accumulated over a long period of time, scattered bones in various states of weathering and decomposition would be expected. Rapid burial is indisputable at the nearby *Stenomylus* bone bed. The "death throes" posture of the camelids and the burial by windborne sediments indicates death was by suffocation in a sandstorm. Evidence for rapid burial at Cita Canyon was equivocal; however, rapid burial is almost always prerequisite for the preservation of an organic fossil. Without rapid burial, weathering, scavenging, and decomposition quickly break down the structure of the organic material. If a fossil exists in a well-preserved state, then rapid burial likely occurred.

The Laramide orogeny and subsequent deposition of the Ogallala Formation probably happened near the end of the Flood since the Ogallala was one of the last continent-scale sediment sheets in North America. Erosion into that surface would have occurred via flow channelization in the recessive stage of the Deluge, but could also occur at any time after the Flood by smaller-scale deposition and burial events. The bone beds of Agate Fossil Beds are found at the base of channels cut into the Ogallala Formation; hence, these fossils postdate the Ogallala Formation deposition. The Cita Canyon bone bed is in a small basin also eroded into the upper surface of the Ogallala Formation (Schultz, 2001). The fossil beds at North Cita Canyon and Agate Fossil Beds were both probably deposited by post-Flood catastrophes.

References

Akridge, A.J., and C.R. Froede, Jr. 2005. Ashfall Fossil Beds State Park, Nebraska: A post-Flood/Ice Age paleoenvironment. *CRSQ* 42(3): 183–192.

Clarey, T. 2018. Palo Duro Canyon rocks showcase Genesis Flood. *Acts & Facts* 47(7), June 29, https://www.icr.org/article/10713.

Faux, C.M., and K. Padian. 2007. The opisthotonic posture of vertebrate skeletons: Postmortem contraction or death throes? *Paleobiology* 33(2): 201–226.

Graham, J. 2009. *Agate Fossil Beds National Monument Geologic Resources Inventory Report*. Natural Resource Report NPS/NRPC/GRD/NRR—2009/080. National Park Service, U.S. Department of the Interior, Denver, CO.

Hood, C.H., and J.R. Underwood, Jr. 2001. Geology of Palo Duro Canyon, In Guy, T.F. (editor), *The Story of Palo Duro Canyon*, Texas Tech University Press, Lubbock, TX.

Hunt, R. 1984. Extinct carnivores entombed in 20 million year old dens, Agate Fossil Beds National Monument, Nebraska. *The George Wright Forum 4, no. 1*, http://www.jstor.org/stable/43597031.

Hunt, R.M., Jr., R. Skolnick, and J. Kaufman. 2018. The carnivores of Agate Fossil Beds National Monument: Miocene dens and waterhole in the valley of a dryland paleoriver. *Zea E-Books*, 74, https://digitalcommons.unl.edu/zeabook/74.

Johnston, C.S., and D.E. Savage. 1955. A survey of various late Cenozoic vertebrate faunas of the Panhandle of Texas, Part 1: Introduction, description of localities, preliminary faunal lists. *University of California Publication Geological Science*, 31:2.

Reed, J.K. 2002. Time warp 1: The Permian-Triassic boundary in the Texas Panhandle. *CRSQ* 39(2): 116–119.

Reed, J.K., and M.J. Oard. 2017. Not enough rocks: The sedimentary record and Earth's past. *Journal of Creation* 31(2): 84–93.

Reed, J.K., and M.J. Oard. 2018. The meaning of unconformities. *Journal of Creation* 32(1): 92–99.

Schultz, G.E. 2001. The paleontology of Palo Duro Canyon. In Guy, D.F. (editor), *The Story of Palo Duro Canyon*, Texas Tech University Press, Lubbock, TX.

USDI (U.S. Department of Interior, National Park Service). 1980. *Agate Fossil Beds*. U.S. National Park Service Publications and Papers, DigitalCommons@University of Nebraska—Lincoln.

Design Revealed by the Spectral "IR Ledge"

Jonathan K. Corrado*

Abstract

Remote sensing is a field designed to enable people to look beyond the range of human vision. Whether it is over the horizon or in a spectral range outside our perception, we search for information about our environment. Remote sensing data is enormously powerful and gives humans more data than can be discriminated directly via our senses. The extraction and analysis of this data reveals important, valuable information. It also implies specific design characteristics that only a designer could invoke. One of the incredible phenomena found through remote sensing is the illumination of the "IR Ledge" in vegetation. The IR Ledge or "red edge" is an essential and dramatic spectral feature found in remote sensing and refers to the region of dramatic change in reflectance of vegetation in the near infrared (NIR) range of the electromagnetic spectrum. This dramatic variation in reflectance facilitates photosynthesis and protects vegetation in the higher energy, longer wavelength region of the electromagnetic spectrum. This article contends that this reflectance phenomenon combined with the unique and precisely tuned blackbody radiation profile of the Sun centered on the visual spectrum displays characteristics that transcend coincidence, meets the definition of Complex Specified Information, and infers causation and, therefore, design.

Key Words: remote sensing, photosynthesis, electromagnetic spectrum, design, infrared (IR), blackbody radiation, Complex Specified Information

Introduction

"Astronomy may be revolutionized more than any other field of science by observations from above the atmosphere. Study of the planets, the Sun, the stars, and the rarified matter in space should all be profoundly influenced by measurements from balloons, rockets, probes and satellites.... In a new adventure of discovery no one can foretell what will be found, and it is probably safe to predict that the most important new discovery that will be made with flying telescopes will be quite unexpected and unforeseen." —Lyman Spitzer, Jr.

Remote sensing is the process of detecting and monitoring the physical characteristics of an area by measuring its reflected and emitted radiation at a distance (typically from a satellite or aircraft) (Chuvieco, 2020). Said more practically, remote sensing is a field designed to enable people to look beyond

* Jonathan K. Corrado, PhD, PE, Cincinnati, OH, corradojk@gmail.com
Accepted for publication May 13, 2022

the range of human vision. Whether it is over the horizon, beyond our limited range, or in a spectral range outside our perception, we are in search of information (Olsen, 2016). Special cameras collect remotely sensed images, which help researchers "sense" things about the Earth. First, cameras on satellites and airplanes take images of large areas on the Earth's surface, allowing us to see much more than we can see when standing on the ground. Second, sonar systems on ships create ocean floor images without needing us to travel to the bottom of the ocean. Finally, cameras on satellites can be used to make images of ocean temperature changes.

Four specific uses of remotely sensed images of the Earth include mapping large forest fires from space to allow rangers to see a much larger area than from the ground. Second, scientific surveillance, e.g., tracking clouds to predict the weather, observing erupting volcanoes, or watching out for dust storms. Third, tracking city growth and changes in farmland or forests over several years or decades. Fourth, the discovery and mapping of the rugged topography of the ocean floor (e.g., huge mountain ranges, deep canyons, and the "magnetic striping" on the ocean floor) (Chuvieco, 2020).

Remote sensing data is enormously powerful and gives humans much more information than can be detected directly via our senses. The extraction and analysis of this data reveal important, valuable information for many different applications but implies specific design characteristics that only a designer could invoke. One such design element is a phenomenon called the "IR Ledge" used by image analysts to highlight vegetation in satellite imagery. The discussion of the IR Ledge and the design implied by this marvel is the substance of this paper, "for his invisible attributes, namely, his eternal power and divine nature, have been clearly perceived, ever since the creation of the world, in the things that have been made. So they are without excuse" (Romans 1:20).

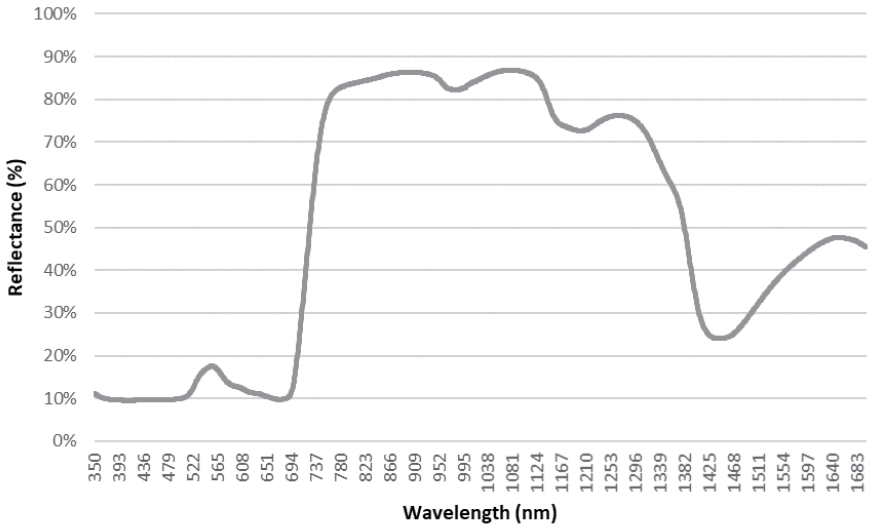

Figure 1. Spectral reflectance curve for an oak leaf (Kokaly et al., 2017).

Reflectance of Materials

Reflection illustrates the process whereby incident radiation recoils off the surface of a material in a single, anticipated direction. Reflection is produced by surfaces that are smooth relative to the wavelength of incident radiation. These smooth, mirror-like surfaces are called "specular reflectors" (Olsen, 2016). The reflectance of most substances varies with wavelength, which allows spectral imagers to distinguish different substances. Figure 1 (spectral image) illustrates reflective spectra. Spectra are the fingerprints of elements, derived from their fundamental atomic characteristics.

Knowledge of spectral signatures is essential in the understanding and interpretation of a remotely sensed image. Wavelength-dependent absorptions distinguish different substances, and these images of reflected solar energy are known as "spectral signatures." The property used to quantify these spectral signatures is called *spectral reflectance*. This reflection is a ratio of the reflected energy to incident energy as a function of wavelength (Kruse, 1999). The graph of the spectral reflectance of an object as a function of wavelength is called the "spectral reflectance curve" (Lillesand and Kiefer, 1999).

The arrangement of the spectral reflectance curves is essential in establishing the wavelength region(s) in which remote sensing data is obtained, as the spectral reflectance curves provide comprehension of the spectral characteristics of an object (Lillesand and Kiefer, 1999). Spectral signatures obtained from multispectral images are isolated compared to the adjoining signatures obtained from hyperspectral images. Adjoining spectral signatures allow for detailed analysis through the recognition of surface materials and their proportion, as well as deductions of biological and chemical processes (Lillesand and Kiefer, 1999). As displayed in Figure 1, the reflectance curve for an oak leaf illustrates the reflectance curve unique to that leaf.

In green vegetation, the plant's coloration regulates the valleys in the visible portion of the spectrum. For example,

chlorophyll absorbs sharply in the blue (450 nm) and red (670 nm) sections of the electromagnetic spectrum, otherwise known as the "chlorophyll absorption bands." Chlorophyll is the primary photosynthetic pigment in green plants (Lillesand and Kiefer, 1999). Thus, the human eye perceives healthy vegetation as green due to the strong absorption of the red and blue wavelengths and the reflection of the green wavelengths. When the plant encounters stress that hinders normal growth and chlorophyll production, less adsorption occurs in the red and blue regions and the amount of reflection in the red waveband increases (Lillesand and Kiefer, 1999).

The spectral reflectance signature illustrates a dramatic increase in the reflection for healthy vegetation at around 700 nm. In the near-infrared (NIR) range between 700 and 1300 nm, a plant leaf will typically reflect between 40 to 50%; the rest is transmitted, with only about 5% being adsorbed. Structural variability in leaves in this range allows one to differentiate between species, even though they might look the same in the visible region (Lillesand and Kiefer, 1999).

The "IR Ledge"

The "IR Ledge" or "red edge" is an important and dramatic spectral feature found in remote sensing, as can be seen around 700 nm on a spectral image of green vegetation. The IR ledge refers to the region of dramatic change in vegetation reflectance in the near-infrared range. This striking wavelength reflectance rise makes vegetation appear bright in the infrared, as displayed in the false-color images in Figures 2 and 3. As previously discussed, the leaf pigments, cell structure and water content all impact the spectral reflectance of vegetation (Carter, 1991). In the visible bands, the reflectance is relatively low as the leaf pigments absorb the most light. For healthy vegetation, the reflectance

Figure 2. Natural- and false-color images from NASA's MESSENGER mission to Mercury showing plant-covered land from the Amazon rainforest to the North American forests (V1Media/*Earth Imaging Journal*, 2014).

Figure 3. QuickBird near-infrared satellite image of Nigeria, Africa (Satellite Imaging Corporation).

is much higher in the near-infrared region than in the visible region due to the cellular structure of the leaves. Therefore, healthy vegetation can be easily identified by the high near-infrared reflectance and generally low visible reflectance.

Live green plants absorb solar radiation in the photosynthetically active radiation (PAR) spectral region, which they use as a source of energy in the process of photosynthesis. Leaf cells also re-emit solar radiation in the near-infrared spectral region (which carries approximately half of the total incoming solar energy) because the photon energy at wavelengths longer than about 700 nm is too small to synthesise organic molecules. Strong absorption at these wavelengths would only result in overheating the plant and possibly damaging the tissues. Hence, live green plants appear relatively dark in the PAR and relatively bright in the near infrared (Gates, 1980). By contrast, clouds and snow tend to be relatively bright in the red (as well as other visible wavelengths) and quite dark in the near infrared. As previously discussed, pigment in plant leaves, chlorophyll, strongly absorbs visible light (from 400 to 700 nm) for use in photosynthesis. The cell structure of the leaves, on the other hand, strongly reflects near-infrared light (from 700 to 1100 nm). The more leaves a plant has, the more these wavelengths of light are affected.

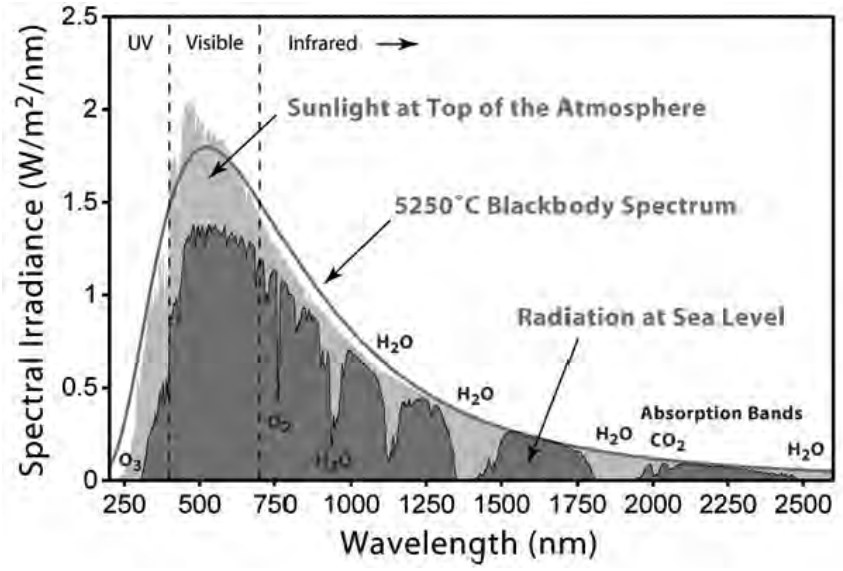

Figure 4. Emission spectra of blackbodies at various temperatures (Tanaka et al., 2010).

The Design of the IR Ledge

Blackbody radiation of the Sun

When an object is heated to a high temperature, it emits light that is more representative of the object's temperature than of its composition. When an object has this characteristic, it is called a "blackbody radiator." Blackbody radiation is the thermal electromagnetic radiation within or surrounding a body in thermodynamic equilibrium with its environment, emitted by a blackbody (an idealized opaque, non-reflective body) (Stewart and Johnson, 2017). Typically, light emitted by these objects has similar characteristics in that the blackbody produces a continuous spectrum (over a wide range of wavelengths). The wavelength of the maximum radiation intensity varies inversely with the temperature. The total energy emitted varies as the fourth power of the temperature, and the power at a given temperature varies inversely with the fifth power of the wavelength (Stewart and Johnson, 2017).

These characteristics result in emission spectra like that shown in Figure 4.

As the temperature increases, the peak of the emitted blackbody radiation curve moves to higher intensities and shorter wavelengths (up and to the left on Figure 4). The 5250°C (9482°F) line in the figure corresponds roughly to the temperature of the Sun's photosphere. Although planets and stars are neither in thermal equilibrium with their surroundings nor perfect blackbodies, researchers use blackbody radiation as a first approximation for the energy planets and stars emit (Stewart and Johnson, 2017).

Anthropic implications

As depicted in Figure 4, the peak of the 5250°C curve centers in the visible spectrum and the most (and highest) energy is emitted within this visual band. As the Sun represents the 5250°C curve, it would effectively need to remain at a stagnate temperature (given the distance from the Sun to Earth), or life of any kind on Earth would be impossible as implied by the "Anthropic Cosmological Principle" (Borrow and Tipler, 1988). If the surface temperature of the Sun increased, two main consequences would result. First, the total energy radiated from the Sun would increase (and so Earth would get hotter). Second, the Sun's light wavelength would decrease (the Sun would become bluer). The first would cause severe climate change, and the latter would result in much higher levels of ultraviolet radiation reaching Earth. If this transition were to happen suddenly, life on Earth would quickly go

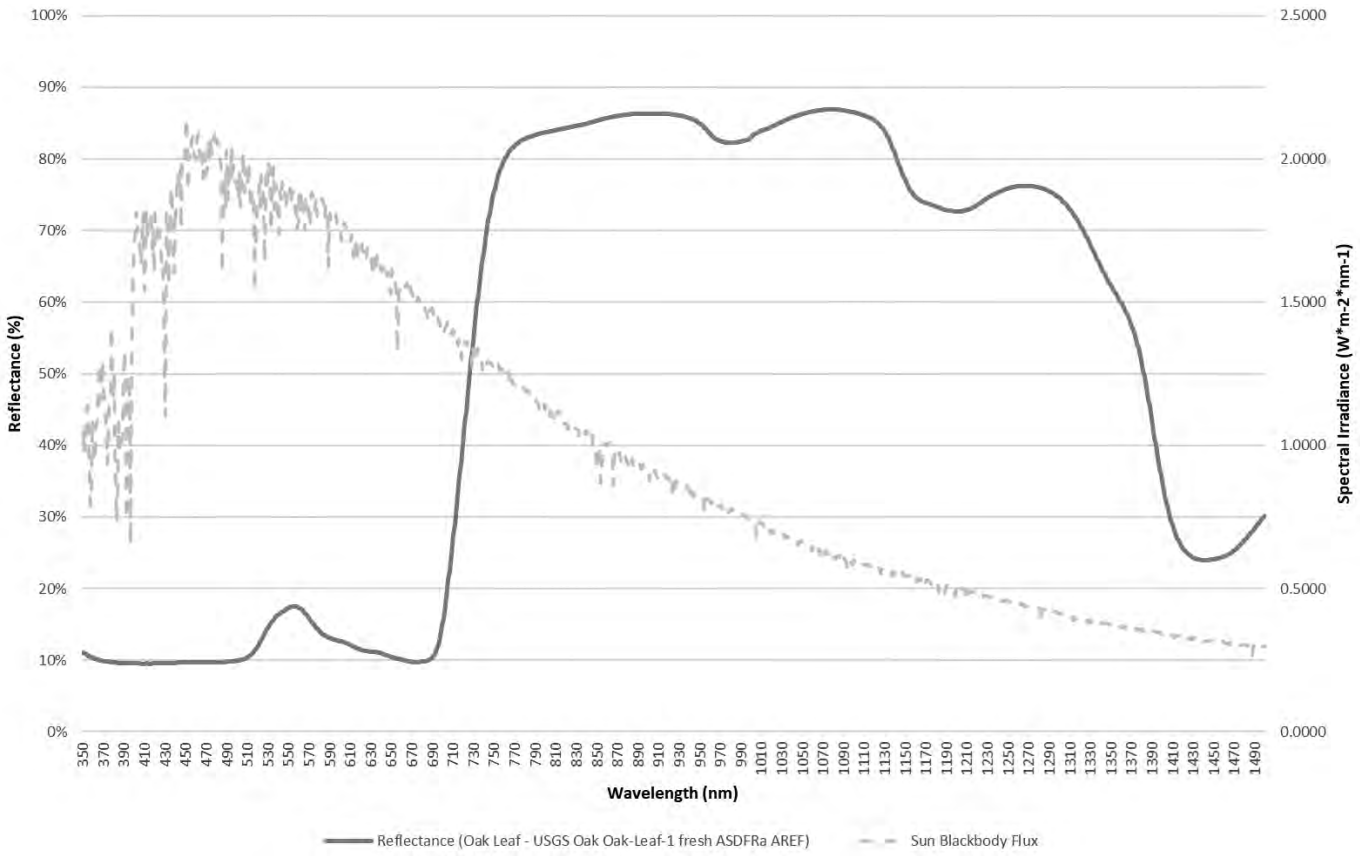

Figure 5. Plot of the Sun's blackbody radiation overlaid on a reflectance curve for an oak leaf (Coddington et al., 2015; Kokaly et al., 2017).

extinct. If it happened gradually, some microbial life-forms might survive in the new environment, but plant, animal, and human life would cease to survive (Borrow and Tipler, 1988).

So, with the understanding that the Sun's temperature has to remain relatively stagnant for life on Earth (as we know it) to remain viable, with the blackbody spectrum remaining constant, it can be logically inferred that the placement of the IR Ledge should be tied to the Sun's blackbody spectrum. As displayed in Figure 5, an overlay of the Sun's blackbody radiation profile on top of a reflectance curve of vegetation clearly shows this tie. From the figure, most of the Sun's energy is emitted within the wavelength range of the visible spectrum, which is precisely the energy absorbed by plant life for the photosynthesis process. Outside the visual spectrum, the Sun's blackbody energy declines rapidly as the plant's reflectance profile increases promptly to repel the energy at wavelengths that would harm the plant. This phenomenon indicates complexity, sophistication, and purpose—as if it were designed by a designer.

The irresolute evolution of photosynthesis

Photosynthesis is a process used by plants and other organisms to convert light energy into chemical energy that, through cellular respiration, can later be released to fuel the organism's metabolic activities. This chemical energy is stored in carbohydrate molecules, such as sugars and starches, which are synthesized from carbon dioxide and water. There are two types of photosythesis. The first is *anoxygenic photosynthesis* that uses molecules other than water to drive the process and does not produce oxygen as a byproduct. The second is *oxygenic photosynthesis*, which separates water into hydrogen and oxygen to drive photosynthesis, and releases oxygen as a byproduct. Oxygenic photosynthesis is the most common and familiar, found in algae, plants, and in some bacteria. Oxygenic photosynthesis is a fundamental process that sustains human and animal life (Bryant and Frigaard, 2006).

For decades, biological evolutionary theory contented that anoxygenic photosynthesis significantly predated oxygenic photosynthesis on the order

of a billion years. However, recent research discovered unique structures in bacteria, specifically *Heliobacterium modesticaldum*, demonstrating that oxygenic photosynthesis was occurring a billion years earlier than commonly thought. By investigating *H. modesticaldum*, research found fully functional photosynthesis was already in place, therefore, one kind of photosynthesis could not have evolved into the other (Cardona, 2019). This discovery leans in favor of intelligent design versus adaptive response over time in that this recent finding points more firmly to the fact that the molecules and processes that enable photosynthesis were purposely formed for that specific function.

Further, the formation of these complex, photosynthetic molecules comprises a set of enzymes that must act in a specific sequence. Per the Granick Hypothesis, these enzymes evolved arbitrarily and the sequence of steps in the synthesis represents the progression of steps in the historical evolution of the process. But the probability of this natural selection bringing about the right enzymes in the right sequence at the right time to produce the end product surpasses reason and transcends incongruity. The Calvin Cycle, a process that plants and algae use to turn carbon dioxide from the air into sugar, necessitates eleven different enzymes, all of which are uniquely coded within the DNA and directed specifically to the chloroplast, a component that contains chlorophyll and in which photosynthesis takes place. For the Calvin Cycle to function correctly, all enzymes must be present (Taiz and Zeiger, 1998).

It thwarts logic to presume the irreducible complexity of photosynthetic systems would have resulted from arbitrary means and randomness. Rather, the specific arrangement and complexity apparent in photosynthesis, a process scientists have merely scratched the surface in comprehending, more comfortably and logically aligns with design. Moreover, the concept of an unevolved photosynthetic process would also suggest against an evolving, shifting electromagnetic spectrum emitted from the Sun. The solar spectrum emitted and the photosynthetic receptors need to be in lockstep for the process to function and life on Earth to exist. As this suggests, 'success tapping' into the electromagnetic wavelengths arriving from the Sun would not be necessary, thus disputing the idea that if a different spectrum reached the surface of the Earth, maybe a different chemical process would have been utilized for photosythesis.

Specified complexity

'The concept of specified complexity' asserts that when something exhibits *specified complexity* (i.e., the item or phenomenon is both complex and specified, *simultaneously*), one can infer an intelligent cause (i.e., that it was designed) rather than being the result of natural processes (Dembski, 1999). Any object or event with an extremely low probability of occurring by chance that matches a discernable pattern displays specified complexity. According to contemporary design theory, the presence of highly specified complexity is an indicator of an intelligent cause. Although the theory of specified complexity derived by William Dembski stemmed from his study of biology, this idea can be expanded to other fields of science and occurrences in nature.

Complex Specified Information (CSI), the qualitative and quantitative measure of specified complexity, is a reliable indicator of design because its recognition corresponds with how researchers identify intelligent causality. In general, to distinguish intelligent causality, one must establish that a choice from a range of contending possibilities was definitely actualized, determine which possibilities were excluded, and then identify the particular possibility that was actualized. Besides, the excluded competing possibilities must be tangible possibilities, suitably numerous, so that identifying the possibility that was actualized cannot be attributed to chance. Regarding probability, this means that the identified possibility is *highly improbable*. Regarding complexity, this means that the identified possibility is *highly complex*. All the components in the general method for identifying intelligent causation (i.e., actualization → exclusion → specification) find an equivalent in CSI (Dembski, 1997).

As displayed in Figure 5, most of the Sun's energy is emitted and peaks in the visual range of the electromagnetic spectrum, thus making life on Earth possible. In tandem, the nested vegetation spectral reflectance curve indicates high absorption within the visual spectrum. This absorption facilitates photosynthesis and rapidly transitions to high reflection values outside the visual band to protect the plant from the more harmful longer wavelengths. Based on the previous discussion of the irresolute evolution of photosynthesis, it can be assumed that the probability of the Sun emitting a majority of its energy in the spectral range to be a low probability. It can also be assumed that the probability of the vegetation's spectral reflectance profile indicating high absorption in the visual range and a rapid transition to the higher reflectance right outside the visual range also to be low. Collectively, the composite probability of these two independent probabilities would yield an even lower probability. This construction reduces the probability of this condition occurring by chance and infers that this is a "complex" relationship as defined in the concept of specified complexity.

The distinction between specified and unspecified information can be defined as follows: "the actualization of a possibility (i.e., information) is specified if independently of the possibility's actualization, the possibility is identifiable by means of a pattern. If not, then the information is unspecified" (Dembski, 1997). Note that this definition implies

an asymmetry between specified and unspecified information. Specified information cannot become unspecified information, though unspecified information may transform into specified information. Unspecified information can become specified as our background knowledge increases. In the context of Figure 5, independently, the blackbody curve and the vegetation reflectance curve can be deemed "specified" per the above definition concerning the visual spectrum and their characteristics within this wavelength range. Taken collectively, logically, the relationship between the two curves can be inferred as a "specified" relationship.

As postulated, the IR Ledge combined with the precisely arranged blackbody radiation profile of the Sun centered on the visual spectrum presented in Figure 5 is determined to be both "complex" and "specified." Therefore the IR Ledge can be labeled "Complex Specified Information," which, per the above discussion qualitatively, infers a high likelihood of causation and thus design.

Conclusion

"*For by him all things were created, in heaven and on Earth, visible and invisible, whether thrones or dominions or rulers or authorities—all things were created through him and for him. And he is before all things, and in him all things hold together*" (Colossians 1:16–17).

Evidence of design is continuously overwhelming our senses. It does not take much rational thought to conclude that our material existence resulted from design in contrast to accidental, evolutionary causes. From the macro to the micro, the elements of our material existence are finely balanced and operate with intricate, shared precision. Some of the most remarkable findings of modern physics and cosmology, especially the indications that our particular universe and its laws seem remarkably tailored to sustain life, support this point of view.

Via remote sensing in the near infrared, one of these interesting yet critical design elements appears in the IR Ledge. This appearance combined with the unique and specially tuned blackbody radiation profile of the Sun centered on the visual spectrum displays characteristics that transcend coincidence, meet the definition of CSI, and thus radiate the inference of design "for from him and through him and to him are all things. To him be glory forever, Amen" (Romans 11:36).

References

Borrow, J., and F. Tipler. 1988. *The Anthropic Cosmological Principle*. Oxford University Press, New York, NY.

Bryant, D.A., and N.U. Frigaard. 2006. Prokaryotic photosynthesis and phototrophy illuminated. *Trends in Microbiology* 14(11): 488–496. doi:10.1016/j.tim.2006.09.001. PMID 16997562.

Cardona, T. 2019. Thinking twice about the evolution of photosynthesis. *Open Biology* 9(3): 180246. http://doi.org/10.1098/rsob.180246.

Carter, G. 1991. Primary and secondary effects of water content on the spectral reflectance of Leaves. *American Journal of Botany* 78(7): 916–924. https://doi.org/10.1002/j.1537–2197.1991.tb14495.x.

Chuvieco, E. 2020. *Fundamentals of Satellite Remote Sensing: An Environmental Approach*, third edition. CRC Press/Taylor & Francis Group, Boca Raton, FL.

Coddington, O., J.L. Lean, D. Lindholm, P. Pilewskie, M. Snow, and NOAA CDR Program. 2015. NOAA climate data record (CDR) of solar spectral irradiance (SSI), NRLSSI version 2. *NOAA National Centers for Environmental Information*. https://doi.org/10.7289/V51J97P6 (accessed April 15, 2021).

Dembski, W. 1997. Intelligent design as a theory of information. *Access Research Network*.

Dembski, W. 1999. *Intelligent Design: The Bridge Between Science and Theology*. Intervarsity Press, Downers Grove, IL.

[See V1 Media (the copyright source of this article) below.]

Gates, D.M. 1980. *Biophysical Ecology*. Springer-Verlag, New York, NY.

Kokaly, R.F., R.N. Clark, G.A. Swayze, K.E. Livo, T.M. Hoefen, N.C. Pearson, R.A. Wise, W.M. Benzel, H.A. Lowers, R.L. Driscoll, and A.J. Klein. 2017. *USGS Spectral Library Version 7: U.S. Geological Survey Data Series 1035*. https://doi.org/10.3133/ds1035.

Kruse, F.A. 1999. Visible-Infrared Sensors and Case Studies. In *Remote Sensing for the Earth Sciences: Manual of Remote Sensing*, third edition. A.N. Renz (editor). Volume 3, pp. 567–611. John Wiley & Sons, New York, NY.

Lillesand, T., and R. Kiefer. 1999. *Remote Sensing and Image Interpretation*. John Wiley & Sons, Inc., Hoboken, NJ.

Olsen, R. 2016. *Remote Sensing from Air and Space*, second edition. Spie Press, Bellingham, WA.

Satellite Imaging Corporation. 2004. QuickBird Near Infrared Satellite Image Nigeria, Africa. *Satellite Imaging Corporation*; image acquired February 3, 2004. https://www.satimagingcorp.com/gallery/quickbird/quickbird-oil-and-gas-near-infrared/ (accessed April 15, 2021).

Stewart, S., and R. Johnson. 2017. *Blackbody Radiation: A History of Thermal Radiation Computational Aids and Numerical Methods*. CRC Press/Taylor & Francis Group, Boca Raton, FL.

Taiz, L., and E. Zeiger. 1998. *Plant Physiology*, second edition. Sinauer Associates, Inc., Massachusetts, MA.

Tanaka, Y., et al. 2010. Long-lasting muscle thinning induced by infrared irradiation specialized with wavelength and contact cooling: A preliminary report. *ePlasty* 10:e40.

V1 Media. 2014. How to interpret a false-color satellite image. *Earth Imaging Journal*, April 11. https://eijournal.com/print/articles/how-to-interpret-a-false-color-satellite-image (accessed April 15, 2021).

Creation Research Society Quarterly 2022 59:21–28

The "Dolomite Problem" Solved by the Flood

Michael J. Oard

Abstract

Dolomite conservatively makes up 10% of all sedimentary rocks and is mostly stoichiometric and ordered, mainly older than the Cenozoic. It can be thick and widespread, especially in the Precambrian and Paleozoic. Although dolomite is forming today, the great mystery is that it is of small scale and not stoichiometric and ordered. Dolomite today is likely formed by the aid of microorganisms that act as catalysts to overcome strong kinetic effects. The "dolomite problem" has been a uniformitarian mystery for over 200 years. Many uniformitarian scientists predominantly believe in replacement of limestone and not the primary precipitation of dolomite. However, replacement, or dolomitization, required tremendous fluid flow from a 'pumping mechanism' with an unlimited amount of Mg available. Evidence does exist for replacement, mainly from hydrothermal fluids associated with faults, but the fluid has to have been very hot. Numerous experiments studying the origin of dolomite use temperatures over 100°C for primary precipitation. In contrast, the short time scale of the Flood would require that most dolomite is primary formed from widespread hot water, especially very early in the Flood when the Precambrian and Paleozoic rocks were being deposited, mostly in basins and rifts. In addition, dolomites may be helpful as a criterion for determining the pre-Flood/Flood boundary.

Key Words: Carbonate, dolomite, dolomitization, dolostone, hydrothermal flow, Genesis Flood, geological column, limestone, Mg, microbial precipitation, pre-Flood/Flood boundary, protodolomite, replacement, uniformitarianism (actualism)

Introduction

The origin of several types of sedimentary rocks have remained major uniformitarian mysteries for a few hundred years. Dott (2003, p. 387) writes:

> When I was a student half a century ago, the origin of pure quartz sheet sandstones, then called orthoquartzites [now called quartz arenites], was considered a major puzzle. Together with the origin of dolomite, red beds, black shale, and banded iron formation, they made up a group of seemingly intractable geological problems. Even now, 50 odd years later, their origins are still being debated.

Dolomite is one of those mystery rocks (Figure 1). It was probably first discovered by the French geologist Deodat Guy de Dolomieu in 1792 in the Dolomite Mountains of northern Italy (Figure 2). Dolomite is the common name

Accepted for publication December 13, 2021

for carbonate rock mostly composed of the mineral dolomite ($CaMg(CO_3)_2$) (Boggs, 2012). It is sometimes called dolostone. To qualify as dolostone, more than 50% of the carbonate must be the mineral dolomite. Intermediates between limestone, calcite ($CaCO_3$), and dolostone are high-magnesium calcite or 'protodolomite' that is commonly synthesized in the lab.

Sedimentary Rock Dolomite Mostly Stoichiometric and Ordered

Sedimentary rocks usually have a high percentage of either limestone or dolomite, but rarely possess much of the intermediates (Pettijohn, 1975). A perfectly stoichiometric, ordered dolomite with 50% calcium and 50% magnesium

Figure 1. Dolomite crystals from Trimouns Talc Mine, Luzenac, Ariège, Midi-Pyrénées, France (size 10 x 6.2cm) (Didier Descouens, Wikimedia Commons CC-BY-SA-4.0).

Figure 2. Cristallo Mountain in the Dolomite Mountains of the southeast Alps in northeast Italy (Kallerna, Wikimedia Commons CC-BY-SA-4.0).

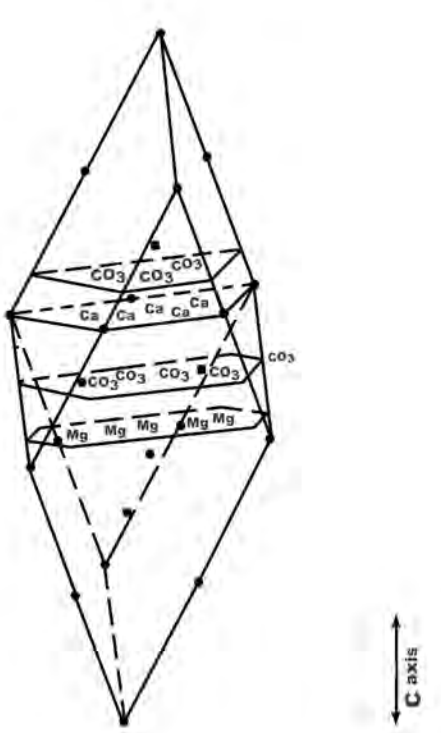

Figure 3. Ordered dolomite crystal (from Morrow, 1982, p. 8; redrawn by Mrs. Melanie Richard).

is rare. There is usually a small percentage more of calcium. The carbonate can have up to 14 mole % more Ca than Mg and still be called a dolomite (Manche and Kaczmarek, 2021). Most dolomites in sedimentary rocks are considered stoichiometric, especially in the Precambrian and Paleozoic, and ordered (Sperber et al., 1984; Manche and Kaczmarek, 2021). Ordered dolomite is the condition in which all calcium ions and all magnesium ions alternate in layers with the CO_3 ion in between (Figure 3). There is little or no mixture of calcium and magnesium ions in any one layer of the dolomite crystal. Dolomite can contain a small percentage of other elements, such as iron.

Many Dolomites Thick and Widespread

Although estimates vary, carbonate rocks make up from 20 to 25% of all sedimentary rocks (Boggs, 2012). Dolomite is more extensive than limestone in the Precambrian (Tucker, 1982). It is also poorly fossiliferous. The abundance of dolomite in the Proterozoic suggests that these rocks were deposited in a different environment from today: "The extraordinary abundance of dolomite in the Proterozoic challenges our understanding of Precambrian marine environments" (Hood et al., 2011, p. 871).

The amount of dolomite varies vertically through the Phanerozoic rock record, once claimed to be more than 50% of all carbonates in the Ordovician to Lower Carboniferous and the Triassic to Mid-Cretaceous of the geological column (Given and Wilkinson, 1987). Limestone dominates the late Paleozoic, the late Mesozoic, and the Cenozoic (Given and Wilkinson, 1987). However, many scientists dispute this trend, claiming the amount of dolomite increases with older age (Zenger, 1989; Manche and Kaczmarek, 2021). Petrash et al. (2017, pp. 559–560) write: "Independent of their origin, the distribution of dolostone in the rock record reflects an apparent monotonic decrease in abundance relative to limestone since the Palaeozoic…."

A conservative estimate of the amount of dolomite is that half the carbonate rocks are dolomite. And if carbonate rocks make up only 20% of all sedimentary rocks, then dolomite would make up about 10% of all sedimentary rocks—no small mystery to account for the origin of dolomite.

Dolomite can be thick and widespread through all the geological column. Fang and Xu (2018, p. 679) state: "Dolomite is one of the most common minerals in sedimentary rocks, ranging from Archean to Holocene." A massive Cambrian dolomite in the Yangtze Gorges area (China) "has a thickness ranging from several hundreds to more than one thousand meters across an area of ~500,000 square kilometers" (Ning et al., 2020, p. 2). The dolomite in the Dolomite Mountains of northern Italy is about 1,000 m thick (McKenzie and Vasconcelos, 2009). Petrash et al. (2017, p. 558) state: "Over the past century a number of models have been developed to explain the vast stratigraphic distribution of authigenic dolomite." Authigenic minerals are minerals formed in place within the sediments and were not transported into the sediments. Uniformitarian scientists consider even large dolomite formations to be authigenic because they believe they originated from a precursor limestone due to replacement (see below). Boggs (2009, p. 401) states that most dolomites are thick and widespread: "Let's return to the problem of explaining the relatively thick, massive, widespread dolomites that constitute most of dolomite in the geological record."

Stoichiometric, Ordered Dolomite Not Forming Today

Secular scientists, being strict uniformitarians, believe that by examining present processes, they should be able to solve the dolomite problem:

> We believe a major insight into the sedimentary dolomite problem can be obtained through detailed study of those environments where the mineral is forming at the present day under earth surface conditions. (Wacey et al., 2007, p. 156)

Dolomite has been discovered in small, warm, saline water since the 1950s, but it is not the volume or type found in the rock record. Dolomite has been discovered at many locations, including a hypersaline lagoon in Kuwait (Gunatilake et al., 1984); saline lakes in western Victoria, Australia (De Decker and Last, 1984); shallow ephemeral lakes in the Coorong region, South Australia (Rosen et al., 1989; Wacey et al., 2007); and in Dohat Faishakh Sabkha, Qatar (Shalev et al., 2021). Not only that, the dolomite is mostly protodolomite, not stoichiometric and not ordered. Other

minerals are also precipitated, such as other carbonates and evaporites (Meister et al., 2013). This has been dubbed the "dolomite problem" (Manche and Kaczmarek, 2021).

Very Strong Kinetic Factors Inhibit the Formation of Dolomite Today

Presently seawater is 10–100 times supersaturated with magnesium (Warren, 2000), yet dolomite is not precipitating today. Land (1998) discovered that dolomite would not precipitate even at 1,000-fold supersaturation at temperatures of 25°C after 32 years. Very strong kinetic barriers have to be overcome. The main kinetic barrier is that Mg ions are surrounded by six water molecules, and it takes much energy to dehydrate the Mg ion so that it can bond: "Dehydration of water from surface Mg^{2+} is most likely the rate-limiting step in the dolomite growth at low temperatures" (Shen et al., 2015, p. 435). The energy barrier is 9.0–10.5 kcal/mole (Shen et al., 2015). Other kinetic inhibitors are the low concentration of dissolved CO_3^{2-} relative to Ca and Mg, the difficulty of ordering, and possibly high dissolved sulfate (Morrow, 1982; Petrash et al., 2017).

Microbes Likely Overcome the Kinetic Barriers Today

So why is dolomite locally forming at all today? It is likely because microorganisms act like catalysts and overcome the kinetic barriers for most precipitation of dolomite (Petrash et al., 2017). It is believed that extracellular polymeric substances excreted by anaerobic microbes cause the catalytic effect (Zhang et al., 2015). Researchers believe that the dolomite produced in the Kuwait lagoon was due to microbial sulfate reduction within the sediments (Gunatilake et al., 1984). The dolomite in Victoria and South Australia is believed to be primary but likely caused by bacteria (De Decker and Last, 1988; Wacey et al., 2007). This has given rise to the microbial theory for dolomite in the sedimentary rocks (McKenzie and Vasconcelos, 2009), but this theory is still under debate (Zhang et al., 2015). For instance, researchers have attempted to apply the microbial model to Ordovician dolomite/limestone laminations from the Appalachian Mountains in Pennsylvania (Fang and Xu, 2018). From the point of view of Flood geology, the microbial theory would be very unlikely, since there would not be enough time for microbes to act to deposit huge volumes of dolomite.

Origin of Dolomite Against Uniformitarianism

Therefore, the origin of dolomite is against uniformitarianism or actualism, the basis upon which almost all geology is interpreted. Hardie (1987, p. 176) states:

> This may explain the strong bias of modern dolomite to form in evaporitic environments, a bias not shared by ancient dolomites (with dolomites, the present is probably not the key to the past).

Ning et al. (2020, p. 1) claim:

> The origin of ancient massive dolostones, i.e. continuous dolostone sequence with a thickness >100 m and a platform-wide distribution, is the key issue of the 'Dolomite Problem' that cannot be clearly demonstrated by any existing dolomitization model individually or sequentially.

Scientists Believe Vast Majority of Dolomite Formed by Replacement

Although scientists think they can solve the dolomite problem by applying uniformitarianism, it is actually because they believe in uniformitarianism that they have a dolomite problem. By applying present processes, they believe dolomite forms at near present-day surface temperatures. Since massive dolomite is not forming today, and presumably in the past with near-present surface temperatures, the majority of geologists have come to believe in the replacement of limestone—for practically all dolomites, whether thick and widespread or local. Primary dolomite is dolomite that precipitates directly from solution, while replacement dolomite, also called dolomitization, is believed to have replaced limestone by high magnesium fluid flow. Tucker (1982, p. 11) states: "The majority of geologists accept that nearly all recent and ancient dolomites are of replacement origin and that primary dolomite is insignificant in the geological record." Kaczmarek and Sibley (2007, p. 424) write:

> Dolomite, $CaMg(CO_3)_2$, is a common mineral in ancient rocks and the thermodynamically stable carbonate phase in modern seawater, yet it is rare in modern marine environments. Why this is so has remained the subject of scientific inquiry of over 200 years. There is very little agreement concerning the details of dolomite formation except that most natural dolomites form at Earth-surface temperatures and pressures (Krauskopf and Bird, 1995). Despite such consensus it has been extremely difficult to synthesize dolomite abiotically at temperatures below 100°C [212°F], even over many years. (Land 1980, 1998)

If widespread, thick dolomite is to be formed by replacement, several conditions must be met. Tremendous fluid flow (Warren, 2000) with a 'pumping mechanism' and enough available Mg must occur. Not only that, the fluid flow must flush out the extra Ca liberated during dolomitization (Boggs, 2009). Furthermore, the porosity and permeability must allow the fluid flow.

The amount of available magnesium would have to be huge (Jones and Rostron, 2000), and the pump and fluid flow must continue for an extended

period of time, since it is estimated that 1,000 units of fluid flow are needed to dolomitize one unit volume (Given and Wilkinson, 1987), and 350 kg of Mg is needed to dolomitize 1 m^3 of limestone with a porosity of 7% (Jones and Rostron, 2000). Of course the fluid flow of magnesium ions decreases away from a potential source—one of the many problems with dolomitizing a huge limestone formation. Such dolomitization needs to occur in the subsurface where temperatures are higher, but porosity and permeability is often reduced by compaction with depth. This is one reason why it supposedly would take millions of years for dolomite to form, according to uniformitarian reckoning. How reasonable is such a replacement process, even given millions of years?

Evidence for Replacement

There is evidence that replacement formed some dolomites. For instance, a close analysis of a 1,600 m-thick carbonate in eastern Spain showed massive dolomite near faults (Yao et al., 2020). It is assumed that hot Mg-rich water issued from the faults to dolomitize the limestone. Further evidence is provided by observations that certain beds are selectively dolomitized, limestone stringers exist within dolostones, and the dolostone ends abruptly. Another indication of replacement is that limestone fossils have been dolomitized, "Dolomitized fossils, ooids, peloids, reefs, and so forth all attest to dolomite replacement of original calcite or aragonite" (Tucker, 1982, p. 7). An ooid is a limestone coating on a small grain or fossil that is usually less than 1 mm in diameter, and they can grow rapidly in the Flood (Oard, 2021a). A peloid is generally another name for a large ooid. Reefs are a matter of interpretation and are likely carbonate banks with fossils.

Such fault-transported dolotomizing fluids were hot. Based on fluid inclusions in the affected rock, the temperature of dolomitization for a Cambrian dolomite in the Western Canadian Sedimentary Basin was 124°–181°C (Koeshidayatullah et al., 2020). It is believed that hot hydrothermal flow in a Triassic carbonate in southern Spain occurred at temperatures of 50–430°C (Mueller et al., 2020). From experimental dolomitization studies, Kaczmarek and Thornton (2017) discovered that cation ordering does not occur below 160°C despite reaction times as great as1,400 hours. Stoichiometry was also correlated with cation ordering.

Researchers sometimes use geochemical indicators, such as oxygen isotope ratios, to arrive at the temperature of dolomitization, but geochemical proxies give equivocal interpretations because of many variables that determine the oxygen isotope ratio. Tucker (1982, p. 10) states: "Many factors affect the fractionation of carbon and oxygen isotopes and determine the isotopic ratios of precipitated minerals." Ryan et al. (2020, pp. 2917–2918) state:

> Geochemical proxy data commonly permit multiple interpretation as to the temperature and chemistry of the dolomitizing fluids and environmental conditions (Machel, 2004), but frequently point to low-temperature near-surface settings…

Davies and Smith (2006, pp. 1655–1656) write that oxygen isotopes understate temperatures for dolomitizing fluid:

> An important corollary of this relationship is that, if the temperature of the fluid forming the dolomite is estimated from $\delta^{18}O$ data assuming a seawater or slightly modified seawater composition (for example, Green and Mountjoy, 2005), an erroneously low fluid temperature may be determined if the precipitating water was a hypersaline brine. This error may be very large…

Oxygen isotope ratios depend upon many variables, such as the oxygen isotope ratio of the fluid, of the carbonate that is replaced, and the temperature of precipitation (Lapponi et al., 2014).

Thus, many researchers believe in the hydrothermal model for dolomitization because of the very hot temperatures required for primary dolomite. Based on a dolomite from northern Spain, Lapponi et al. (2014) determined that hydrothermal dolomitization occurred at temperatures of 80–120°C. So, hot temperatures seem to be required for replacement of limestone:

> The degree of order and the stoichiometry of the dolomite product is a function of both the temperature and length of time of the reaction. Increase in temperature or greater length of time results in a more ordered and stoichiometric dolomite. (Gregg and Sibley, 1984, p. 914)

Temperatures >100°C Needed for Primary Precipitation

There have been numerous experiments forming dolomite in the lab at higher temperatures. It is known that dolomite much more easily precipitates at higher temperatures, higher Mg/Ca ratios, and high Mg supersaturation (Burns et al., 2000). Scientists used to think high sulfate inhibited the formation of dolomite (Wright, 1997), but this has likely been disproven (Zhang et al., 2012). Stoichiometry and ordering increase under these conditions, similar to many dolomites found in the rock record. Hot water is required for primary precipitation of dolomite: "Only at temperatures over about 100°C, well beyond those expected for synsedimentary dolomite formation, can dolomite be readily precipitated in experiments" (Burns et al., 2000, p. 53). Morrow (1982, p. 6) states:

> The absence of a widely accepted theory concerning the chemistry of dolomitization is due primarily to the difficulty in precipitating dolomite from appropriate solutions at temperatures less than 100°C.

Hardie (1987, p. 166) states: "At elevated temperatures the dolomite problem essentially disappears (ordered dolomite can be made in the laboratory in days at 100°C)." Machel and Mountjoy (1986, pp. 185, 190) state:

> …and to date it has not been possible to experimentally precipitate stoichiometric, well ordered dolomite below 100°C. … Beyond about 100°C this kind of diagram is rendered meaningless since almost all know kinetic inhibitors become ineffective.

The temperature should be over 150°C, and the higher the temperature, the faster dolomite precipitates and the more ordered the atomic structure (Arvidson and MacKenzie, 1999; Li et al., 2015). High temperatures are used to study the formation of dolomite in the lab, which should provide a hint to the conditions needed to form dolomite rapidly, such as in the Flood (see below): "High temperature experiments (>100°C) provide insight into the general process of dolomitization…" (Nordeng and Sibley, 1994, p. 191).

The Claim that Many Precambrian Dolomites are Primary

Not only is there more dolomite in the Precambrian than the Phanerozoic by volume percent, but some scientists believe Precambrian dolomites are primary. In fact, early geologists first assumed the dolomite was primary (Glover and Sippel, 1967). Based especially on the Beck Springs Dolomite in the Death Valley region of the United States and the Porsanger Dolomite in Arctic Norway, Tucker (1982, p. 7) states:

> The data suggest that in Precambrian time dolomite was the principal carbonate mineral precipitated from seawater and during diagenesis, and this implies that Precambrian seawater was different from that of the Phanerozoic.

One of Tucker's main evidences is that the replacement destroys the limestone fabric, but this has been questioned (Ricketts, 1982; Zenger, 1982).

Dolomite Shows Early Floodwaters Were Very Hot

It is possible that some Precambrian dolomite is from the very early Flood (Oard and Reed, 2017; Oard, 2021b). The large scale of some dolomites in the rock record matches the scale of sedimentation expected in the Flood. Because of the short time available for forming thick, widespread dolomites, many dolomites are likely primary. Replacement dolomites would be localized near faults, as in the Ordovician section in the Williston Basin, by hydrothermal flow of very hot water. Precipitation of dolomite requires water over 100°C. This would have been early in the Flood, when some Precambrian and all Paleozoic rocks were deposited. Since limestone was also precipitated, this primary dolomite formation likely occurred on a local to regional scale, and mainly in basins and rifts. The increasing proportion of limestone over time suggests increasingly cooler water, possibly because deposited sediments insulated the Floodwaters from deep, hot rocks. It is also possible that there was more mixing with cooler seawater.

Implications for Flood Models

Local, very hot early Floodwaters have several implications (Oard, 2021b). Dolomite may be a criterion for determining the pre-Flood/Flood boundary. There does not seem to be any significant change in dolomite/limestone ratios from the Precambrian up into the Paleozoic, suggesting that these rocks are all Flood rocks. Moreover, the high percentage of dolomite in the Precambrian and the consistency through the late Paleozoic would indicate many dolomites were deposited in the Flood, not before. Since dolomite even occurs in the Archean, it could imply that some Flood rocks even extend into the Archean. Such a deduction is reinforced by raindrop imprints, black shale, and impacts in the Precambrian that continue up into the Paleozoic (Oard, 2013, 2014).

A Flood model must account for hot water early in the Flood. Very hot water could have resulted from several mechanisms such as the eruption of the "fountains of the great deep," volcanism, tectonic friction, and impacts. The early hot temperatures, especially in the developing Precambrian and Paleozoic basins and rifts, could account for the present-day geothermal gradient of 25–30°C/km (Fridleifsson et al., 2008) in sedimentary rocks of the subsurface. The subsurface was not necessarily heated by millions of years of accumulating overburden, as uniformitarian scientists believe, but by the deposition of sediments in hot water early in the Flood. Such hot water temperatures, plus overburden, could also account for the rapid origin of coal and oil in the Flood.

Conclusions

Dolomite, a common rock, has been a uniformitarian mystery for over 200 years. It is uniformitarianism that creates the "dolomite problem." Dolomite cannot be deposited under normal surface temperatures because of very strong kinetic barriers. However, dolomite is being precipitated locally today, likely because microbes catalyze the kinetic factors. But this dolomite is not stoichiometric or ordered like practically all sedimentary dolomite. Experiments have shown that very hot temperatures also overcome the kinetic barriers for primary precipitation. But uniformitarianism would have us believe that mean water temperatures were never very hot. Therefore, they believe dolomite forms by replacement of limestone, but this also requires hydrothermal flow through

faults. It is also highly unlikely that replacement dolomitization can account for all of the thick, widespread layers documented throughout the world.

The short timescale of the Flood requires formation of primary dolomite. This implies that very early Floodwaters were very hot locally and probably were present in rifts and basins. Since there is no significant change in the percentage of dolomite, as well as other geological variables, through at least the early Paleozoic, it is unlikely that late Neoproterozoic and Precambrian/Cambrian boundaries mark a universal pre-Flood/Flood boundary.

References

Arvidson, R.S., and F.T. MacKenzie. 1999. The dolomite problem; control of precipitation kinetics by temperature and saturation state. *American Journal of Science* 299(4): 257–288.

Boggs, Jr., S. 2009. *Petrology of Sedimentary Rocks*, second edition. Cambridge University Press, Cambridge, UK.

Boggs, Jr., S. 2012. *Principles of Sedimentology and Stratigraphy*, fifth edition. Prentice Hall, New York, NY.

Burns, S.J., J.A. McKenzie, and C. Vasconcelos. 2000. Dolomite formation and biogeochemical cycles in the Phanerozoic. *Sedimentology* 47(Suppl. 1): 49–61.

Davies, G.R., and L.B. Smith, Jr. 2006. Structurally controlled hydrothermal dolomite reservoir facies: An overview. *AAPG Bulletin* 90(11): 1641–1690.

De Decker, P., and W.M. Last. 1988. Modern dolomite deposition in continental, saline lakes, western Victoria, Australia. *Geology* 16(1): 29–32.

Dott, Jr., R.H. 2003. The importance of eolian abrasion in supermature quartz sandstones and the paradox of weathering on vegetation-free landscapes. *Journal of Geology* 111(4): 387–405.

Fang, Y., and H. Xu. 2018. Study of an Ordovician carbonate with alternating dolomite-calcite laminations and its implications for catalytic effects of microbes on the formation of sedimentary dolomite. *Journal of Sedimentary Research* 88(6): 679–695.

Fridleifsson, I.B., R. Bertani, E. Huenges, J.W. Lund, A. Ragnarsson, and L. Ryback. 2008. The possible role and contribution of geothermal energy to the mitigation of climate change. In Hoymeyer, O., and T. Triton (editors), *Proceedings of IPCC Scoping Meeting on Renewable energy Sources*, pp. 59–80. Intergovernmental Panel on Climate Change (IPCC), Lübeck, Germany.

Given, R.K., and B.H. Wilkinson. 1987. Dolomite abundance and stratigraphic age: Constraints on rates and mechanisms of Phanerozoic dolostone formation. *Journal of Sedimentary Petrology* 57(6): 1068–1078.

Glover, E.D., and R.F. Sippel. 1967. Synthesis of magnesium calcites. *Geochimica et Cosmochimica Acta* 31(4): 603–613.

Gregg, J.M., and D.F. Sibley. 1984. Epigenetic dolomitization and the origin of xenotopic dolomite texture. *Journal of Sedimentary Petrology* 54(3): 908–931.

Gunatilake, A., A. Saley, A. Al-Temeemi, and N. Nassar. 1984. Occurrence of subtidal dolomite in a hypersaline lagoon, Kuwait. *Nature* 311(5985): 450–452.

Hardie, L.A. 1987. Perspectives dolomitization: A critical view of some current views. *Journal of Sedimentary Petrology* 57(1): 166–183.

Hood, A.V.S., M.W. Wallace, and R.N. Drysdale. 2011. Neoproterozoic aragonite-dolomite seas? Widespread marine dolomite precipitation in Cryogenian reef complexes. *Geology* 39(9): 871–874.

Jones, G.D., and B.J. Rostron. 2000. Analysis of fluid flow constraints in regional-scale reflux dolomitization: Constant versus variable-flux hydrogeological models. *Bulletin of Canadian Petroleum Geology* 48(3): 230–245.

Kaczmarek, S.E., and D.F. Sibley. 2007. A comparison of nanometer-scale growth and dissolution features on natural and synthetic dolomite crystals: Implications for the origin of dolomite. *Journal of Sedimentary Research* 77(5): 424–432.

Kaczmarek, S.E., and B.P. Thornton. 2017. The effect of temperature on stoichiometry, cation ordering, and reaction rate in high-temperature dolomitization experiments. *Chemical Geology* 468:32–41.

Koeshidayatullah, A., H. Corlett, J. Stacey, P.K. Swart, A. Boyce, H. Robertson, F. Whitaker, and C. Hollis. 2020. Evaluating new fault-controlled hydrothermal dolomitization models: insights from the Cambrian dolomite, Western Canadian Sedimentary Basin. *Sedimentology* 67(6): 2945–2973.

Land, L.S. 1998. Failure to precipitate dolomite at 25°C from dilute solution despite 1000-fold oversaturation after 32 years. *Aquatic Geochemistry* 4:361–368.

Lapponi, F., T. Bechstädt, M. Boni, and D.A. Banks. 2014. Hydrothermal dolomitization in a complex geodynamic setting (Lower Palaeozoic, northern Spain). *Sedimentology* 61(2): 411–443.

Li, W., B.L. Beard, C. Li, H. Xu, and C.M. Johnson. 2015. Experimental calibration of Mg isotope fractionation between dolomite and aqueous solution and its geological implications. *Geochimica et Cosmochimica Acta* 157:164–181.

Machel, H.G., and E.W. Mountjoy. 1986. Chemistry and environments of dolomitization – A reappraisal. *Earth Science Reviews* 23(3): 175–222.

McKenzie, J.A., and C. Vasconcelos. 2009. Dolomite Mountains and the origin of the dolomite rock of which they mainly consist: Historical developments and new perspectives. *Sedimentology* 56(1): 205–219.

Manche, C.J., and S.E. Kaczmarek. 2021. A global study of dolomite stoichiometry and cation ordering through the Phanerozoic. *Journal of Sedimentary Research* 91(5): 520–546.

Meister, P., J.A. McKenzie, S.M. Bernasconi, and P. Brack. 2013. Dolomite formation in the shallow seas of the Alpine Triassic. *Sedimentology* 60(1): 270–291.

Morrow, D.W. 1982. Diagenesis 1. Dolomite—Part 1: The chemistry of dolomitization and dolomite precipitation. *Geoscience Canada* 9(1): 5–13.

Mueller, M., et al. 2020. Testing the preservation potential of early diagenetic dolomites as geochemical archives. *Sedimentology* 67(2): 849–888.

Ning, M., X. Lang, K. Huang, C. Li, T. Huang, H. Yuan, C. Xing, R. Yang, and B. Shen. 2020. Towards understanding the origin of massive dolostone. *Earth and Planetary Science Letters* 545(16403): 1–8.

Nordeng, S.H., and D.F. Sibley. 1994. Dolomite stoichiometry and Ostwald's step rule. *Geochimica et Cosmochimica Acta* 58(1): 191–196.

Oard, M.J. 2013. Raindrop imprints and the location of the pre-Flood/Flood boundary. *Journal of Creation* 27(2): 7–8, https://creation.com/images/pdfs/tj/j27_2/j27_2_7–8.pdf.

Oard, M.J. 2014. Precambrian impacts and the Genesis Flood. *Journal of Creation* 28(3): 99–105, https://creation.com/precambrian-impacts-and-the-genesis-flood.

Oard, M.J. 2021a. Ooids grew rapidly in the Flood. *Journal of Creation* 36(1): 13–14.

Oard, M.J. 2021b. A more likely origin of massive dolomite deposits. *Journal of Creation* 36(1): 3–5.

Oard, M.J., and J.K. Reed. 2017. *How Noah's Flood Shaped Our Earth*. Creation Book Publishers, Powder Springs, GA.

Petrash, D.A., O.M. Biali, T.R.R. Bontognali, C. Vasconcelos, J.A. Roberts, J.A. McKenzie, and K.O. Konhauser. 2017. Microbially catalyzed dolomite formation: From near-surface to burial. *Earth-Science Reviews* 171:558–582.

Pettijohn, F.J. 1975. *Sedimentary Rocks*, third edition. Harper and Row, New York, NY.

Ricketts, B.D. 1982. Comments and reply on 'Precambrian dolomites: Petrographic and isotopic evidence that they differ from Phanerozoic dolomites,' Comment. *Geology* 10(12): 663.

Rosen, M.R., D.E. Miser, M.A. Starcher, and J.K. Warren. 1989. Formation of dolomite in the Coorong region, South Australia. *Geochimica et Cosmochimica Acta* 53(3): 661–669.

Ryan, B.H., S.E. Kaczmarek, and J.M. Rivers. 2020. Early and pervasive dolomitization by near-normal marine fluids: New lessons from an Eocene evaporative setting in Qatar. *Sedimentology* 67(6): 2917–2944.

Shalev, N., T.R.R. Bontognali, and D. Vance. 2021. Sabkha dolomite as an archive for the magnesium isotope composition of seawater. *Geology* 49(3): 253–257.

Shen, Z., J. Szlufarska, P.E. Brown, and H. Xu. 2015. Investigation of the role of polysaccharide in the dolomite growth at low temperature by using atomistic simulations. *Langmuir* 31(38): 435–442.

Sperber, C.M., B.H. Wilkinson, and D.R. Peacor. 1984. Rock composition, dolomite stoichiometry, and rock/water reactions in dolomitic carbonate rocks. *The Journal of Geology* 92(6): 609–622.

Tucker, M.E. 1982. Precambrian dolomites: Petrographic and isotopic evidence that they differ from Phanerozoic dolomites. *Geology* 10(1): 7–12.

Wacey, D., D.T. Wright, and A.J. Boyce. 2007. A stable isotope study of microbial dolomite formation in the Coorong Region, South Australia. *Chemical Geology* 244(1–2): 155–174.

Warren, J. 2000. Dolomite: Occurrence, evolution and economically important associations. *Earth-Science Reviews* 52(1): 1–81.

Wright, D.T. 1997. An organogenic origin for widespread dolomite in the Cambrian Eilean Dubh Formation, northwestern Scotland. *Journal of Sedimentary Research* 67(1): 54–64.

Yao, S., E. Gomez-Rivas, J.D. Martín-Martín, D. Gomez-Gras, A. Travé, A. Griera, and J.A. Howell. 2020. Fault-controlled dolostone geometries in a transgressive—regressive sequence stratigraphic framework. *Sedimentology* 67(6): 3290–3316.

Zenger, D.H. 1982. Comments and reply on 'Precambrian dolomites: Petrographic and isotopic evidence that they differ from Phanerozoic dolomites,' COMMENT. *Geology* 10(12): 662.

Zenger, D.H. 1989. Dolomite abundance and stratigraphic age: Constraints on rates and mechanisms of Phanerozoic dolostone formation—discussion. *Journal of Sedimentary Petrology* 59(1): 162–164.

Zhang, F., H. Xu, H. Konishi, E.S. Shelobolina, and E.E. Roden. 2012. Polysaccharide-catalyzed nucleation and growth of disordered dolomite: A potential precursor of sedimentary dolomite. *American Mineralogist* 97(4): 556–567.

Zhang, F., H. Xu, E.S. Shelobolina, H. Konishi, B. Converse, Z. Shen, and E.E. Roden. 2015. The catalytic effect of bound extracellular polymeric substances excreted by anaerobic microorganisms on Ca-Mg carbonate precipitation: Implications for the "dolomite problem." *American Mineralogist* 100(2–3): 483–494.

Creation Research Society Quarterly 2022 59:29–38

Latent Heat Could Solve Accelerated Nuclear Decay's Heat Problem—Part 1

Barbara S. Helmkamp*

Abstract

A phase change for the condensed matter comprising large nuclei is proposed as a heat sink during an episode of accelerated nuclear decay, being particularly relevant to the formation of radiohalos. The proposed nuclear phase change would occur in ^{206}Pb nuclei, being the final stable progeny in the ^{238}U decay chain. With each cascade of decays, the latent heat for this presumed first order phase transition would be taken from (via heat transfer, generically invoked), and thereby continuously cool, the radio-center's immediate environment wherein the thermal energy is deposited. Arguing by analogy with atomic/molecular systems, the plausibility of providing sufficient cooling (absorbing enough energy) by a phase change is explored. The lower entropy phase for large, unstable nuclei during accelerated decay might consist of alpha clusters as compared with primarily nucleon pairings for the normal phase. The nuclear phase change would occur with/at the switch from unstable parent isotope to stable daughter in accordance with the dependence of a hypothetical nuclear phase diagram on the decreased strength of the nuclear force (a shallower nuclear potential) for unstable nuclei characterizing an episode of accelerated decay as compared with normalcy, as will be explained in Part 2.

Key Words: radiohalo, heat sink, latent heat, cooling, phase diagram, accelerated decay, uranium, polonium, nuclear decay, alpha cluster, condensed matter

Editorial Comment: Neither the reviewers, the physics editor, nor the author of this article were fully satisfied with the explanation of how heat could be transferred from the surroundings into the nucleus, but it was decided to leave that for future research.

* Barbara S. Helmkamp, Ph.D. Physics, B.S. Eng. Physics, Kepler Education consortium, Parker, CO, barbara.helmkamp@gmail.com

Accepted for publication July 14, 2022

Introduction: A Change of Phase for the Nucleus

As a novel solution to the heat problem associated with accelerating nuclear decay, herein described in the context of radiohalo production during an episode of accelerated decay, a spontaneous endothermic process, occurring inside each new ^{206}Pb nucleus at the culmination of the ^{238}U decay chain,[1] is proposed. That is, an energy-absorbing phase change occurs in the newly formed lead nuclei at the radio-center thereby removing much of the heat just produced by the preceding chain of decays. The requisite latent heat for the phase change is taken[2] at Series' End from the adjacent rock where it is being deposited in rapid fire at a ring's radial distance away. This process is akin to an entropy-increasing first-order phase transition between two condensed states of matter in (nonnuclear) chemistry like the melting of an ice cube ($\Delta G < 0$, $\Delta H > 0$, $\Delta S > 0$), here due to an abrupt change in the nuclear force (the mean field describing the nuclear potential) when the nuclide switches (crosses over) from being unstable to being stable with the last alpha decay in the uranium series (^{210}Po $\rightarrow$ ^{206}Pb + α).[3] It is assumed (or asserted) that *only unstable nuclei are significantly affected by the change in the nuclear force* (residual strong force that holds the nucleus together) *responsible for accelerated decay*. That is, the phase of stable nuclei remains a condensed fluid, consistent with the Liquid Drop Model and current scientific consensus, regardless of accelerated nuclear decay, while the unstable nuclei undergoing accelerated decay find themselves in an unknown lower entropy state. This condition is necessary for the proposed solution to work, as will become apparent to the reader, and it is plausible that a change in the strong force would only affect a particular class of nuclides, like the unstable ones, given the inherent complications of few-body quantum physics. While every nuclide is its own system with significant dependence on size (neutron and proton counts) affecting various properties, classes of nuclides do share behaviors—like stability vs. instability against alpha or beta decay, low- vs. high-binding energy per nucleon, being symmetrical vs. deformed, etc.—all of which point to distinctions in how the strong force plays out in determining nucleon interactions and nuclear phase.

The Conundrum of Radiohalos

A radiohalo is a microscopic[4] heat scar commonly found in granitic rocks (within the black biotite specks, typically) that depicts the alpha decays in a radioactive decay series by a set of concentric spherical shells, or rings, in cross-section.[5] A hundred million to a billion parent isotopes in the halo's radio-center[6] have to decay to cause the discoloration that makes a fully developed radiohalo. On the low end of counts the outer rings are too faint to readily see while on the high end the inner rings are blurred from too much radiation damage. The only decay-series parent isotopes with high enough (and concentrated enough) natural abundances in Earth's rocks to make, or to have made, radiohalos appear to be uranium-238 and thorium-232. Yet polonium-218, polonium-214, and polonium-210 radiohalos are also found, and herein lies the conundrum because a fully naturalistic explanation for these halos and their radio-sources is lacking (Gentry, 1992, pp. 30–31).

What of polonium halos? All polonium being radiogenic and short-lived, if there were any primordial polonium, it would have decayed away within a few years of its creation. Among polonium's naturally occurring isotopes (decay progeny from ^{238}U, ^{237}Np, ^{235}U, and ^{232}Th), the ^{210}Po isotope is longest-lived by far with a half-life of 138 days, all the others having half-lives of 3 minutes or less.[7] Thus, polonium is mainly found as ^{210}Po dispersed in uranium ores[8] at about mg per metric ton (1 part in 10^{10}), uranium being 99.3% ^{238}U (0.7% ^{235}U) and the ^{210}Po isotope being ^{238}U's last unstable daughter in the uranium series.

At first take, this would seem to confine polonium halos to creation rock (Gentry, 1992, pp. 33–37), yet they are found spanning the geologic column chiefly in granitic plutons (melts or remelts) from Precambrian through Mesozoic (Snelling, 2005) and even Tertiary[9] but also in coalified wood from the Colorado Plateau (Gentry et al., 1976). Importantly, polonium

1 Or, occurring inside each new ^{208}Pb nucleus at the culmination of the ^{232}Th decay chain.

2 Just how the thermal energy gets into the nucleus to affect the phase change is unknown.

3 Or, with the last alpha decay in the thorium series (^{212}Po $\rightarrow$ ^{208}Pb + α).

4 Uranium radiohalos in granitic rocks are about 70 microns in diameter.

5 The leaves comprising biotite (mica) provide natural translucent thin sections for viewing radiohalos in cross-section under an ordinary optical microscope.

6 The radio-center approximates a point source, with rings differentiated, if it is smaller than the ring spacing.

7 Even the longest-lived of *all* polonium isotopes ^{209}Po (produced by proton bombardment of bismuth in a particle accelerator) has a half-life of only 125 years.

8 Ores include uraninite, UO_2, also known as pitchblende, as well as uranothorite (Th,U) SiO_4.

9 Radiohalos are ubiquitous in granitic rocks up through the Mesozoic while there is only one Tertiary halo-bearing sample in the *RATE* data set; however, the latter is from an index granite making its location in the geologic column relatively certain.

halos come in only three kinds: ^{218}Po, ^{214}Po, and ^{210}Po which are uranium-238's three polonium daughters. But any primordial ^{218}Po halos or primordial ^{214}Po halos—one of the latter being famously pictured on a book jacket (Gentry, 1992)—would not have survived their first ring's own heat production (6.0 MeV per decay and 7.7 MeV per decay, respectively, times ~500 million decays)[10] given the near-adiabatic heating due to their very short half-lives (3 min and 164 μs, respectively). Incidentally, the same goes if a radio-center's worth of ^{218}Po or ^{214}Po abruptly materialized in a host rock at any time (for any reason) in Earth's history: the halo would not survive its own heat. Radiohalos cannot survive high temperatures (≳150°C in biotite) because the rings of radiation damage, as assemblages of scorch marks, get annealed away (if not vaporized in production!). It is not enough only to explain the presence of polonium halo source isotopes.

Aside from the heat problem, the conundrum of the polonium halo finds resolution in the *RATE*[11] model (Snelling, 2005, pp. 152–174) in which polonium halos are really just partial uranium halos. That is, the U-halo's trailing rings—the rings due to emissions by polonium isotopes—are merely displaced from the origin U-halo(s). This one-atom-at-a-time displacement arguably occurred by the aqueous transport of the gaseous radon-222 daughter ($t_{½}$ = 3.8 d), some of which escapes the zircon (housing the uranium inclusion) into the surrounding biotite (mica) before decaying into polonium-218. The essential moving water (between flakes of mica and through microfractures) was chemically produced as the host granite crystallized with the flow slowing to a halt once the temperature dropped below ~75°C. This scenario presents a severely short time window of about five days[12] (at most) corresponding to a temperature window 150°C <T <75°C for radiohalos (uranium as well as polonium) to have formed.

This model presupposes (or requires) a Flood-Year episode of accelerated decay because *the U-halos and Po-halos necessarily formed simultaneously* despite their spectacularly disparate half-lives. During such episode, it is understood that the longest-lived, least-unstable isotopes like uranium-238 ($t_{½}$ = 4.5 Ga) experience the greatest increase in decay rate (by a billionfold) while the shortest-lived isotopes like polonium-214 ($t_{½}$ = 164 μs) are nominally affected, and the alpha particle energies (ring radii) remain essentially unchanged regardless of half-life. Being named for the longest half-life (primordial) isotope in the chain, alpha decay rates in a series tend to increase (half-lives decrease) until the chain culminates with the stable isotope[13] though there can be hiccups in this trend (preceding the grand one at Series' End) like there is at polonium-210 in the uranium series.[14] Regardless, the final alpha decays for the uranium series are the three poloniums (as are the two poloniums for the thorium series), all of which would experience negligibly small changes in their half-lives (while preserving ring order) when decay rates are accelerated.

Just as importantly though not generally put in such terms, this model implicitly presupposes (or requires) a commensurate and concurrent cooling (energy absorption) that allows each halo to survive its own heat, for each decay necessarily generates frictional heat as an alpha particle comes to a stop, scorching and discoloring the host rock (e.g., the mica in granitic rocks) along its track in the random direction it goes off (isotropically) but primarily at a stopping distance where the linear energy transfer peaks in accordance with its kinetic energy. In principle, the alpha particle's kinetic energy is determined from the almost-eigenstate of the quasi-bound alpha particle[15] inside the parent nuclide.

10 Not that rings form consecutively—rather, they develop simultaneously from multitudinous individual cascades—but by way of categorizing heat contributions.

11 *RATE* stands for *Radioisotopes and the Age of the Earth*, referencing the significant young-Earth creationist research initiative that published results in 2005.

12 Mean lifetime is ~1.4 times greater than half-life: $\tau = \frac{t_{½}}{\ln 2}$. So, 5 days is used instead of 4.

13 The stable isotope might be thought of as having infinite half-life as the limiting case.

14 Uranium series with its eight alpha decay half-lives:

$^{238}_{92}$U @ 4.5×10^9 y | $^{234}_{90}$Th, $^{234}_{91}$Pa | $^{234}_{92}$U @ 2.5×10^5 y |

$^{230}_{90}$Th @ 7.5×10^4 y | $^{226}_{88}$Ra @ 1600 y | $^{222}_{86}$Rn @ 3.8 d |

$^{218}_{84}$Po @ 3 m | $^{214}_{82}$Pb, $^{214}_{83}$Bi | $^{214}_{84}$Po @ 164 μs | $^{210}_{82}$Pb, $^{210}_{83}$Bi |

$^{210}_{84}$Po @ 138 d | $^{206}_{82}$Pb @ ∞ |.

Thorium series with its six alpha decay half-lives:

$^{232}_{90}$Th @ 1.4×10^{10} y | $^{228}_{88}$Ra, $^{228}_{89}$Ac | $^{228}_{90}$Th @ 1.9 y |

$^{224}_{88}$Ra @ 3.7 d | $^{220}_{86}$Rn @ 55.6 s | $^{216}_{84}$Po @ 144 ms |

$^{212}_{82}$Pb , $^{212}_{83}$Bi | $^{212}_{84}$Po @ 299 ns | $^{208}_{82}$Pb @ ∞ |.

Beta decay half-lives (not given here) are typically but not always intermediate in value between the sandwiching alpha decay half-lives. Alpha decay half-lives were found from the Decay Radiation Search at the National Nuclear Data Center https://www.nndc.bnl.gov/nudat3/indx_dec.jsp

15 An alpha particle is a helium nucleus consisting of two protons and two neutrons, denoted $^{4}_{2}\mathrm{He}$ or $^{4}_{2}\alpha$, where the preceding subscript is the atomic number Z (number of protons) and the preceding superscript is the mass number A (number of nucleons or protons plus neutrons), generically $^{A}_{Z}X$. A beta (minus) particle is an electron, denoted $^{-1}_{0}\beta$ or $^{-1}_{0}e$ or β^-, or simply β.

However, the very same heat that makes the halo by scarring the rock must necessarily prevent and/or undo the discoloration (scarring) unless it can dissipate into the surroundings faster than it is produced such that the host rock's temperature in the immediate vicinity of the halo remains below the annealing temperature ($T \lesssim 150$°C in biotite). During an episode of accelerated decay, per the transport-via-escaping-radon model for polonium (alongside uranium) halo formation, the vast majority of this heat cannot possibly get away in time given the time scales involved, with at least a hundred million decays occurring inside a 35-micron radius (^{214}Po's ring) in a matter of days. Thus, adiabatic heating gives the right order of magnitude, not just an upper limit, for the increase in temperature experienced by a halo *in the absence of any cooling*. Moreover, because natural annealing of radiohalos in samples taken from deep drill holes is found to be consistent with the temperature-depth profile for the drill holes (Laney and Laughlin, 1981), with the alpha particle tracks either surviving to the present or being erased accordingly, *as though no local heat surge from accelerated nuclear decay occurred*, the cooling (energy absorption) must be nearly commensurate with each halo's frictional heat generation. In other words, radiohalos act like there is no heat problem associated with accelerated decay.

Simply by energy conservation, such near-adiabatic heating requires a near-commensurate cooling of ~40–50 MeV per decay cascade;[16] otherwise, halos cannot have formed much less persist once formed. The adiabatic temperature rise is at least 1800°C for one U-halo or 180°C for one ^{210}Po halo where $\Delta T \sim Q/(\rho V c) \times 10^8$ for a sphere of biotite ($\rho = 2.9$ g/mL; $c = 0.88$ J/g°C; $V = \frac{4}{3}\pi r^3$) using polonium-214's ring radius ($r = 35$ μm) and heat $Q = 52$ MeV per decay cascade for a ^{238}U radio-center or $Q = 5.4$ MeV for a ^{210}Po radio-center (1 MeV ≈ 1.6 10^{-13}J; 1 μm^3 = 10^{-12} mL). Arguably the temperature increase could be 5–10 times greater, as much as 18,000°C for a fully developed U-halo. For comparison, the adiabatic temperature-rise for a typical pluton undergoing accelerated decay, encompassing *all* radioactive decay therein, has been estimated at 22,400 K (Snelling, 2005, p. 184). In other words, accelerating nuclear decay by upwards of 100 million-fold presents no small heat problem to solve (Worraker, 2018).

A Change of Phase for the Nucleus, Continued

Some kind of Liquid-Liquid Phase Transition for the lead nuclei, from a lower entropy (lower density?)[17] state where alpha particle clusters would dominate due to stronger many-body forces, to a higher entropy (higher density?) state mainly consisting of nucleon spin-antispin pairs, seems most likely. But the relative latent heat for atomic/molecular systems undergoing such phase transitions (like water) is too small to translate into the needed amount of cooling for radiohalos to have formed. Rather, the latent heat for the unknown phase transition in lead nuclei is compared to the latent heat of melting for a salt (e.g., *NaCl*), as justified later in this paper and continued in Part 2.

For a ^{238}U nuclide undergoing accelerated decay, it seems quite plausible that all eight departing alpha particles ($pnnp$ or $n_\beta nnn_\beta$)[18] are pre-formed, or pre-forming, as such in the nucleus, instead of just one at a time, with these clusters of nucleons—32 nucleons as 22 neutrons (n) and 10 protons (p) in order of decay as: $pnnp$, $n_\beta nnn_\beta$, 4 × $pnnp$, $n_\beta nnn_\beta$, $n_\beta nnn_\beta$—occupying quasi-bound alpha particle states above a stable ^{206}Pb-like core. In modeling alpha decay/tunnelling, half-life is often underpredicted, perhaps by about 2% to 20%, meaning that some hindrance factor is not accounted for in the basic formulation (Duarte and Siegel, 2010). Called the preformation factor, the discrepancy is interpreted as the *percentage of time* the outgoing alpha particle's composite quad of nucleons is an alpha particle versus not; but equivalently, the preformation factor could be seen as the percentage of the parent isotope's nucleon quads that are alpha particles *at any given time*.

Recent evidence for the tetraneutron as an extremely short-lived entity outside the nucleus makes a quad of sometimes-neutrons ($n_\beta nnn_\beta$) clustering in the nucleus seem not unreasonable (Kisamori et al., 2016; Duer et al., 2022). An excess of neutrons at the surface of neutron-heavy nuclei, termed the neutron skin, is also confirmed by experiment: the neutron skin thickness was recently measured for ^{208}Pb as 0.28 fm (Adhikari et al., 2021) which translates into about 20 of its 208 nucleons, 126 of which are neutrons ($A - Z = 208 - 82$).[19] Applying a comparable ratio of skin thickness to nuclear radius

16 The total energy released in the uranium series ($^{238}_{92}\mathrm{U} \rightarrow {}^{206}_{82}\mathrm{Pb} + 8\alpha + 6\beta^-$) is 51.7 MeV including the kinetic energies of the alphas and betas (with their neutrinos) as well as nuclear recoil; its alpha particle energies subtotal 43.7 MeV. For comparison, the thorium series ($^{232}_{90}\mathrm{Th} \rightarrow {}^{208}_{82}\mathrm{Pb} + 6\alpha + 4\beta^-$) is 42.6 MeV with an alpha subtotal of 37.5 MeV.

17 The low-density liquid (LDL) phase has lower entropy and the high-density liquid (HDL) phase higher entropy because the Liquid-Liquid Phase Transition (LLPT) is observed specifically for water-like liquids for which their solid phase floats in its own liquid; that is, water-ice floats.

18 n_β represents the *proton-plus-electron* that replaces a neutron (n) in beta decay ($n \rightarrow p + \beta^- + \bar{\nu}_e$), the idea being that the neutron is in some sense already a proton (p) plus electron (β^-) prior to decay.

19 Again, Z is the element's atomic number or proton count while A is the isotope's mass number or nucleon count.

to the slightly bigger ^{238}U translates into 22 of its 238 nucleons, 146 of which are neutrons ($A - Z = 238 - 92$).[20] Interestingly, this is precisely the number of neutrons lost in the chain of decays from ^{238}U to ^{206}Pb. Necessarily, there are no occupied positive energy (quasi-bound or resonant) states for lead's *stable* isotopes (including ^{206}Pb at the end of the uranium series, ^{207}Pb at the end of the actinium series, and ^{208}Pb at the end of the thorium series, besides primordial non-radiogenic ^{204}Pb)[21] while the 22 beta decay neutrons in ^{238}U (when acting like nucleons in spin-antispin pairs instead of alpha particles) would be resonances above the neutron well.[22] The existence of such surface neutrons in the energy sense is supported by the apparent existence of surface (skin) neutrons in the geometric sense based on scattering experiments.

So, like ice cubes cooling a beverage by heat transfer from the beverage (as the cube's surroundings) to the ice, thereby melting the cubes, *here the alpha clusters comprising an unstable nucleus undergoing accelerated decay would disassemble into nucleon pairs and sometimes dimers once they find themselves in a stable nucleus*. As a phase transition, presumed to be first-order,[23] this would absorb its latent entropic heat from the surroundings, both the local rock matrix and any connate water in microfractures, thereby making the radio-center (i.e., its radiation-source nuclides) also a heat sink (i.e., its end-product nuclides) *as a natural response to accelerated nuclear decay*. So, the radio-center's unstable nuclei are the source of the alpha particles, causing the surrounding rock matrix to heat up in stopping them, and the stable lead nuclei absorb the heat. Though radiohalos are the focus here, this energy absorption is not limited to radio-centers (concentrations of uranium or thorium in settings like a zircon which contain their progeny): each newly formed stable nucleus at Series' End (^{206}Pb for the uranium series and ^{208}Pb for the thorium series) would be a heat sink individually during an episode of accelerated decay whether the uranium or thorium is dispersed throughout the rock or concentrated as inclusions in zircons—though the energy balance argument would not necessarily apply.

Just how the transfer of heat to the nucleus, or absorption of energy by it, would occur is a subject for future research. While thermal conduction, per kinetic molecular theory, is understood to occur by momentum transfer between atoms/molecules, and absolute temperature describes this motion statistically as a mean kinetic energy,[24] how the nucleons that comprise an atom's nucleus might couple to this molecular motion to effect the heat transfer is unknown. But the thermal energy (as blackbody radiation?)[25] must be able to get back into the nucleus. For one, it must be in the right energy range to be absorbed by lead nuclei (such as occurs with vibrational levels of small spacing) and the resulting nuclear excitation effects the phase change (Chaffin, 2022). But for the present, heat transfer is invoked without a specific mechanism offered for consideration, though the author welcomes ideas in this regard. This important issue aside, to further explain and justify the idea of a phase change for lead nuclei being a heat sink during an episode of accelerated nuclear decay—where an unknown phase comprised of alpha clusters reverts to the normal state as a condensed fluid of nucleon pairs and sometimes dimers—requires reviewing some basic nuclear chemistry and noting which model(s) of the nucleus make successful predictions for stable vs. unstable nuclides.

Nuclear Chemistry: Quantum Shells or Liquid Drop?

The success of the quantum *nuclear shell model*, as a mean field approximation, is highly surprising: how can one member (proton or neutron) of a *few-body* system of nucleons act like an independent particle moving in the field made by the remaining particles; that is, by the one-fewer few-body system? Yet the nuclear shell model rightly predicts the nuclear magic numbers

20 While neutron-heavy nuclei are deformed (prolate) spheroids and the skin might be tougher (denser) than the interior, uniform density and spherical symmetry are assumed for simplicity, the quoted value of 0.28 fm for ^{208}Pb being, in effect, an average. Thus, $\frac{\Delta V}{V} \approx 3\frac{\Delta R}{R}\left(1 - 2\frac{\Delta R}{R}\right) = 9.4\%$ with radius $R \approx 1.3\,A^{1/3}$ fm $= 1.3(208)^{1/3}$ fm $= 7.7$ fm.

21 Interestingly, lead is the last element in the Periodic Table with stable isotopes, though the very nearly stable $^{209}_{83}Bi$ with its magic number of 126 neutrons lies between lead ($Z = 82$) and polonium ($Z = 84$).

22 The nuclear shell model is depicted as side-by-side neutron and proton potentials yielding the magic numbers separately when counting neutrons vs. protons. The neutron well is deeper than the proton well for neutron-heavy nuclides, and there is a Coulomb barrier for the proton well but not for neutron (neutrons being neutral). As such, positive energy solutions for the neutron well are called resonances (unbound but not free) while they are quasi-bound states for the proton well (depicted schematically in Part 2 in the context of describing uranium-238 during accelerated nuclear decay, hypothetically).

23 There is a latent heat only for first-order phase transitions for which the first derivative of the free energy with respect to one of its dependent thermodynamic variables is discontinuous.

24 That is, $k_BT \propto (\frac{1}{2}\, mv^2)$ where m is particle mass, v particle velocity and k_B Boltzmann's constant.

25 This being the relevant form for accelerated decay's thermal energy per another paper that addresses the heat problem (Humphreys, 2018, p. 735), though it takes a very different approach.

for neutrons and protons[26] corresponding to high nuclear stability (as long as the model includes energy-level splitting due to spin-orbit coupling). This success is akin to how the single electron model of the atom rightly predicts the atomic magic numbers corresponding to the noble gases (Group XVIII elements) as well as inter-atomic bonds giving rise to molecules and compounds and the residual intermolecular forces giving rise to the various phases of matter. In both systems, spin-antispin pairing means that otherwise identical quanta can occupy the same level (like pairs of shared electrons comprise an atomic bond) *making these pairs rather particle-like* by virtue of their having the same energy and locale (orbital). The quantum parallel between atomic and nuclear systems holds despite the atom being mostly empty space and electrons planet-like in a quantum solar system, while the nucleus is densely packed with no empty space for its nucleons to move around in any classical sense so its orbitals would not seem at all orbit-like.[27]

While predicting magic numbers validates the nuclear shell model, especially for nuclides with $Z \le 82$ and $N \le 126$, it is a (semi-classical) *alpha particle model* that predicts the logarithmic relationship between the escaping alpha particle's energy and parent isotope's half-life, whether it is very short-lived polonium-214 or very long-lived uranium-238. That is, the nucleus acts like an assemblage of alpha particles (*alpha particles being the quanta* instead of nucleons) where the outermost shell is quasi-bound with positive energy (instead of a bound state with negative energy) so that the alpha particle can escape (tunnel out)—even when far from being a so-called 4*n* nucleus (i.e., $A = Z + N = 2Z = 4n$) meaning its set of *A* nucleons does not translate into an integer number of alpha particles. Surprisingly, a simple square well potential and semi-classical approach gives Gamow's analytical formula[28] for the half-life of even-even nuclei as well as the Geiger-Nuttall Law.[29] For polonium-214 ($E_\alpha = 7.7$ MeV), Gamow's model predicts a 370 μs half-life while experiment gives 164 μs, and for uranium-238 ($E_\alpha = 4.27$ MeV), it predicts a 40.6 Ga half-life while experiment gives 4.5 Ga. In the first case the model's decay rate is quite close (half-life too long by a factor of two) while in the second the model's rate is too low (half-life too long by a factor of ten). Nonetheless, it is truly remarkable that the huge disparity (microseconds vs. giga-anna) in half-lives for ^{214}Po vs. ^{238}U is rightly predicted with

$$t_{½} \sim \left(10^{\,1/\sqrt{E_\alpha}}\right)^{aZ}$$

for alpha decays from even-even nuclei with Z = 78–118 (Qi et al., 2012).

A quantized alpha particle model with a Lennard-Jones shaped potential[30] plus a Coulomb barrier has been used to model light 4*n* nuclei including ^{8}Be, ^{12}C, and ^{16}O with limited success (Blatt and Weisskopf, 1952, pp. 292–293). Modeled thus, such nuclei are geometric structures (^{16}O being a tetrahedron of alpha particles, for example) possibly contradicting

26 The shells for protons and for neutrons are independent of each other meaning each has its own Woods-Saxon potential $V(r) = \frac{-V_0}{1+e^{(r-R)/a}}$ which differ when $N \neq Z$; for example, $V_0 = 51 \pm 33\left(\frac{N-Z}{A}\right)$ giving $V_0 = 58.5$ MeV for the deeper neutron well and $V_0 = 43.5$ MeV for the proton well, for $^{238}_{92}$U. This presents like a broken degeneracy due to a lost symmetry where the pairs of pairs (*nn* & *pp*) no longer have the same energies.

27 The fact that the single-electron model of the atom works as well as it does is itself rather surprising (why should the Z – 1 electrons occupy shells as determined for the two-body problem?), but less so than the nuclear shell model's success.

28 For potential $V(r) = -V_0$ for $r < R$ and $V(r) = \frac{zZ_De^2}{r}$ for $r < R$ where $R = R_0A^{⅓}$, the decay constant becomes $\lambda \approx \frac{v_{in}}{R}e^{-\gamma}$ with $\gamma = \frac{2}{\hbar}\int_R^{R'}\sqrt{2M_0\left(\frac{zZ_De^2}{r} - Q_\alpha\right)}dr$ where $z = 2$ for alpha decay while $M_0 = \frac{M_\alpha M_D}{M_\alpha + M_D}$ is the reduced mass with $M_\alpha = 2u$. If the parent nuclide is ^{238}U then $Z_D = 234$, $M_D = 234u$; $Q_\alpha = \frac{1}{2}M_0v_{in}^2 = \frac{zZ_De^2}{R'} = 4.27$ MeV is the alpha particle's energy (purely kinetic inside the well and purely potential upon emerging from the tunnel). Integrating gives $\gamma = \frac{zZ_De^2}{\hbar v_{in}}\left(\cos^{-1}\sqrt{\frac{Q_\alpha}{V(R)}} - \sqrt{\frac{Q_\alpha}{V(R)}}\sqrt{1-\frac{Q_\alpha}{V(R)}}\right)$ but for thick barriers with $\frac{R}{R'} \ll 1$, $\gamma \approx \frac{2\pi zZ_De^2}{\hbar v_{in}} - \frac{4}{\hbar}\sqrt{2zZ_De^2M_0R}$. The quoted numbers use $R_0 = 1.4$ fm but 1.3 fm is also common.

29 Either: $\log_{10}t_{½} = aZ / \sqrt{Q_\alpha} + b$ where $t_{½}$ is the half-life for the alpha decay, Q_α is the total alpha decay energy ($Q_\alpha \approx E_\alpha$ for large nuclei), Z is the parent isotope's proton number, and *a*, *b* are constants for a given Z though $a \approx 1.5$ is very nearly constant across Z for even-even isotopes with $Z \ge 84$, $N \ge 128$. Or: $\log_{10}\lambda = c\log r + d$ when given in terms of the decay constant λ (instead of the half-life) and the alpha particle's range *r* (instead of the alpha particle's energy E_α) with constants *c*, *d*. Note that range corresponds to ring radius for a radiohalo though the medium is generally air or water for range measurements.

30 The Lennard-Jones "12–6" potential $V(r) = 4\varepsilon\left[\left(\frac{\sigma}{r}\right)^{12} - \left(\frac{\sigma}{r}\right)^{6}\right]$ with well depth ε and particle size σ (measured center-to-center making it a diameter) is used to model intermolecular (Van der Waals) forces *classically* and has a corresponding phase diagram for the so-called *Lennard-Jonesium* substance with temperature scaled as k_BT/ε. Nuclear wells describing the *α*–*α* interaction have ε~50 MeV compared to ε~10 *MeV* for molecular wells describing the *Ar*–*Ar* interaction (for example); this means that any terrestrial temperature lies at the bottom of such a phase diagram for nuclear condensed matter (where $k_BT = 26$ meV at 25°C or 36 meV *at* 150°C). In this region ($k_BT/\varepsilon < 0.687$) with appropriate density ($\rho\sigma^3 \lesssim 1$), the phase is solid, same as for real argon.

the liquid-like saturation that motivates and justifies the Liquid Drop Model (Blatt and Weisskopf, 1952, pp. 300–305). The saturation or flat topping exhibited by the binding energy per nucleon BE/A vs. the number of nucleons A (Figure 1) is fluid-like with a constant latent heat of evaporation as the binding energy per fluid molecule, while the nuclear density $A/R^3 \sim 1/r_0^3$, where A is the nucleon count and R and r_0 are nuclear and nucleon radii respectively, argues for a condensed state like an incompressible fluid (i.e., liquid).

Interestingly, the (quantum) alpha particle model with its finite structures does show saturation on a per-bond basis at about 2.4 MeV (or 4.1 MeV once corrected for Coulomb repulsion between alpha particles) as compared to the per-nucleon value of 8.8 MeV where the binding energy curve tops out for ^{56}Fe and/or ^{62}Ni. In any case, "they [the modelers] were aware of the shortcomings of a naïve alpha particle model [like the exclusion of all not-4n nuclides] and suggested that the alpha particles, rather than being stable structures inside a nucleus, be considered to have only a short-lived identity. After a certain time…the alpha particle dissolves into its constituents, and the remains of this and other dissolved alpha particles rearrange themselves into a new alpha particle structure, etc." (Blatt and Weisskopf, 1952, p. 293). Since then, the nucleus as a superfluid condensate of alpha particles has also been studied (Ring et al., 1983). Now, alpha particles have been seen experimentally in nuclei (Tanaka et al., 2021), and there is evidence suggesting if not confirming an alpha particle condensate for carbon-12 nuclei (Funaki et al., 2003) and oxygen-16 nuclei (Funaki et al., 2008). It would seem that alpha particles really do exist pre-formed in the nucleus (or forming, disintegrating, and re-forming), *and the nucleus is apparently subject to changing phase* (Chaffin, 2008).

Moreover, the success of modeling beta decay as an electron tunnelling out of the nucleus for the case of bound-state beta decay[31] (Woodmorappe, 2001) implies that the neutron acts like a proton-plus-electron inside the nucleus ($n \leftrightarrow p + \beta^- + \bar{\upsilon}_e$) prior to the beta decay event in the same sense that a pair of nucleon pairs makes an alpha particle in the nucleus ($n_\uparrow n_\downarrow + p_\uparrow p_\downarrow \leftrightarrow \alpha$)[32] prior to the alpha decay event (Subedi et al., 2008). An either/or model (shell nucleons sometimes organizing into alpha particles) with various adjustable parameters (making it semi-empirical) is commonly studied computationally where a typical model potential generally includes adjustable well-bottom V_0 and surface thickness a for a standard Woods-Saxon potential $V(r) = \frac{-V_0}{1+e^{(r-R)/a}}$ with nuclear radius $R = 1.3A^{⅓}$ fm plus a Coulomb barrier outside the nucleus ($r > R$). An escaping pair of pairs (neutron pair plus proton pair) is thought to assemble into an alpha particle "near the surface" occupying the first (lowest positive) quasi-bound alpha particle state, which must correspond with paired states above the neutron and proton wells respectively per the nuclear shell model.[33] In the end, getting an accurate half-life (better than within a decade) requires correcting for systematically under-predicting the true half-life. In other words, the calculated barrier potential decay rate is multiplied by whatever "preformation factor" P is needed to get the decay rate λ that is found experimentally: $\lambda_{expt} = P\lambda_{calc}$ or $t_{½expt} = \ln 2/\lambda_{expt} = P^{-1}t_{½calc}$ where $t_{½}$ is half-life. For uranium-238 ($^{238}_{92}\mathrm{U} \rightarrow {}^{234}_{90}\mathrm{Th} + {}^{4}_{2}\alpha$), the value of P is perhaps about 20% (Duarte and Siegel, 2010) and understood to be the percentage of time the four nucleons act like an alpha particle. Though it seems like merely a fudge factor, the variation in P from isotope to isotope within the scope of a particular model is measuring or reflecting something that is hindering decay.

All this is to say that nuclei generally act like assemblages of nucleons (spin-antispin pairs filling energy levels in separate neutron- and proton-potential wells) per the nuclear shell model's rightly predicting nuclear magic numbers, while large, unstable nuclei also act like assemblages of alpha particles per the alpha/tunnelling model's rightly describing alpha decay half-lives.[34] While four nucleon clusters can occur within the normal nuclear "liquid drop" phase whether a nucleus is stable or unstable (forming and breaking up on the surface of large nuclei, and tunnelling out as alpha particles if unstable), it is assumed that all the nucleon pairings would be paired up into alpha clusters in the unknown lower entropy phase describing unstable nuclei undergoing accelerated decay. All along the chain, the rapidly decaying nucleus would be characterized by this unknown phase comprised of alpha clusters but then would revert to the normal, higher entropy phase with a presumed first-order phase transition occurring for stable lead at Chain's End.

31 If a nucleus is stripped of atomic electrons, the beta decay electron can tunnel out more easily to occupy an atomic bound state (e.g., the ground state) rather than having to reach the continuum. The dramatic decay-rate acceleration (half-life shortening) observed for plasmas is explained thereby.

32 Or possibly $np + pn \leftrightarrow \alpha$ as the deuteron (np) has also been seen in the nucleus.

33 Exactly what quanta should be said to be filling the well, whether nucleons or alpha particles, is unclear. It is also unclear whether all underlying (negative) bound states are filled though it would seem they must be for spontaneous decay because the nucleus is not in an excited state.

34 An alpha particle's escape by tunnelling translates into the Geiger-Nuttall Law.

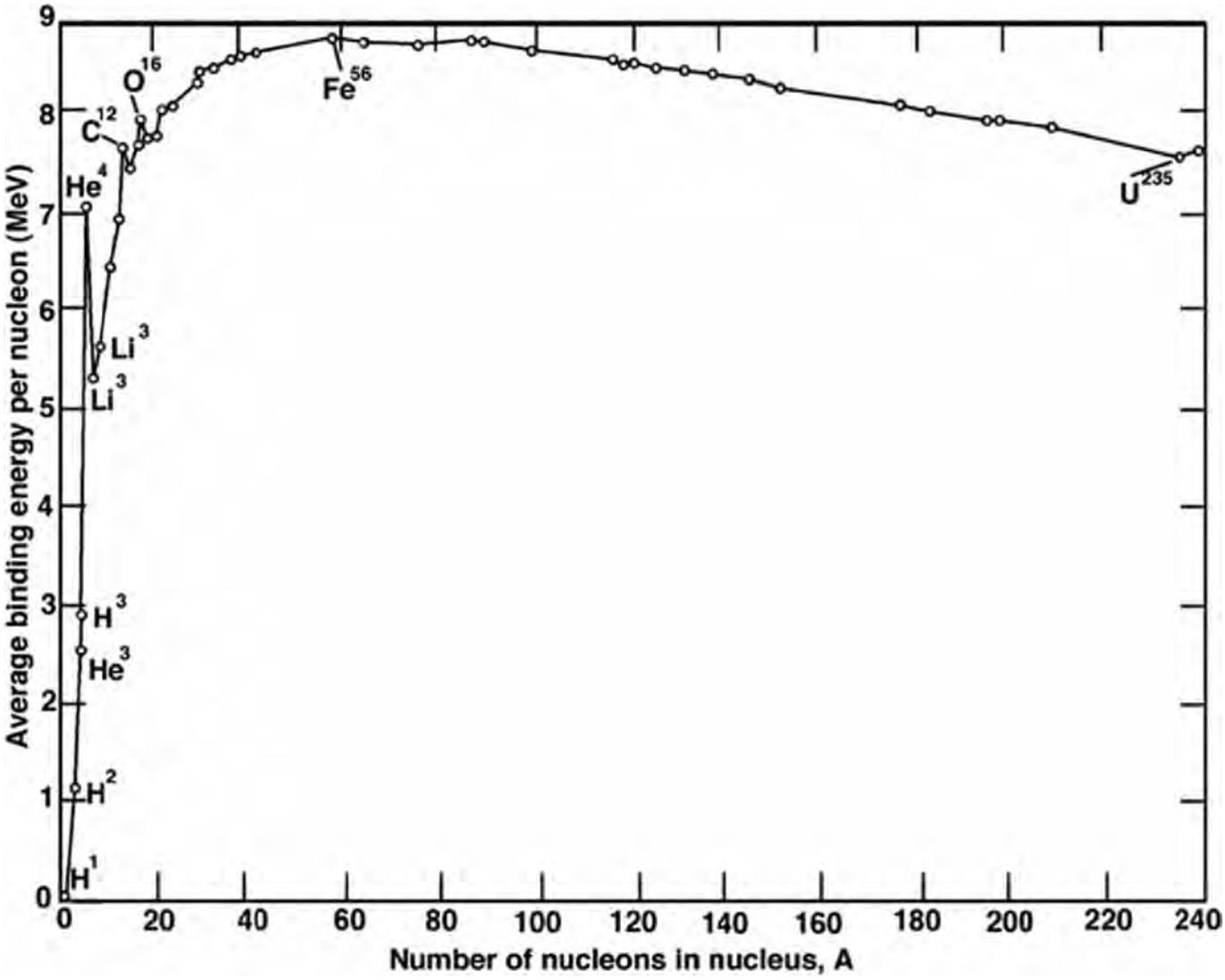

Figure 1. The saturation or flat-topping exhibited by the curve for the binding energy per nucleon vs. the number of nucleons (BE/A vs. A) is fluid-like with a constant latent heat of evaporation as the binding energy per fluid molecule, thus supporting the Liquid Drop Model of the nucleus.

This file is in the public domain in the United States because it was solely created by NASA and duly noted as free of copyright. http://imagine.gsfc.nasa.gov/Images/teachers/posters/elements/booklet/energy_big.jpg.

Nuclear Phase by Analogy

Since the nuclear force between hadrons is *residual*, "leftover" from the strong force that holds quarks as hadrons together, it follows that *inter-nucleon* forces are more like the *intermolecular* forces that determine a material's phase than they are like the intramolecular forces (i.e., covalent bonds) that determine a material's chemical composition. In this sense, bonds between ions as charged molecules (i.e., ionic bonds) can be understood as very strong intermolecular forces. Thus an ionic melt is perhaps the best analogy for the normal nuclear phase: the alpha particle's total binding energy of 28.3 MeV translates into ~4 MeV for the nuclear "ionic" bond[35] (that is, the bond *between*

35 Here, the coordination number counts nearest anions around a cation or vice versa. Six corresponds to simple cubic (sc), like the structure for Na^+Cl^-: ⅙([28.3 MeV – 2(2.225 MeV)] = 3.975 MeV > 2.225 MeV.

$n_\uparrow n_\downarrow$ and $p_\uparrow p_\downarrow$ by analogy) which is significantly *greater than* (certainly not weaker than) the bond in each diatomic ion (that is, *within* $n_\uparrow n_\downarrow$ or $p_\uparrow p_\downarrow$ by analogy) as approximated by the binding energy of the deuteron *np* (2.225 MeV).[36] It is therefore not unreasonable to treat the nucleon spin-antispin pair as a mono-atomic ion by analogy. Treating nucleon spin-antispin pairs as interacting entities is not new to nuclear physics (Chaffin, 2008). Nor is such pairing a stranger to atomic/molecular physics: the electron spin-antispin pair is treated as an entity (a bond) with repulsion between bonds explaining molecular geometry via Valence Shell Electron Pair Repulsion (*VSEPR*). The Cooper Pair of superconductivity is yet another example.

Consider a molten salt like NaCl. This ionic melt is a fluid consisting of its cations and anions, Na^+ and Cl^-, not really free from each other yet also not really bound (having no fixed crystalline array). Vaporized sodium chloride is not merely a gas of its ions but exhibits neutral polar-molecule-like pairings NaCl and Na_2Cl_2 (McCaffrey et al., 2007; Galamba, 2010) so its liquid phase surely exhibits such pairings too. Interestingly, liquid water's polar molecules occasionally morph back into cation plus anion $2HOH \rightleftharpoons H_3O^+ + OH^-$ where water's *pH* (or *pOH*) measures hydronium (or hydroxide) concentration. Or, consider that the liquid phase of nonpolar beryllium dichloride, Cl·Be·Cl (nonpolar as a molecule though its bonds are polar), includes both monomers $BeCl_2$ and dimers Be_2Cl_4, while its lower-entropy phase is a polymer (Pavlatou and Papatheodorou, 2000). Point being fluids are known to have "structure" (clustering tendencies) given their X-ray diffraction patterns and corresponding radial distribution functions.

Thus one might envision the unknown higher-entropy liquid phase of lead nuclei as consisting of the monomers $n_\uparrow n_\downarrow$ and $p_\uparrow p_\downarrow$ (analogous to cation and anion for an ionic melt) as well as sometimes-dimers, the paired pairings (or alpha clusters) *nppn* or *pnnp*, in contrast to a lower-entropy unknown phase consisting of all alpha clusters, possibly a distinct fluid with its own "structure" (rings or chains of alpha clusters: … *pnnppnnppnnppn*…). This would explain the preformation of alpha particles in nuclei, by this analogy with atomic/molecular systems, as dimers within the higher-entropy phase. In the present context the unknown lower-entropy phase is purely hypothetical, imagined as existing only in unstable nuclei during an episode of accelerated decay as a result of a change in the strong force miraculously wrought by God.

36 There is also an *np* pairing in the nucleus important for nuclides with the same number of neutrons as protons (Chaffin, 2021, p. 193) for which the nucleons are farther apart than for the deuteron ^2H (Isaule et al., 2016) possibly suggesting a weaker attraction for nucleon pairings inside the nucleus and thus a somewhat lower number than the deuteron's 2.225 MeV.

Summary

To reiterate, a phase change for the condensed matter comprising large nuclei is proposed as a heat sink during an episode of accelerated nuclear decay, being particularly relevant to the formation of radiohalos. The proposed nuclear phase change would occur in ^{206}Pb nuclei, being the final stable progeny in the ^{238}U decay chain. With each cascade of decays, the latent heat for this presumed first-order phase transition would be taken from (via heat transfer, generically invoked), and thereby continuously cool, the radio-center's immediate environment wherein the thermal energy is deposited. Arguing by analogy with atomic/molecular systems, the plausibility of providing sufficient cooling (absorbing enough energy) by a phase change is explored. The lower-entropy phase for large, unstable nuclei during accelerated decay might consist of alpha clusters as compared with primarily nucleon pairings for the normal phase. The nuclear phase change would occur with/at the switch from unstable parent isotope to stable daughter in accordance with the dependence of a hypothetical nuclear phase diagram on the decreased strength of the nuclear force (a shallower nuclear potential) for unstable nuclei characterizing an episode of accelerated decay as compared with normalcy, as will be explained in Part 2.

References

Adhikari, D., et al. (PREX Collaboration). 2021. Accurate determination of the neutron skin thickness of ^{208}Pb through parity-violation in electron scattering. *Physical Review Letters* 126(17):172502. [7 pages]

Blatt, J.M., and V.F. Weisskopf. 1952. *Theoretical Nuclear Physics*. Wiley and Sons, New York, NY.

Chaffin, E.F. 2008. Studies of the dependence of nuclear half-lives on changes in the strength of the nuclear force. In Snelling A.A. (editor), *Proceedings of the International Conference on Creationism Volume 6*, pp. 179–192. Creation Science Fellowship, Pittsburgh, PA, and Institute for Creation Research, Dallas, TX.

Chaffin, E.F. 2021. Supernova light curves and accelerated decay. *Creation Research Society Quarterly* 57:185–199.

Chaffin, E.F. 2022. Personal communication, May 31.

Duarte, A., and P.B. Siegel. 2010. A potential model for alpha decay. *American Journal of Physics* 78 (9):949–953.

Duer, M., et al. 2022. Observation of a correlated free four-neutron system. *Nature* 606:678.

Funaki, Y., et al. 2003. Analysis of previous microscopic calculations for the second 0^+ state in ^{12}C in terms of 3α particle Bose-condensed state. *Physical Review C* 67(5):051306. [5 pages]

Funaki, Y., et al. 2008. α-particle condensation in ^{16}O studied with a full four-body orthogonality condition model calculation. *Physical Review Letters* 101(8):082502. [4 pages]

Galamba, N. 2010. Molecular dynamics study of the vaporization of

an ionic drop. *The Journal of Chemical Physic*s 133(12):124510. [12 pages]

Gentry, R.V. 1992. *Creation's Tiny Mystery* (Third Edition). Earth Science Associates, Knoxville, TN.

Gentry, R.V., W.H. Christie, D.H. Smith, J.F. Emery, S.A. Reynolds, R. Walker, S.S. Christy, and P.A. Gentry. 1976. Radiohalos in coalified wood: New evidence relating to the time of uranium introduction and coalification. *Science* 301:315–318.

Humphreys, D.R. 2018. New mechanism for accelerated removal of excess radiogenic heat. In Whitmore, J.H. 2018. *Proceedings of the Eighth International Conference on Creationism*, pp. 731–739. Creation Science Fellowship, Pittsburgh, PA.

Isaule, F., H.F. Arelano, and A. Rios. 2016. Di-neutrons in neutron matter within a Brueckner-Hartree-Fock approach. *Physical Review C* 94:034004. [26 pages]

Kisamori, K., et al. 2016. Candidate resonant tetraneutron state populated by the 4He(8He,8Be) reaction. *Physical Review Letters* 116:052501. [5 pages].

Laney, R., and A.W. Laughlin. 1981. Natural annealing of the pleochroic haloes in biotite samples from deep drill holes, Fenton Hill, New Mexico. *Geophysical Research Letters* 8(5):501–503.

McCaffrey, P.D., et al. 2007. Accurate equilibrium structures obtained from gas-phase electron diffraction data: Sodium chloride. *The Journal of Physical Chemistry* A 111(27):6103–6114.

Pavlatou, E.A., and G.N. Papatheodorou. 2000. Raman spectroscopic study of $BeCl_2$ in the crystalline, glassy and liquid states and of molten $BeCl_2$–CsCl mixtures. *Physical Chemistry Chemical Physics* 2(5):1035–1043.

Qi, C., R.J. Liotta, and R. Wyss. 2012. Generalization of the Geiger-Nuttall Law and alpha clustering in heavy nuclei. In *Rutherford Centennial Conference on Nuclear Physics Journal of Physics: Conference Series* 381:012131. [6 pages]

Ring, P., P. Shuck, and Y.K. Gambhir. 1983. Nuclei: A superfluid condensate of α-particles? A study within the interacting boson model. *International Conference of Nuclear Physics*, Florence, Italy, August 29–September 3, 1983; Gambhir, Y.K., P. Ring, and P. Schuck. 1983. Nuclei: A superfluid condensate of a particles? A study within the interacting-boson model. *Physical Review Letters* 83:1235–1238.

Snelling, A.A. 2005. Radiohalos in granites: Evidence for accelerated nuclear decay. In Vardiman, Snelling, and Chaffin (editors). *Radioisotopes and the Age of the Earth Volume II*, pp. 101–207. Institute for Creation Research, El Cajon, CA, and Creation Research Society, Chino Valley, AZ.

Subedi, R., et al. 2008. Probing cold dense nuclear matter. *Science* 320:1476–1478.

Tanaka, J., et al. 2021. Formation of α clusters in dilute neutron-rich matter. *Science* 371:260–264.

Woodmorappe, J. 2001. Billion-fold acceleration of radioactivity demonstrated in laboratory. *Journal of Creation* 15(2):4–6.

Worraker, W. 2018. Heat problems associated with Genesis Flood models—Part 1: Introduction and thermal boundary conditions. *Answers Research Journal* 11:171–191.

Creation Research Society Quarterly 2022 59:39–50

Petrified Ideas of the Williston Basin
Part III: Coal and Oil

Peter Klevberg*

Abstract

The Williston Basin of central North America contains prodigious quantities of coal and oil. Could the antediluvian biosphere have provided this carbon mass, or did it require many millions of years to accumulate? In this concluding part, we focus on fossil fuels. As we have seen many times in many places, what appear to be strong arguments against the Biblical view of Earth history turn out to be strong arguments against uniformitarianism.

Key Words: petrogenesis, coal, oil, Williston Basin, Bakken Formation, lignite, pyrolysis

Introduction

The geologic setting of the Williston Basin was provided in Part I of this series, while Part II focused on fossil wood. While the nearly 5,000 m (over 16,000 ft.) of sediments filling the Williston Basin (Figure 1) are said to represent all the geologic systems in the standard story of Earth history, providing an impressive argument against the Biblical account closer examination in the light of recent scientific advances puts the shoe on the other foot. The idea of gradual deposition in a gradually subsiding basin in concert with eustatic depth changes in the basin now appears to be a petrified idea with many scientific difficulties.

Likewise, the Fort Union Group strata that form the bulk of the badlands in North Dakota exhibit evidence of rapid, continuous deposition. Instead of huge swamps with gradual soil formation leading to coal formation and fossilization of trees, catastrophic conditions of at least regional extent would have been necessary to preserve the wood and other organic matter, and coalify or fossilize it. The mineralogy and sedimentology of the Fort Union Group supports this view rather than the traditional story. This paper addresses fossil fuels in the Williston Basin. The focus is the deeper part of the basin as shown in Figure 2.

Importance

While the Williston Basin has produced lignite-rank coal and crude oil for many years, it was the advent of two technologies that revolutionized production in the basin. Directional drilling with horizontal completion and hydrofracturing ("fracking") tapped the enormous potential of the Bakken Formation and triggered the Bakken oil rush, which the lead author experienced, working in Watford City, North Dakota, the heart of the Williston Basin. Nearing the North Dakota border at night, one could see a thousand giant gas flares from new oil wells across the prairie. There was memorable hoopla when North Dakota oil production exceeded one million barrels per day (Table I).

Estimates of total reserves of the basin, by the USGS and others, range from a century to a millennium at today's production rates. The amount in the Bakken Formation alone is mind bog-

* Peter Klevberg, grebvelk@yahoo.com
Accepted for publication November 16, 2021

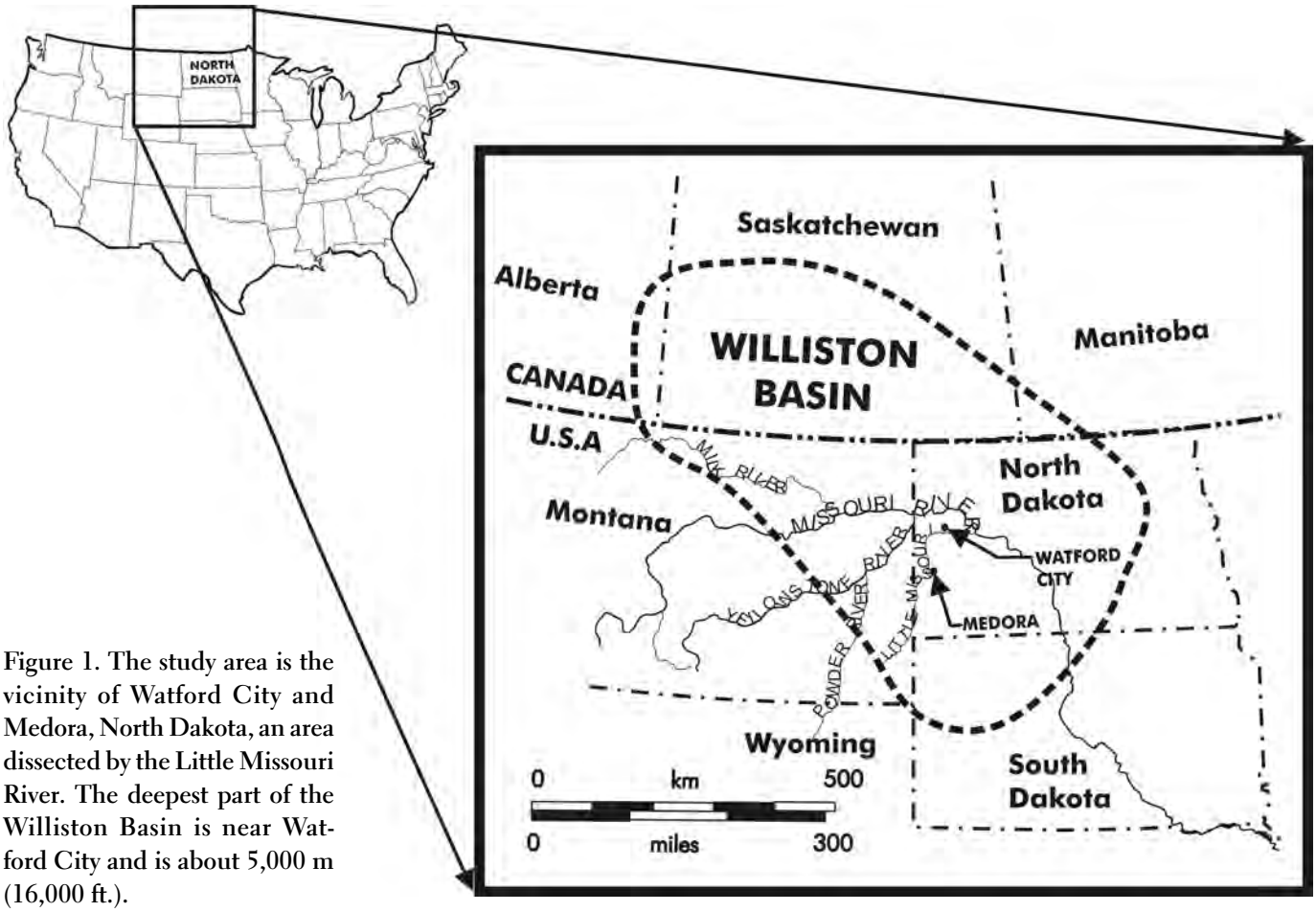

Figure 1. The study area is the vicinity of Watford City and Medora, North Dakota, an area dissected by the Little Missouri River. The deepest part of the Williston Basin is near Watford City and is about 5,000 m (16,000 ft.).

gling. Crude oil and sub-par kerogenous matter are found in lesser quantities in the Three Forks and other formations (Figure 3). The strata nearer the surface are characterized by abundant lignite.

The Williston Basin: Endless Supplies of Fuel?

Enormous amounts of organic matter, largely terrestrial vegetation and marine algae, were buried in the basin. In deeper formations, it forms crude oil and natural gas. In the shallower strata of the Fort Union Group, most of it is preserved as low-rank coal (lignite or "brown coal").

Conventional Plays

Oil has been extracted from several fields in the basin for many years. "Conventional plays" are those where oil has migrated from carbon-rich source rocks to reservoirs, usually sandstones, and is extracted by vertical wells. These plays tend to be found in structural traps such as the Nesson Anticline, Poplar Dome, and Cedar Creek Anticline (Figure 2).

The Bakken Formation

Type localities are usually outcrops representative of the formation. However, the type locality of the Bakken Formation is from subsurface drill cores (subcrop). The Bakken is easily located geophysically and is buried deep in the basin (Figure 3, number 11). It consists of four members (LeFever et al., 2012; Stroud, 2012; Sonnenberg, 2017), not all of which are present at all places: the basal *Pronghorn Member* ("Sanish sand"), consisting of sandstones, siltstones, and carbonaceous mudstones of limited areal extent; the *lower shale member*, an organic-rich black shale source rock; the *middle member*, consisting of silty dolostone, limestone, and sandstone; and the *upper shale member*, similar to the lower shale. The shales are interpreted by sequence stratigraphers as hemipelagic muds from transgressive systems tracts (see Part I), with the Bakken at the base of the Kaskaskia Megasequence. This interpretation has, however, been disputed (e.g., Petty, 2019). Evidence of bioturbation appears at odds with an anoxic (euxinic to dysoxic) environment, which supposedly explains the 3% to 10% total organic carbon content (Egenhoff and Fishman, 2013). Multiple sediment sources or directions are postulated (Mohamed, 2015).

Petroleum Systems

Six petroleum systems (source rocks generating oil and gas, collected in reservoir rocks, and capped by seals) are recognized in the Williston Basin (Nordeng, 2013). These are shown in Figure 3. Oil in the Three Forks Formation is part of the Bakken system, as it is believed to derive from Bakken source rocks. The Bakken is the primary producer today. Petroleum systems are identified by physical properties, geochemistry, and biomarkers of the oils (Jarvie, 2001; Lillis, 2013; Auers et al., 2014; Yang et al., 2017).

The Fort Union Group

The Fort Union Group (Fort Union Formation in Montana) contains several similar formations (or members) of weak, clastic sedimentary rocks (Klevberg and Oard, 2021). These strata are laterally extensive but not continuous across the Williston Basin. Marker beds, usually major coal seams, are not abundant. Bentonite is common, derived from volcanics but with fragments of metamorphic rocks transported from mountains more than one hundred miles to the west or southwest. Where coal has burned, it forms clinker beds. These rocks weather

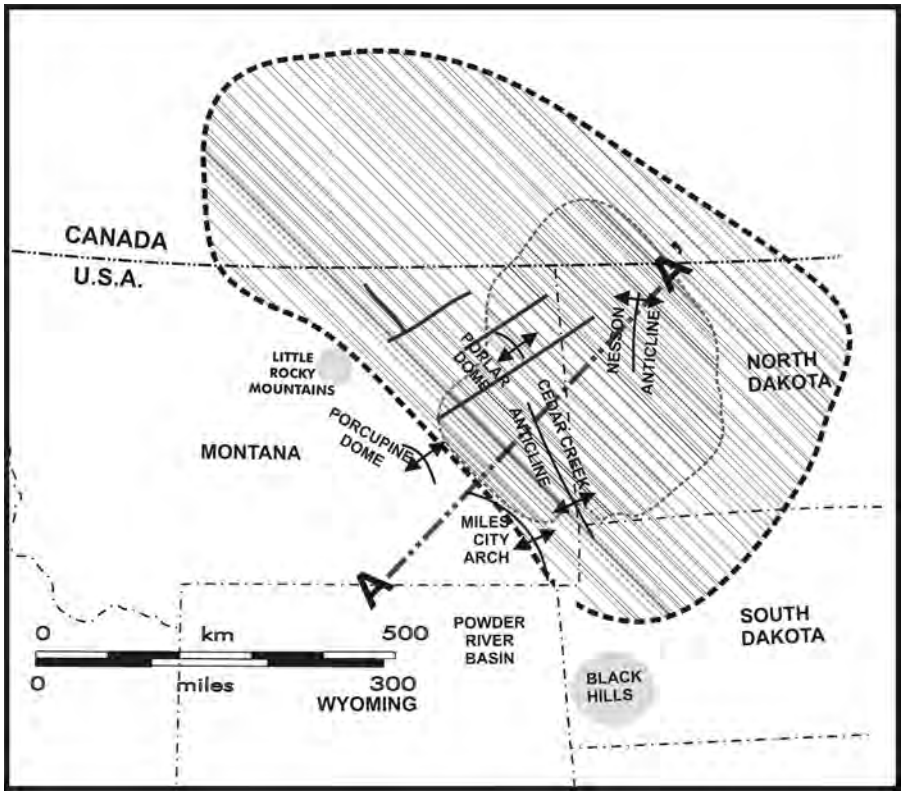

Figure 2. Relation of Williston Basin to nearby structures. Antiforms are found within the basin as well as to the west. Area of darker hatching is central (deeper) part of basin. Cross section indicated by line A–A' is shown in Figure 3.

Table I

Bakken Development History			
Year	**Field**	**Event**	**Location (Figure #)**
1953	Antelope	Earliest discovery	Southeast spur of Nesson Anticline
1961	Elkhorn Ranch	Shell well completed in upper shale	Halfway between Watford City and Medora
1976	Bakken Fairway	Next well in Bakken, first in Fairway	Between Nesson and Cedar Creek Anticlines
1987	Fairway	First horizontal well, in upper shale	
2006	Parshall	Discovery of Parshall Field, beginning of boom	East of Nesson Anticline
2007	Elm Coulee	Development of middle Bakken	Southeast of Poplar Dome
2012	entire Williston Basin	peak of 217 active drilling rigs	Closely hatched (inner area) inside gray dashed line
2014		production first exceeded one million barrels a day	

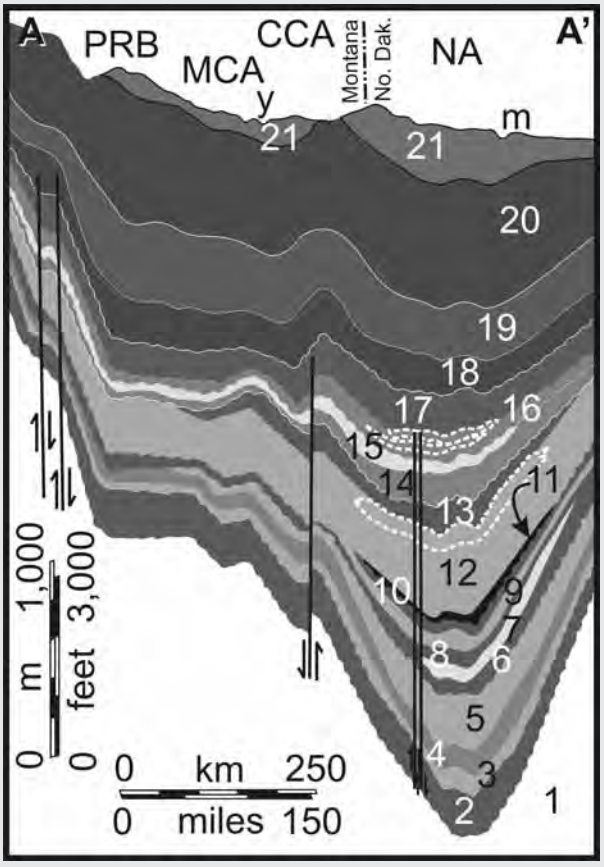

Figure 3. Southwest–northeast cross section through Williston Basin along line indicated on Figure 2. Figure modified from Peterson (1988). Charles Formation and Spearfish Formation Fine Salt and Dunham Salt Members indicated by dashed white lines.

PRB Powder River Basin
MCA Miles City Arch
CCA Cedar Creek Anticline
NA Nesson Anticline
y Yellowstone River
m Missouri River
italics indicates petroleum system source rocks

1 Metamorphic basement
2 Deadwood Formation
3 Winnipeg Group (Black Island, Ice Box, and Roughlock Formations)
4 *Red River*, Stony Mountain, and Stonewall Formations, undivided
5 Interlake Formation
6 *Winnipegosis* Formation
7 Prairie Formation (Prairie Salt)
8 Manitoba Group (Dawson Bay and Souris River Formations)
9 Jefferson Formation (*Duperow* and Birdbear Members)
10 Three Forks Formation
11 *Bakken* Formation
12 *Madison* Group (Lodgepole, Mission Canyon, and Charles Formations; Charles indicated by dashed line)
13 Big Snowy Group (Kibbey, Otter, and Heath Formations)
14 Amsden Group (*Tyler*, Alaska Bench, and Devil's Pocket Formations; eastward may be referred to as Tyler, Amsden, and Minnelusa Formations)
15 Opeche and Minnekahta Formations, undivided
16 Spearfish Formation (Fine Salt and Dunham Salt Members indicated by dashed lines)
17 Ellis Group (Piper, Rierdon, and Swift Formations; strata assigned to Morrison Formation included)
18 Dakota Group (Inyan Kara, Skull Creek, Newcastle, and Mowry Formations; some refer to Inyan Kara Group with Lakota, Fusion, Fall River—Dakota; Skull Creek and above assigned to Colorado Group)
19 Colorado Group (Graneros—Mowry, Belle Fourche, Greenhorn, Carlisle, and Niobrara Formations; Skull Creek and Newcastle included by some at base)
20 Montana Group (Telegraph Creek, Eagle, Claggett, Judith River—Pierre—Bearpaw, Fox Hills, and Hell Creek Formations)
21 Fort Union Group (Ludlow, Slope, Cannonball, Bullion Creek, and Sentinel Butte Formations; in Montana, Fort Union Formation with Tullock, Ekalaka, Lebo, and Tongue River Members)

to badlands topography which cuts deeply into the group (Figure 4). The Fort Union strata are the lowest exposed rocks in the area; deeper formations are all subsurface.

Fort Union Lignite

The Fort Union Group contains immense amounts of lignite (Figure 5).

> The lignite area covers more than 28,000 square miles (18 million acres). More than 100 beds over four feet in thickness have been identified…. Strippable reserves are estimated to total 16.1 billion tons…. (Dalsted and Leistritz, 1974, p. 4).

More than a century ago, the enormous extent of this resource was already recognized and being tapped (Herald,

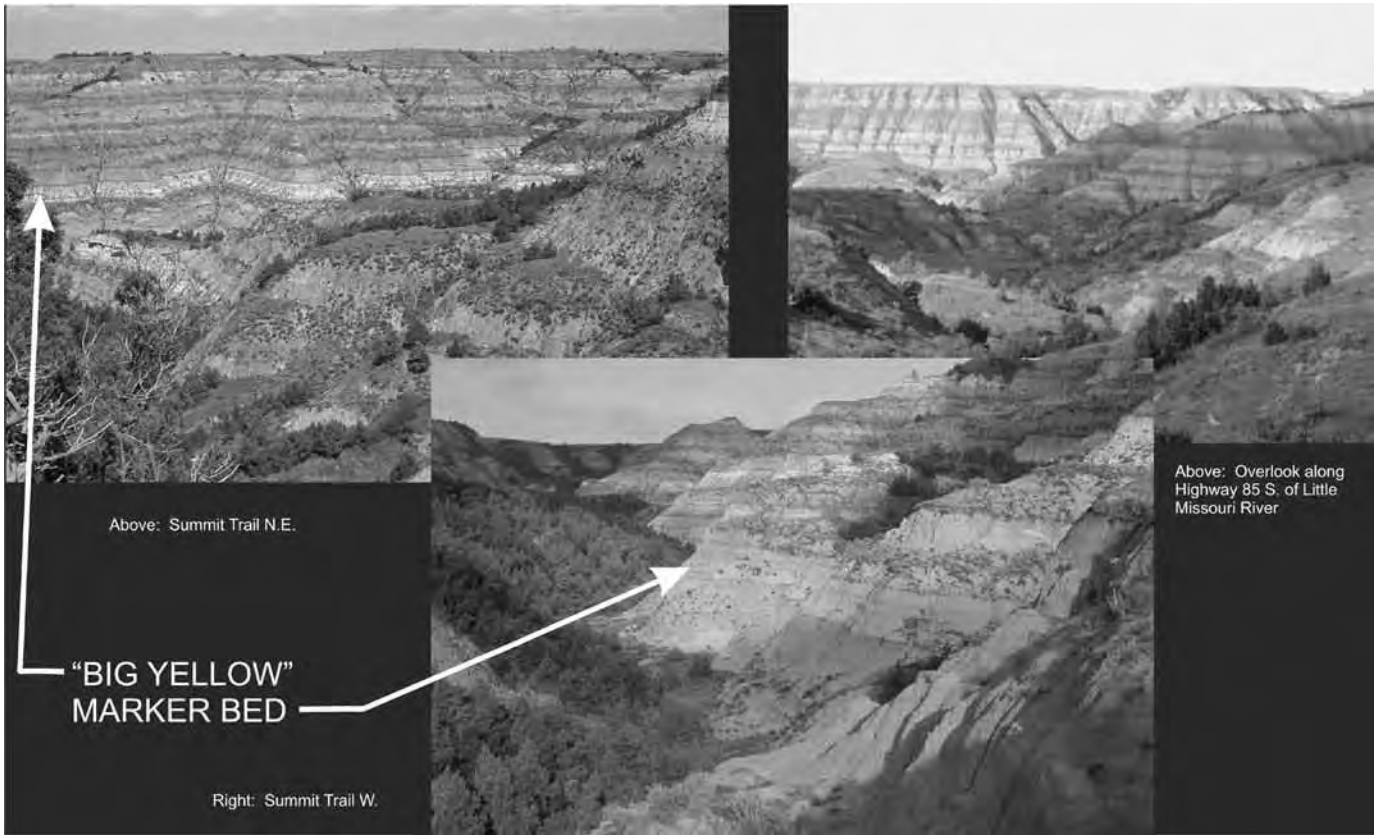

Figure 4. The uppermost formation in the Fort Union Group is the Sentinel Butte Formation, and the deeply dissected badlands provide abundant exposures. These three views from the badlands of McKenzie County show the lateral continuity of strata. Marker beds such as the "big yellow," "big blue," HT lignite, L lignite, and "upper yellow" are important stratigraphic markers, but none extends the width of the basin. The coal therefore did not form from a mass of vegetation of basinal extent but instead from large but isolated mats or masses.

1911). Many of the seams are thin (Figure 6), but thick, extensive ones serve as marker beds.

The lignite of the Williston Basin (Figure 5) seems like the continuation of the extensive coal in the Powder River Basin, deposited by a north-to-northeast diluvial current. Several of the 47 Tertiary coal seams greater that 1.5 m (5 ft.) thick in the Powder River Basin exceed 30 m (100 ft.) in thickness (Jones, 2010; Luppens et al., 2015). The Powder River coal is low sulfur, subbituminous A to subbituminous C. The differences in coals can be explained by the subsequent overburden and erosion. Assuming a geothermal gradient of 26–27°C/km (24–26°F/1,000 ft.), lignite requires an overburden of 100–1,600 m (330–5,250 ft.), while the Powder River Basin coal would require 1,600–3,200 m (5,250–10,500 ft.) (Thomas, 2013, p. 111).

The Pyrolysis Problem

Thermal maturity is the degree to which kerogen converts to petroleum or coal by pyrolysis. The concept is simple: heat at depth breaks carbon-carbon bonds in large molecules. Reduction in oxygen, sulfur, nitrogen, and hydrogen, and hydrogenation of the resulting fragments, forms smaller ones. Branched alkanes and aromatics are also formed. Though straightforward, several problems arise. Difficulties forming petroleum from organic matter have caused some to look for an abiologic source. Thermodynamic stability relations (free energies and activation energies) argue against common explanations. The enthalpy of the system must decrease. If vast time is required, it may not be possible for the molecules to persist. Carefully managed processes in oil refineries that use exotic catalysts may make poor analogues for natural processes.

Organic versus Inorganic Origin

Petroleum is largely believed to be biogenic. Kenney et al. (2002) argued

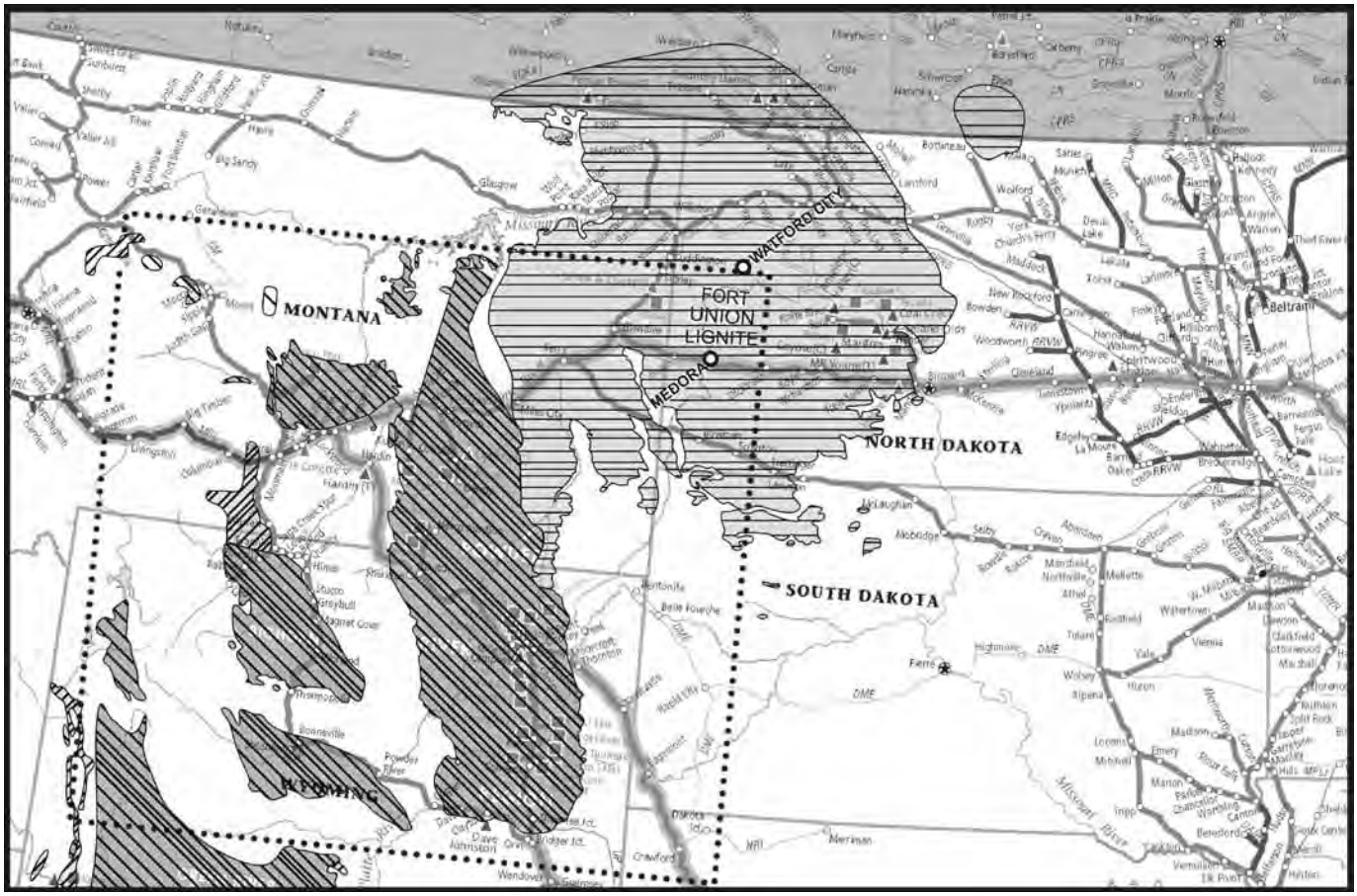

Figure 5. Map derived from BNSF Railway 2013 Coal Map with coal mines and railroad system shown. Sub-bituminous and bituminous coal indicated by diagonal hatching and lignite by horizontal hatching. Dotted square is primary Powder River Basin coal mining and rail haulage area.

on chemical thermodynamic grounds for an abiologic origin in the mantle, a view largely promoted by Russian researchers but not accepted in the West. Experimental evidence for the possibility of thermodynamically favorable generation of methane and larger hydrocarbons from carbonate minerals at high pressures has been presented (Scott et al., 2004). Vestiges of chlorophyll, sulfur bacteria, and other levorotary (left-handed chirality) biogenic molecules appear to argue in favor of a biologic origin (Jiang et al., 2001; Yang et al., 2017) as does a preponderance of odd-numbered alkanes in various crude oils. Matthews (2008, p. 154) disputes this and proffers a "theobaric" origin for most oil: "A very specific burial history must occur for the kerogen to be heated to the correct temperatures for the correct amount of time to form oil." This burial history is the object of basin modeling.

Basin History

Burial history is commonly modeled by PETROMOD or BASINMOD software (Figure 7). Model output can be quite impressive, but the reasoning is circular, and results can diverge from field conditions (Matthews, 2008). The time required for petrogenesis as commonly modeled has also been refuted by observation of recently formed oil in the Gulf of California, the result of hydrothermal activity on the sea floor and not the multistep process commonly modeled.

> Such a slow, multistep mechanism differs significantly from hydrothermal petroleum formation, which can be geologically fast… in which generation occurs almost concurrently with expulsion and migration (Didyk and Simoneit, 1989, p. 69).

Stability and Time

"The generation of hydrocarbons, even at these temperatures [100–120°C], is very slow and requires time on the scale of millions of years to produce significant

volumes of hydrocarbons" (Nordeng, 2013, p. 11). Higher temperatures cause oil to break down into condensate and natural gas, but lower temperatures greatly slow the pyrolytic reactions. However, petroleum hydrocarbons experimentally generated from carbonate minerals were quenched to prevent transformations that may have occurred if the apparatus had been cooled slowly (Kenney et al., 2002). Anaerobic conditions, even deep in the Earth, do not preclude microbial degradation of hydrocarbons (Gray et al., 2010). We rely on anaerobic degradation to clean up petroleum pollution on a year-to-decade scale, so even if deep microbial activity is three orders of magnitude slower than near the surface, millions of years should result in complete conversion to methane and heavy oil or inert kerogen. Thus, conflicting ideas include source *and* time.

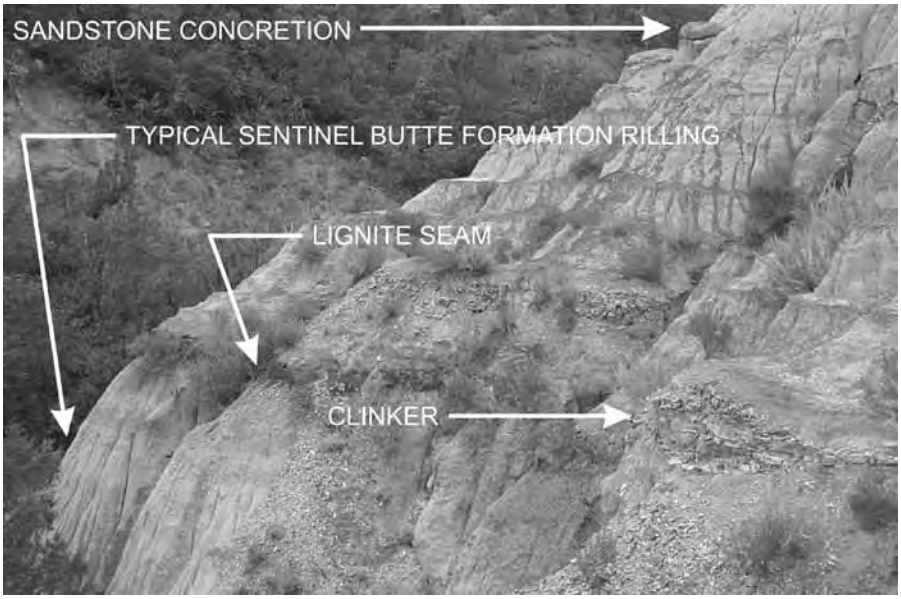

Figure 6. Typical exposure of Sentinel Butte Formation in McKenzie County, North Dakota. Concretions in sandstone are common. The rilling shown here is typical of the Sentinel Butte strata, as is the thinness of the lignite seam. Lignites and clinker are often associated, sometimes transitioning laterally where oxygen deprivation probably prevented further burning of the coal.

Problems for Diluvialists

Diluvialists are significantly restricted by time. While the formation and filling of the Williston Basin is difficult for evolutionists (Klevberg and Oard, 2021), petrogenesis presents challenges for creationists. Can oil form that rapidly? Was it abiogenic, biogenic, or both? Or is it a mystery transcending natural explanation (Matthews, 2008). Creationists have only provided preliminary answers (Ouweneel, 1977; McQueen, 1986; Snelling, 1990), but recent experiments provide illumination.

Experimental evidence indicates oil can form rapidly. Torbanite is oil shale, boghead coal, or cannel coal (Figure 8) that is believed to be derived primarily from algal kerogen and can yield paraffinic or asphaltic oil when heated. Experiments on torbanite and brown coal over a period of six years provided some very important results (Saxby et al., 1986, p. 80):

> Overall, the two most significant results are (i) the absence of olefins and carbon monoxide in all major products, as in naturally-occurring hydrocarbons and (ii) remarkable experimental verification of the vitrinite coalification line from brown coal to anthracite…the results show that natural maturation reactions can be simulated both in the presence and absence of water.
>
> The present experiments clearly show that altering the time-scale of source rock pyrolysis from seconds to years (i.e. a factor of 10^7) changes the product distribution to that of natural petroleum. In many geological situations much longer time intervals are available but evidently the molecular mechanism of the decomposition is little changed by the additional time. Thus, within sedimentary basins, heating times of several years are sufficient for the generation of oil and gas from suitable precursors.

As shown on Figure 8, boghead or cannel coal mature through the oil window on the path to anthracite coal. Synthetic crude oil from algae (Helman, 2013) and slaughterhouse waste (Lemley, 2006) has been produced at both bench and plant scales in less than one hour. The Carthage, Missouri, plant (Lemley, 2006) subjected the slaughterhouse waste to 20 minutes at 260°C (500°F) and 4.1 MPa (600 psi) to produce 500 barrels per day of high-quality light crude oil. Laboratory results indicate that many oil properties can be produced at high temperatures for short times versus low temperatures for long times (Liang et al., 2015). Some differences in relative abundances of alkanes and other compounds varied with temperature. "The temperature range of maximum hydrocarbon generation for Type I kerogen corresponds to 350–450°C" (Liang et al., 2015, p. 212). For planktonic (Type II) kerogen,

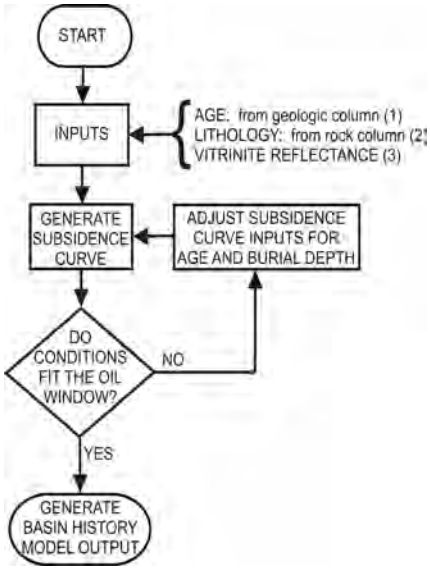

Figure 7. PETROMOD and BASIN-MOD rely on several inputs: (1) age is *assumed* starting with the geologic column, (2) lithology is scientifically derived from the rock column, which is usually a combination of drilling and geophysical data, but the sediment is *assumed* to have begun cold and warmed as it was slowly buried *assuming* the current geothermal gradient, (3) vitrinite reflectance, a measured value, is *assumed* to accurately indicate thermal *maturity*, though this may not be the case (Wenger and Baker, 1987). The program goes through iterations to compute burial depth and rate based on assumed initial conditions and pyrolysis. Pyrolysis is *assumed* to have taken place over vast ages, i.e., equilibrium conditions, which places a relatively low maximum temperature on the system; otherwise, molecules would have been reduced to natural gas (see Figure 8).

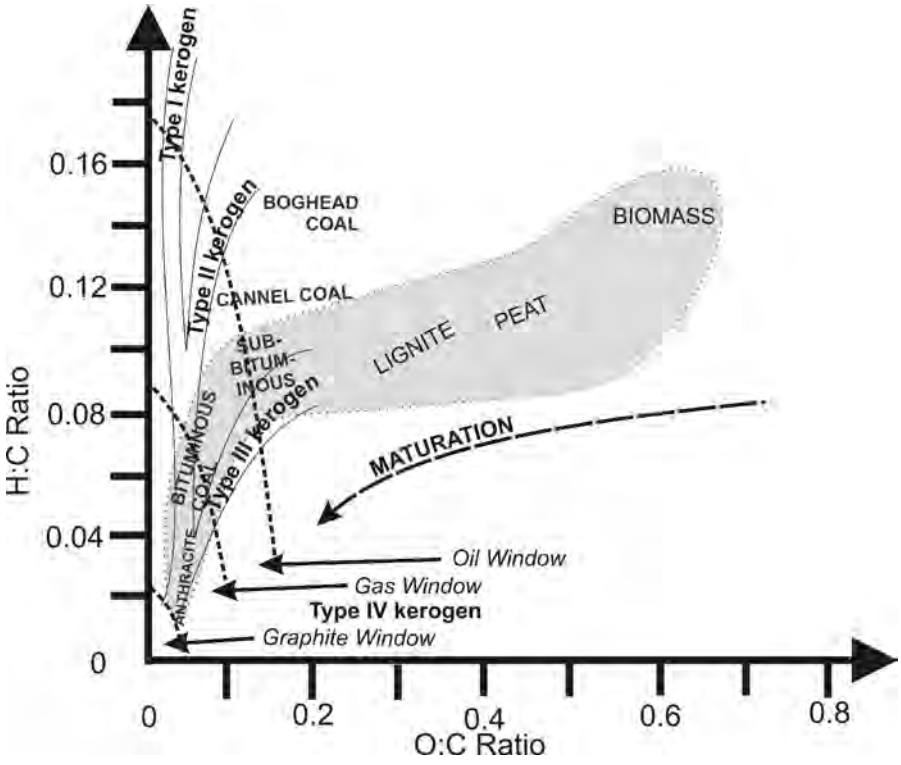

Figure 8. Van Krevelen diagram derived from Harwood (1977) and a multitude of other sources. The oxygen:carbon is the abcissa, and the hydrogen:carbon is the ordinate. Maturation (heavy dashed line) results in lowering of both ratios as hydrogen and oxygen are released. Kerogen types (Table II) show different ratios and plot in different parts of the diagram. Primary path of coal maturation follows the shaded area. Maturation of petroleum follows the general maturation trajectory with the "oil window" and "gas window" demarcated by the curves with short-dashed lines. Thus, oil will form inside the "oil window" and turn to gas after passing into the "gas window" with further maturation (pyrolysis). A residue of pure carbon from which all O and H have been stripped by pyrolysis would be graphite.

maximum productivity was between 300 and 450°C.

Matthews (2008) noted the objection to migration of hydrocarbons per Darcy's Law on a scale of thousands of years. However, many assumptions are involved in that calculation, including: viscosity and interaction with water, porosity changes, and migration pathways. Viscosity is temperature related, and the assumption that organic matter began cool and heated gradually with burial is shaky. In a diluvial model, we would expect elevated temperatures during the Genesis Flood.

Coal maturation is similar to that of petroleum (Figure 8). While Type II kerogen may have mixed terrigenous and marine organic materials, Type III is dominated by woody plants and more likely to produce coal and natural gas (Table II). Oard and Klevberg (2022) noted the role of floating mats of logs and woody debris in coal formation in the Fort Union strata. Other creationists have provided evidence for rapid transport, deposition, and burial of plant matter to form fossilized wood or coal (see Appendix).

The Carbon Quantity Conundrum

The amount of organic material in petroleum and coal has been estimated as being many times that of the

Table II

Types of Kerogen				
Type	**Description**	**Source**	**Prominent Maceral**	**Products**
I	sapropelic	bacteria, algae, proteins, waxes, fatty acids	alginite	oil
II	planktonic	plankton, bacteria, marine organic matter	exinite	oil and gas
III	humic	cellulose, woody plants	vitrinite	gas, coal
IV	inert	charcoal, peat, polyaromatic hydrocarbons	inertinite	coal, graphite

present biosphere, a point addressed by Froede (1995), Wiant (1974), and Woodmorappe (1999). Archer (2010) estimated that there is eight times as much carbon in coal as in the current terrestrial biosphere. Uniformitarians have millions of years for organic matter to accumulate in anoxic basins; creationists must find another answer. In the case of coal, the organic matter was largely terrestrial plants. As shown in Table III, greatly accelerated rates of production of Types I and II kerogen would be expected during the Deluge, but this would not explain the apparent lack of *volume* of terrestrial plants. Type IV kerogen also would have had terrestrial plant precursors (Achten and Hofmann, 2009). This is a large amount of vegetation, but there are possible explanations: the land/sea ratio was larger, there were few if any deserts or semi-arid areas, and/or the climate was warmer and wetter (Oard and Reed, 2017). Given these, the carbon reservoir of the antediluvian world could have been sufficient.

Problems for Uniformitarians

Hydrocarbon formation is problematic for uniformitarians too. In addition to the pyrolysis problem, gradual accumulation in anoxic basins might be exceeded by anaerobic microbial degradation. Furthermore, bioturbation is evident in the "oxygen-deprived" environment of the Bakken! The idea of slow pyrolysis of kerogen followed by slow migration to reservoirs per Darcy's Law has been called into question by recent field and laboratory studies. Oil has been created from slaughterhouse waste, algae, and plastic garbage in less than one hour, at reasonable temperatures and pressures. Basin modeling software assumes deep time; the fallacy of begging the question (*petitio principii*). Preservation of organic matter and generation of kerogen and bitumen is best accomplished through rapid burial in a hot environment.

Another problem is the existence of over-pressured reservoirs in the Williston Basin (Sonnenberg, 2017), North Sea (Matthews, 2008), and elsewhere (Armstrong, 1972). No geologic seal is perfect, and after many millions of years, pressures should be greatly reduced regardless of how slight the leakage.

Oil is also found in the "wrong" places. In some cases, downward migration from source rocks appears plausible. Sun et al. (2019) invoke bacteria as the source for Hongshuizhuang Formation shale source rocks (Gaoyuzhuang Formation carbonate reservoir) but explain anomalous biomarkers by contamination. In deep petroleum systems, evolutionists *must* invoke contamination since they believe few living things existed when the rocks were deposited.

The origin of coal has been extensively debated, though the prehistoric swamp theory adorns signs and booklets at tourist traps like Medora, North Dakota (Figure 1). The architecture of the Fort Union Group (Figure 4) is too laterally extensive to fit the uniformitarian model of migrating delta swamps transgressing the isochronous horizon. As has been pointed out many times (see Appendix), the texture or fabric of many coals refutes a peat origin. Evidence for an allochthonous (floating mat) origin has mounted in recent decades. It gained traction with Austin's (1979) study of Appalachian coal and those of Mt. Saint Helens catastrophism (Morris and Austin, 2003; Coffin et al., 2005; Oard and Reed, 2017). Kerogen III (Table II), while primarily terrigenous, often contains marine materials, and marine fossils occur in some coals (Coffin et al., 2005). Alleged paleosols underlying coals have been widely disproven (Froede, 1998), as have those in conjunction with petrified wood (Oard and Klevberg, 2022). The extent, thickness, and textures of

Table III

Carbon Sources		
Source	**Kerogen**	**Diluvial Conditions**
bacteria	I	Probably large blooms when nutrients and temperatures elevated.
algae	I	Probably large blooms when nutrients and temperatures elevated.
plankton	II	Probably large blooms when nutrients and temperatures elevated.
plants	III and IV	Probably assembled into mats by marine currents and deposited in large masses.
mantle (abiogenic)		Abiogenic carbon and hydrocarbons could have been released from fountains of the deep.
carbonates		Hydrocarbons could have formed from deep carbonates, possibly erupted with carbonatites.

coal do not fit with the swamp explanation. While belief in an *old earth* would not preclude acceptance of catastrophism or rapid, continuous deposition of the Fort Union strata, commitment to *uniformitarianism* would. Uniformitarians also have difficulty explaining the purity of the Powder River Basin coal. Why are there not more fluvial sediments and volcanic ash within the coal seams?

Inferences and Conclusions

The Williston Basin is a key source of fossil fuels: gas, oil, and coal. Organic matter occurs in high concentrations in several formations there. Six petroleum systems are generally recognized, the most important being the unconventional Bakken play. Lignite is found in great quantity in the Fort Union Group near the surface.

The pyrolysis problem is one of temperature versus time. By assuming vast time, researchers are limited to relatively low temperatures or hydrocarbons will "overmature" to dry gas. Darcy's Law often suggests long periods of time for hydrocarbon migration to reservoir rocks. Basin models are based on this multistep, slow process and assume deep time. These models mix inputs from science and history; only the former is subject to direct testing. Model results often fail to correspond to field conditions, suggesting a problem with the historical component of the model. Pyrolysis can occur in as little as 20 minutes at the right temperatures and pressures. It appears in nature at advanced rates with hydrothermal activity. Hydrothermal petrogenesis results in maturation simultaneous with migration in agreement with the diluvial geologic paradigm. Initial conditions during the Deluge would likely have included warmer temperatures favoring pyrolysis and faster migration of pyrolytic products. Experimental evidence also shows that light hydrocarbons can be generated directly from carbonate minerals at mantle temperatures and pressures without kerogen. Petroleum may therefore be produced from both biologic and abiologic sources in short periods of time. Over-pressured reservoirs also expose this time discrepancy. Petrified thinking—adherence to belief in deep time and uniformitarianism—appears to be the primary reason for the slowness to adopt these new findings in modeling and exploration.

The carbon problem is one of mass. Uniformitarians appeal to anoxic basins for preservation of slowly accumulating organic matter, an exercise in extended equilibrium inconsistent with the Bakken Formation. The vast amounts of carbon found in the rock record can be partly explained by optimal conditions during the Deluge for production of types I and II kerogen, but this does not apply to types III and IV. These types of kerogens can be explained by a lush antediluvial terrestrial biosphere, potentially greater land area, and the BEDS model (Oard, 2014; Oard and Reed, 2017).

Coal has traditionally been interpreted as forming in in swamps, but evidence favors allochthonous formation, probably largely from mats of vegetation swept onto depositional surfaces by marine or diluvial currents (Oard, 2014). The same arguments presented in Part II of this series for the preservation of wood via fossilization applies to the preservation of wood as fossil fuel: the former process involved silicification; the latter, pyrolysis.

Problems remain in explaining how the enormous deposits of fossil fuels may have formed in the Williston Basin; however, many of these problems result from petrified thinking—blind adherence to belief in deep time, uniformitarianism, and evolution. Plausible explanations are more readily found from the diluvial perspective.

Acknowledgements

Klevberg thanks his employer for use of the company truck in roaming western North Dakota over several seasons and coworkers and others for information on the composition of Bakken crude. *Deum laudamus* (Proverbs 8:28).

References

CRSQ: Creation Research Society Quarterly

CRSA: Creation Research Society Annual

PNAS: Proceedings of the National Academy of Sciences U.S.A.

Achten, C., and T. Hofmann. 2009. Native polycyclic aromatic hydrocarbons (PAH) in coals—a hardly recognized source of environmental contamination. *Science of the Total Environment* 407(8):2461–2473.

Archer, D. 2010. *The Global Carbon Cycle*. Princeton University Press, Princeton, NJ.

Armstrong, H. 1972. Comments on scientific news and views. *CRSQ* 9(1):71–75.

Austin, S.A. 1979. *Depositional Environment of the Kentucky No. 12 Coal Bed (Middle Pennsylvanian of Western Kentucky, with Special Reference to the Origin of Coal Lithotypes.* Ph.D. thesis, Pennsylvania State University, Old Main University Park, PA.

Coffin, H.G., with R.H. Brown and L.J. Gibson. 2005. *Origin by Design*, Revised Edition. Review and Herald Publishing Association, Washington, D.C.

Dalsted, N.L., and F.L. Leistritz. 1974. North Dakota coal resources and development potential. *Farm Research*, July–August, pp. 3–11.

Didyk, B.M., and B.R.T. Simoneit. 1989. Hydrothermal oil of Guaymas Basin and implications for petroleum formation mechanisms. *Letters to Nature* 342(6245):65–69.

Froede, C.R., Jr. 1995. Greenhouse conditions in antediluvian times? *CRSQ* 32:79.

Froede, C.R., Jr. 1998. *Field Studies in Catastrophic Geology*. Creation Research Society Monograph Series 7, Chino Valley, AZ.

Gray, N.D., A. Sherry, C. Hubert, J. Dolfing, and I.M. Head. 2010. Methanogenic degradation of petroleum hydrocarbons in subsurface environments: Remediation, heavy oil formation, and energy recovery. *Advances in Applied Microbiology* 72:137–161.

Harwood, R.J. 1977. Oil and gas generation by laboratory pyrolysis of kerogen. *AAPG Bulletin* 61(12):2082–2102.

Helman, C. 2013. Green oil: Scientists turn algae into petroleum in 30 minutes. *Forbes*, December 23, 2013, energy page (Green Oil: Scientists Turn Algae Into Petroleum In 30 Minutes (forbes.com)

Herald, F.A. 1911. The Williston Lignite Field, Williams County, North Dakota. In Campbell, M.R. *Contributions to Economic Geology, Part II—Mineral Fuels*. U.S. Geological Survey, Washington, D.C.

Jiang, C., M. Li, K.G. Osadetz, L.R. Snowdon, M. Obermajer, and M.G. Fowler. 2001. Bakken/Madison petroleum systems in the Canadian Williston Basin. Part 2: Molecular markers diagnostic of Bakken and Lodgepole source rocks. *Organic Geochemistry* 32(9):1037–1054.

Jones, N.R. 2010. *Genesis of Thick Coal deposits and Their Unique Angular Relationships: Powder River Basin, Wyoming*. Wyoming State Geological Survey Report of Investigations No. 60, 55 p., 3pls.

Lemley, B. 2006. Anything into oil. *Discover*, April 1, 2006, technology page (https://www.discovermagazine.com/technology/anything-into-oil-03)

Kenney, J.F., V.A. Kutcherov, N.A. Bendeliani, and V.A. Alekseev. 2002. The evolution of multicomponent systems at high pressures: VI. The thermodynamic stability of the hydrogen-carbon system: The genesis of hydrocarbons and the origin of petroleum. *PNAS* 99(17):10976–10981, August 12.

Klevberg, P., and M.J. Oard. 2021. Petrified Ideas of the Williston Basin—Part I: Geologic Setting. *CRSQ* 58(2):85–103.

Liang, M., Z. Wang, J. Zheng, X. Li, X. Wang, Z. Gao, H. Luo, Z. Li, and Y. Qian. 2015. Hydrous pyrolysis of different kerogen types of source rock at high temperature–bulk results and biomarkers. *Journal of Petroleum Science and Engineering* 125:209–217.

Luppens, J.A., D.C. Scott, J.A. Haacke, L.M. Osmonson, and P.E. Pierce. 2015. Coal Geology and Assessment of Coal Resources in the Powder River Basin, Wyoming and Montana. *U.S.G.S. Professional Paper 1809*, United States Geological Survey, Washington, D.C.; 10.3133/pp1809.

Matthews, J. 2008. The origin of oil—a creationist answer. *Answers Research Journal* 1: 145–168.

McQueen, D.R. 1986. The chemistry of oil—explained by Flood geology. *Acts and Facts* 15(5)—*Impact*, May 1.

Mohamed, T.I. 2015. Sequence stratigraphy and provenance of the Bakken Formation in southeast Alberta and southwest Saskatchewan. M.Sc. thesis, University of Calgary: Calgary, Alberta, Canada.

Morris, J., and S.A. Austin. 2003. *Footprints in the Ash: The Explosive Story of Mount St. Helens*. Master Books, Green Forest, AR.

Oard, M.J. (ebook). 2014. *The Genesis Flood and Floating Log Mats: Solving Geological Riddles*. Creation Book Publishers, Powder Springs, GA.

Oard, M.J., and J.K. Reed. 2017. *How Noah's Flood Shaped Our Earth*. Creation Book Publishers, Powder Springs, GA.

Oard, M.J., and P. Klevberg. 2022. Petrified ideas of the Williston Basin, Part II: Fossil wood. *CRSQ* 58(3):204–219.

Ouweneel, W.J. 1977. Panorama of science. *CRSQ* 14(2):70–72.

Peterson, J.A. 1988. Geologic summary and hydrocarbon plays, Williston Basin, Montana, North and South Dakota, and Sioux Arch, South Dakota and Nebraska, U.S. *U.S. Geological Survey Open-File Report 87–450-N*.

Saxby, J.D., A.J.R. Bennett, J.F. Corcoran, D.E. Lambert, and K.W. Riley. 1986. Petroleum generation: Simulation over six years of hydrocarbon formation from torbanite and brown coal in a subsiding basin. *Organic Geochemistry* 9(2):69–81.

Scott, H.P., R.J. Hemley, H-K. Mao, D.R. Herschbach, L.E. Fried, W.M. Howard, and S. Bastea. 2004. Generation of methane in the Earth's mantle: *In situ* high pressure-temperature measurements of carbonate reduction. *PNAS* 101(39):14023–14026.

Snelling, A.A. 1990. How fast can oil form? *Creation* 12(2):30–34.

Sonnenberg, S.A. 2017. Sequence stratigraphy of the Bakken and Three Forks, Williston Basin, U.S.A. Presentation at American Association of Petroleum Geologists, Rocky Mountain Section, annual meeting, Billings, MT.

Sun, Q., F. Xiao, X. Gao, W. Zong, Y. Li, J. Zhang, S. Sun, and S. Chen. 2019. A new discovery of Mesoproterozoic erathem oil, and oil-source correlation in the Niuyingzi area of western Liaoning Province, NE China. *Marine and Petroleum Geology* 110:606–620.

Thomas, L. 2013. *Coal Geology*, Second Edition. Wiley-Blackwell, Chichester, West Sussex, UK.

Wenger, L.M., and D.R. Baker. 1987. Variations in vitrinite reflectance with organic facies—Examples from Pennsylvanian cyclothems of the Midcontinent, U.S.A. *Organic Geochemistry* 11(5):411–416.

Wiant, H.V., Jr. 1974. A quantitative comparison of the carbon in the biomass and coal beds of the world. *CRSQ* 11:142–148.

Woodmorappe, J. 1999. *Studies in Flood Geology*. Institute for Creation Research, Dallas, TX.

Yang, X.-F., Y.-F. Xie, Z.-W. Zhang, Z.-Z. Ma, Y.-B. Zhou, Y.-M. Liu, D.-D. Wang, and Y.-B. Zhao. 2017. Hydrocarbon generation potential and depositional environment of shales in the Cretaceous Napo Formation, Eastern Oriente Basin, Ecuador. *Journal of Petroleum Geology* 40(2):173–193.

Glossary

allochthonous—formed by processes operating elsewhere, transported and deposited where now found.

autochthonous—formed in place by processes that acted where the deposit is now found.

bitumen—organic matter that is soluble as opposed to the insoluble portion, which is kerogen.

Darcy's Law—relation between hydraulic head, hydraulic conductivity, and average rate of flow of a fluid through a porous medium ($Q = -k \bullet dx/dy$).

Deluge—the unique global flood cataclysm described in Genesis (*mabbul* in Hebrew).

diluvialist—one who believes the Deluge was the salient geologic event in Earth history.

isochronous horizon—a plane or surface representing a single time in the past which may cut across sedimentary features, such as the growth of a delta with subsequent deposits at the same level as previous ones.

kerogen—organic matter in sediments that is insoluble in common organic solvents but which may release hydrocarbons upon heating. See Table II.

pyrolysis—breakdown of large organic molecules in kerogen from heating, producing mobile molecules with shorter carbon chains (petroleum) and releasing hydrogen, nitrogen, oxygen, and sulfur to leave carbon-rich insoluble material (coal).

Appendix

Bibliography on Rapid Deposition and Coalification

The following references may be consulted regarding formation of coal, petrification, and polystrate fossils:

Rapid formation of coal, allochthonous formation

Allen, B.F. 1972. The geologic age of the Mississippi River. *CRSQ* 9(2):96–114.

Allen, M.W. 2008. The Heavener roadcut: Deltaic environment or flood deposit? *CRSQ* 44:301–307.

Austin, S.A. 1986. Mount St. Helens and catastrophism. In Walsh, Robert E. (editor), *Proceedings of the First International Conference on Creationism*, I:3–9. Creation Science Fellowship, Pittsburgh, PA.

Clark, H.W. 1971. Paleoecology and the Flood. *CRSQ* 8:19–23.

Coffin, H.G. 1968. A paleoecological misinterpretation. *CRSA* 5:85–87.

Froede, C.R., Jr. 2000. Coal-bearing strata within an in-situ (?) fossilized paleo-ferntree forest: which models and settings apply? *CRSQ* 37:123–127.

Froede, C.R., Jr. 2004. Jökulhlaups and catastrophic coal formation. *CRSQ* 41:17–21.

Peters, W.G. 1970. The cyclical black shales. *CRSQ* 7(4):193–200.

Rupke, N.A. 1966. Prologomena to a study of cataclysmal sedimentation. *CRSA* 3:16–37.

Petrified wood associated with coal

Mulfinger, G. 1973. A unique creationist exhibit. *CRSQ* 10:62–68.

Williams, E.L. 1996. The log that has been through more than one fossilization "mill." *CRSQ* 33(1):5.

Polystrate trees and rapid deposition

Coffin, H.G. 1969. Research on the classic Joggins petrified trees. *CRSQ* 6:35–44,70.

Coffin, H.G. 1997. The Yellowstone petrified "forests." *Origins* 24(1):5–44.

Clarey, T. 2020. *Carved in Stone: Geological Evidence of the Worldwide Flood*. Institute for Creation Research, Dallas, TX.

Hergenrather, J., T. Vail, M. Oard, and D. Bokovoy. 2012. *Your Guide to Yellowstone and Grand Teton National Parks: A Different Perspective*. Master Books, Green Forest, AR.

Juby, I.A. 2006. Photographic essay—the fossil cliffs of Joggins, Nova Scotia. *CRSQ* 43:48–53.

Oard, M.J., and H. Giesecke. 2007. Polystrate fossils require rapid deposition. *CRSQ* 43:232–240.

Rusch, W., Sr. 1966. Analysis of so-called evidences of evolution. *CRSA* 3:4–15.

Author and Title INDEX for Volume 58, 2021–2022

David V. Bassett*

This title/author index covers articles, panorama notes, and other features. For items with two or more pages, the reference is to the first page only. After the page number, a letter indicates which type of entry is involved: article (A), panorama note (P), research note (N), letter to the editor (L), book or video review (R), conference abstract (CA), cover photo (CP), or other departments (such as editorials, editor's forum, laboratory director's comments, president's remarks, photo essays, etc.) (D).

A

B

*David V. Bassett, M.S., Cedar Hill, TX

G

H

I

J

K

L

M

N

O

P

Q

R

S

T

W

Notes from the Panorama of Science

Rock Wrens: Living Life on the Rock

Rocks are important.

Simon Peter himself was a little rock, yet his God-given faith in what God revealed about Jesus—namely, that Jesus is the divine Messiah-Savior (i.e., see Matthew 7:24)—was comparable to a huge boulder-sized rock formation (see Matthew 7:24–27), the truth foundation of Christianity (see also John 20:31). In other words, to understand the Greek wordplay that Christ used (in Matthew 16:18), it is necessary to see how Christ used the term "rock" (i.e., the feminine noun PETRA) in Matthew 7:24–27, in His parable about the wise man building his house upon the "rock" (PETRA). Simon Peter came to believe in Jesus as the Scripture-defined Messiah, and Peter's belief in that Messianic truth is the equivalent of Peter wisely building his faith (and life) upon the right "rock."

In fact, even birds appreciate the value of rocks!

Albeit birds are known for habituating trees (Daniel 4:14; Matthew 13:19) and mountains (Psalm 11:1; Psalm 50:11; Psalm 104:12; Isaiah 18:6), some birds are famous for living in rocky habitats (Job 39:27–29; Jeremiah 49:16; Obadiah 1:4).

Consider the following birds: **Rock** Ptarmigan (*Lagopus muta*), **Rock** Partridge (*Alectoris graeca*), **Rock** Bush Quail (*Perdicula argoondah*), Southern **Rock**hopper Penguin (*Eudyptes chrysocome*), Northern **Rock**hopper Penguin (*Eudyptes moseleyi*), **Rock** Shag (*Phalacrocorax magellanicus*), **Rock** Kestrel (*Falco rupicolus*), **Rock** Sandpiper (*Calidris/Erolia ptilocnemis*), **Rock** Pratincole (*Glareola nuchalis*), **Rock** Dove (*Columba livia*—a/k/a "common pigeon"), Chestnut-quilled **Rock** Pigeon (*Petrophassa rufipennis*), White-quilled **Rock** Pigeon (*Petrophassa albipennis*), New Zealand **Rock** Wren (*Xenicus gilviventris*), Andean Cock-of-the-**Rock** (*Rupicola peruvianus*—a/k/a "tunki"), Cape **Rock**jumper (*Chaetops frenatus*—a/k/a Rufous **Rock**jumper), Common **Rock** Thrush (*Monticola saxatilis,*—a/k/a rufous-tailed rock thrush), **Rock** Sparrow (*Petronia petronia*), and **Rock** Wren (*Salpinctes obsoletus*).

The **Rock Wren** is a hearty passerine that often dwells in habitats devoid of thick forests, such as some of the rock-dominated deserts of America's Great West.

It was Friday, March 3rd in A.D. 2018 (while part of an ICR field study/hiking activity), when I spied a Rock Wren inside Palo Duro Canyon, a huge canyonland featuring rocky wilderness within the Texas Panhandle. The sighting occurred during a hike along Lighthouse Trail, an area dominated by canyon rocks sprinkled by scrubby pines and mesquite trees. The **Rock Wren** was perched in the branches of a mesquite tree, a welcome sign of life in an otherwise fairly desolate and dry desert.

The hike and Rock Wren sighting were the occasion for composing this limerick:

Rock Wrens Are Tough Enough For Palo Duro Canyon
In the canyon, near Lighthouse Trail,
'Twas a bird, with an upturned tail;
In weather-worn mesquite,
It sang out a trill-tweet—
Though petite, Rock Wrens aren't frail!

In other words, Rock Wrens are tough enough to survive (and even thrive) in the hot wilderness canyonland of Palo Duro Canyon (Texas), where the wildlife must tolerate months without any precipitation—and (non-winter) temperatures well above 100 degrees Fahrenheit.

To sum it up, there are quite a few birds (including the Rock Wren) that thrive, thanks to God's providence, in rocky habitats—you might say *these resilient birds really rock!*

James J.S. Johnson

Letters to the Editor

The policy of the editorial staff of CRSQ *is to allow letters to the editor to express a variety of views. As such, the content of all letters is solely the opinion of the author, and does not necessarily reflect the opinion of the* CRSQ *editorial staff or the Creation Research Society.*

Williston Basin Comments

I want to thank Oard and Klevberg for their article on Petrified Ideas of the Williston Basin Part II in the Winter 2022 issue. In it, they point out that petrification requires rapid burial in an environment high in silica-rich solutions. As a biologist, I found that some possible explanations for why wood and other plant tissues could be so well-preserved in a very short time quickly came to mind. On page 216, the authors wrote, "Moreover, modern examples of wood petrifying are rare and show that the wood is only partially silicified, even in very special environments, such as the silica-rich hot springs of Yellowstone National Park (Hellawell et al., 2012)." Later in the article they said, "However, the silica in the volcanic ash needs to be dissolved by much heat and enter the wood in hydrothermal solutions, since the solubility of quartz does not occur until a temperature of 70°C and increases exponentially above 70°C (Bjorlykke, 2014)." These comments made me think of two possible explanations of why petrification occurred so rapidly and completely in many fossilized trees. First, the partial silicification at Yellowstone is probably due to the low pressure, whereas completely fossilized wood under heavy sediment would have been under high pressure and temperature that would greatly improve fossilization. Second, temperatures above 70°C would destroy bacteria and fungi, that would otherwise contribute to rapid decay. Wood buried deep in volcanic ash would be under high pressure, with temperatures easily at or above the normal boiling point of water. This would further promote the sterilization of any biological material, as well as speeding up silicification. This could also explain in part why some dinosaur fossils, for example, have such extremely well-preserved and unfossilized tissues, which, under normal conditions, would have decayed rapidly.

Fred Groves, Ph.D.
Springfield, Missouri

References

Bjørlykke, K. 2014. Relationships between depositional environments, burial history and rock properties. Some principal aspects of diagenetic process [sic] in sedimentary basins. *Sedimentary Geology* 301:1–14.

Hellawell, J., C. Ballhaus, C.T. Gee, G.E. Mustoe, T.J. Nagel, R. Wirth, J. Rethemeyer, F. Tomaschek, T. Geisler, K. Greef, and T. Mansfeldt. 2015. Incipient silification of recent conifer wood at a Yellowstone hot spring. *Geochimica et Cosmochimica Acta* 149:79–87.

Comments on the Review of The Republican Brain

In his review of *The Republican Brain: Why They Deny Science and Reality* by Chris Mooney, Jerry Bergman (2000) notes that Mooney accepts Paul MacLean's debunked triune brain hypothesis which asserts that we have a lizard brain under our mammal brain, which is itself under our neocortical primate/human brain. Bergman cites Toker (2018), who holds that "all vertebrates, including reptiles, birds, amphibians, and fish, have analogues of a cortex." That may be true, but MacLean's hypothesis can be falsified on other grounds, and whatever damage cortical analogues do to the hypothesis the analogues can be viewed as supportive of evolution even as discontinuities in nature (e.g., molecular and fossil) are creation friendly, since we can imagine a Creator who likes diversity and implemented variations of themes. With this in view, the following comments focus on whether the neocortex has a reptilian homologue, that is, a similar structure inherited from a common ancestor, since homologous structures arguably would have greater evidentiary value in demonstrating common ancestry as they are said to have developed in related species sharing a similar developmental pattern.

Earlier researchers at times sounded quite pessimistic as to whether the neocortex even has a reptilian homologue, and neuroscientists continue to wrestle with the question of its identity today. Butler et. al. (2011) and Aboitiz (2011) have summarized research on this issue, especially in respect to cell populations, sensory connectivity, and developmental evidence. While cell populations and connectivity data may favor the reptilian dorsal ventricular ridge (DVR) as the primary precursor of the neocortex, Aboitiz believes that it originated from an expansion of the dorsal pallium of reptiles, citing genetic, developmental and embryonic factors (the mammalian neocortex and sauropsidian DVR originate in different embryonic domains). This may involve a speculative "dorsalization process" (Aboitiz and Montill, 2007) of a substantial cell migration from the ventral to the dorsal cortex.

Butler et. al. (2011) call the developmental (epigenetic) evidence "indecisive," but the case for the DVR—which is a target of visual, sensory, somesthetic and motor projections (Butler, 1978)—by virtue of similarly connected neuron pools (the homologous cell population hypothesis) is weakened, as Webster (1979) observed, because it "cannot be directly tested (and) appears sufficiently procrustean to make possible an explanation for any and every set of observations." Even more bluntly, Lohman and Smeets (1990) wrote that "...the question 'is there a reptilian homologue of the mammalian cortex?' must be answered in the negative," consistent with a separate creation of both brains.

William Sabol

References

Aboitiz, F. 2011. Genetic and developmental homology in amniote brains. Toward reconciliating radical views on brain evolution. *Brain Research Bulletin* 84:125–126.

Aboitiz, F. and J. Montiel. 2007. *Origin and Evolution of the Vertebrate Telencephalon with Special Reference to the Mammalian Neocortex: 193, Advances in Anatomy, Embryology and Cell Biology.* Springer-Verlag, Berlin-Heidelberg, p. 54.

Bergman, J. 2020. Review of *The Republican Brain: The Science of Why They Deny Science and Reality. CRSQ* 56:55–56.

Butler, A.M. 1978. Forebrain connections in lizards and the evolution of sensory systems. In Greenberg, N. and P.D. Maclean (editors), *Behavior and Neurology of Lizards: An Interdisciplinary colloquium, DHEW Pub. No. (ADM)77–491, NIMH*, Rockville, MD., pp. 65–78.

Butler, A.M., A. Reiner and H.J. Karten. 2011. Evolution of the amniote pallium and the origins of mammalian neocortex. *Annals of the New York Academy of Sciences; New Perspectives on Neurobiological Evolution* 1225:14–27.

Lohman, A.H.M. and J.A.J.S. Smeets. 1990. The dorsal ventricular ridge and cortex of reptiles in historical and phylogenetic perspective. In Finlay, B.L., G.M. Innocenti and H. Scheich (editors), *The Neocortex: Ontogeny and Phylogeny*, pp. 59–74. Plenum Press, NY.

Toker, D. 2018. You don't have a lizard brain. http:thebrainscientist.com/2018/04/11/you-don't-have-a-lizard-brain/

Webster, K.E. 1979. Some aspects of the comparative study of the corpus striatum. In Divac, I. and R.G.E. Oberg (editors), *The Neostriatum*, pp. 107–126. Pergamon Press, Oxford.

Media Reviews

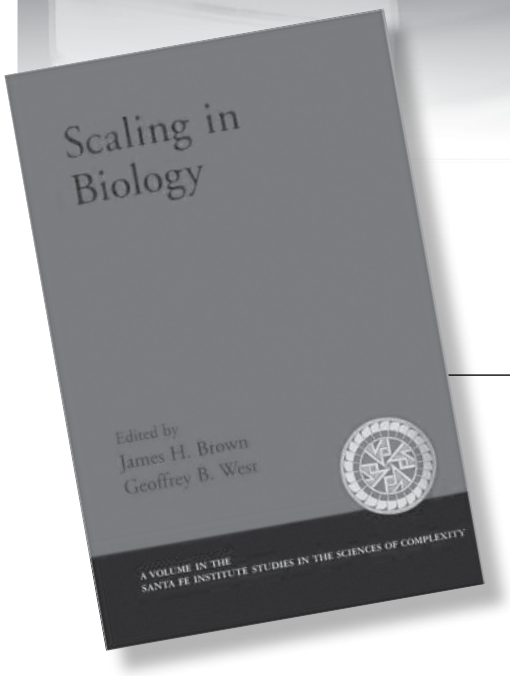

Scaling in Biology

James H. Brown and Geoffrey B. West, editors

Oxford University Press, England, 2000, 352 pages, $83.00

Scaling in Biology is a collection of 17 papers presented at a 1997 multidisciplinary symposium hosted by the Santa Fe Institute. This symposium examined the manner in which living things vary in size. More precisely, the conference focused on *allometry* (derived from "allo" meaning "other" and "metric" meaning "measure"), the manner in which biological characteristics often "scale" with an organism's overall size in different ways. For instance, ants have very thin legs, but elephants need much thicker legs in order to support their much greater body weights. These relationships can often be expressed in the form of $Y = a\ M^b$, where Y is some biological characteristic (limb length, number of heartbeats, lifespan, etc.), *a* and *b* are constants, and *M* is the organism's mass.

One of the most well-known (and perhaps controversial) of these "scaling laws" is Kleiber's Law, which states a relationship between an organism's mass and its basal metabolic rate, the amount of energy required per unit time to support minimal biological functions. According to Kleiber and other biologists, basal metabolic rate is proportional to body mass raised to the $^3/_4$ power. This result surprised biologists, who were expecting, based on a simple geometric argument, that metabolic rate should vary as mass raised to the $^2/_3$ power. This rule was originally thought to apply to only warm-blooded mammals and birds, but it was later extended to include cold-blooded vertebrates and invertebrates and one-celled organisms. If the rule is indeed valid, it is applicable to organisms whose masses vary over more than 21 orders of magnitude.

Among the gems contained in this volume is a discussion of how one might expect hummingbirds and bees to generate similar airflows in order to hover, despite their large differences in body mass. Such an expectation implies that wing beat frequency times the square of wing length, divided by the square root of body mass, should have a nearly constant value, an expectation born out by observations. Likewise, theoretical arguments were presented to explain the manner in which leg length and muscle mass vary in juvenile locusts and frogs.

Another valuable entry is a discussion of the manner in which the mammalian cardiovascular system is optimally designed. It turns out that this system has been impedance matched to minimize the loss of pulsatile energy at branches in the vascular network. For non-physicists, impedance matching is the practice of designing circuits to maximize the amount of power (energy per unit time) transmitted, with minimal losses.

The highlight of the book is a theoretical justification for the $^3/_4$ power in Kleiber's Law. This derivation is presented by physicist Geoffrey B. West and biologists Brian J. Enquist and James H. Brown (WEB). WEB made three key assumptions in their derivation. First, an organism's nutrient supply network (e.g. a plant's vascular network or a mammalian circulatory system) can be treated as a branching hierarchical network, the subsequent "levels" of which decrease in size in a regular manner. In particular, WEB assumed that the sum of the cross-

sectional areas of the branches at one level equaled the sum of the areas of the branches in the next level. Second, they assumed that the terminal branches of the network were always the same size (size invariant), regardless of the overall size of the organism. Third, and most intriguingly from a design perspective, they assumed that the supply network was designed so as to minimize the energy needed to run the network. After using the method of Lagrange multipliers and turning the theoretical crank, out popped the power of $^3/_4$!

WEB combined their model with mechanical and hydrodynamical constraints to explain why maximum tree heights are on the order of 100 meters. They also obtained allometric exponents that related a plant's number of leaves, number of branches, branch length, conductivity, and other characteristics to the plant's mass, and these theoretical values agreed well with available observations.

Alas, the paper authors never give the Creator credit for these evidences of design optimization. Rather they invariably attribute these remarkable outcomes to evolution and natural selection. Yet in spite of this, they can't help but mention design as they discuss these biological systems, despite their refusal to acknowledge a Designer.

Some biologists have been critical of WEB's work, claiming that empirical support for a $^3/_4$ scaling exponent is lacking and/or that WEB have made subtle errors in reasoning. As best as I can tell, this criticism is in no way related to this apparent support for design, as evolutionists, including WEB, attribute these remarkable results, in almost a knee-jerk reaction, to evolution and natural selection. My initial impression from reading the literature is that WEB have the better arguments and that their derivation is a breakthrough in the field of biophysics.

Scaling in Biology is more than twenty years old and it seems to have gone unnoticed by most creation researchers. Nevertheless, many of this volume's chapters greatly strengthen the case for design in living systems. In recent years, there has been increased interest in creationist and intelligent design circles in using engineering principles to understand biological systems. Though written by evolutionists, *Scaling in Biology* is a wealth of examples of design optimization in biological systems that should provide much food for thought for biologists, engineers, and creation/intelligent design theorists. It is somewhat technical, but it should be accessible to anyone who has some calculus expertise.

Jake Hebert
jhebert@icr.org

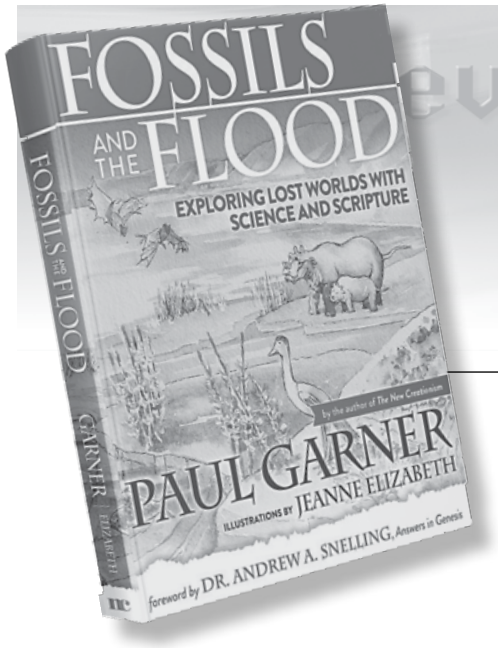

Fossils and the Flood

by Paul Garner

New Creation, Nashville, 2021, 148 pages, $45.00

Author Garner holds a graduate geoscience degree from University College, London. He has a special interest in paleobiology and previously wrote *The New Creationism* (2017). Garner currently is a lecturer and researcher for Biblical Creation Trust, a United Kingdom ministry.

This book is hard bound and 9x11 inches in size. Many endorsements are included with a Foreword written by geologist Andrew Snelling. Garner is well-versed in the fossil record and has traveled widely on research field trips.

A unique book feature is the original artwork. Jeanne Elizabeth has provided more than 200 original watercolor paintings of landscapes and fossils specimens. Most related books are filled with fossil photographs; however, the watercolor illustrations provide a fresh perspective.

Book sections include pre-Flood biomes, the Flood event itself, and the post-Flood recovery of earth systems. There is a pre-Flood suggestion of an original, vast, continent-sized floating forest. This floating island is described as a unique biome of aquatic and semi-aquatic plants along with abundant fauna (p. 138). Broken up and buried during the Flood, this vegetation mat is credited for producing many of the world's coal seams.

Author Garner promotes runaway crustal plate subduction during the Flood, also called catastrophic plate tectonics. Accompanying supersonic steam jets are assumed and illustrated (pp. 49, 54). Crustal plate motion of several meters/second is described. Detailed explanation is given for the placement of fossils due to progressive, catastrophic biome burial. Following the Flood event and animal dispersal from the Ark, Garner supposes speciation rapidly occurred. The mechanism described for this variation involves mobile genetic elements, a topic for which Garner has expertise (71).

Perhaps the most valuable part of this book is the illustrated description of plant and animal fossils, covering 30 pages. Here the many watercolor images are artistic and insightful. As a non-biologist I enjoyed every page and also learned from the glossary. For example, the familiar astronomy word *asteroid* also refers to the group of echinoderms with five distinct arms, that is, starfish (p. 135).

Fossils and the Flood is a colorful, quality publication. It includes a glossary, references, resources and an index. The book is supported by the website www.fossilsandtheflood.net. The author hopes that the book will encourage others to take up the study and understanding of earth's fossil and Flood record (p. 128). May it be so.

Don B. DeYoung
DBDeYoung@Grace.edu

Instructions to Authors

Submission

Electronic submissions of all manuscripts and graphics are preferred and should be sent to the editor of the *Creation Research Society Quarterly* in Word, WordPerfect, or Star-Office/Open Office (see the inside front cover for address). Printed copies also are accepted. If submitting a printed copy, an original plus two copies of each manuscript should be sent to the editor. The manuscript and copies will not be returned to authors unless a stamped, self-addressed envelope accompanies submission. If submitting a manuscript electronically, a printed copy is not necessary unless specifically requested by the *Quarterly* editor. Manuscripts containing more than 35 pages (double-spaced and including references, tables, and figure legends) are discouraged. An author who determines that the topic cannot be adequately covered within this number of pages is encouraged to submit separate papers that can be serialized.

All submitted manuscripts will be reviewed by two or more technical referees. However, each section editor of the *Quarterly* has final authority regarding the acceptance of a manuscript for publication. While some manuscripts may be accepted with little or no modification, typically editors will seek specific revisions of the manuscript before acceptance. Authors will then be asked to submit revisions based upon comments made by the referees. In these instances, authors are encouraged to submit a detailed letter explaining changes made in the revision, and, if necessary, give reasons for not incorporating specific changes suggested by the editor or reviewer. If an author believes the rejection of a manuscript was not justified, an appeal may be made to the *Quarterly* editor (details of appeal process at the Society's web site, www.creationresearch.org).

Authors who are unsure of proper English usage should have their manuscripts checked by someone proficient in the English language. Also, authors should endeavor to make certain the manuscript (particularly the references) conforms to the style and format of the *Quarterly*. Manuscripts may be rejected on the basis of poor English or lack of conformity to the proper format.

The *Quarterly* is a journal of original writings, and only under unusual circumstances will previously published material be reprinted. Questions regarding this should be submitted to the Editor (CRSQeditor@creationresearch.org) prior to submitting any previously published material. In addition, manuscripts submitted to the *Quarterly* should not be concurrently submitted to another journal. Violation of this will result in immediate rejection of the submitted manuscript. Also, if an author uses copyrighted photographs or other material, a release from the copyright holder should be submitted.

Appearance

Manuscripts shall be computer-printed or neatly typed. Lines should be double-spaced, including figure legends, table footnotes, and references. All pages should be sequentially numbered. Upon acceptance of the manuscript for publication, an electronic version is requested (Word, WordPerfect, or Star-Office/Open Office), with the graphics in separate electronic files. However, if submission of an electronic final version is not possible for the author, then a cleanly printed or typed copy is acceptable.

Submitted manuscripts should have the following organizational format:

1. Title page. This page should contain the title of the manuscript, the author's name, and all relevant contact information (including mailing address, telephone number, fax number, and e-mail address). If the manuscript is submitted by multiple authors, one author should serve as the corresponding author, and this should be noted on the title page.

2. Abstract page. This is page 1 of the manuscript, and should contain the article title at the top, followed by the abstract for the article. Abstracts should be between 100 and 250 words in length and present an overview of the material discussed in the article, including all major conclusions. Use of abbreviations and references in the abstract should be avoided. This page should also contain at least five key words appropriate for identifying this article via a computer search.

3. Introduction. The introduction should provide sufficient background information to allow the reader to understand the relevance and significance of the article for creation science.

4. Body of the text. Two types of headings are typically used by the *CRSQ*. A major heading consists of a large font bold print that is centered in column, and is used for each major change of focus or topic. A minor heading consists of a regular font bold print that is flush to the left margin, and is used following a major heading and helps to organize points within each major topic. Do not split words with hyphens, or use all capital letters for any words. Also, do not use bold type, except for headings (italics can be occasionally used to draw distinction to specific words). Italics should not be used for foreign words in common usage, e.g., "et al.", "ibid.", "ca." and "ad infinitum." Previously published literature should be cited using the author's last name(s) and the year of publication (ex. Smith, 2003; Smith and Jones, 2003). If the citation has more than two authors, only the first author's name should appear (ex. Smith et al., 2003). Contributing authors should examine this issue of the *CRSQ* or consult the Society's web site for specific examples as well as a more detailed explanation of manuscript preparation. Frequently-used terms can be abbrevi-

ated by placing abbreviations in parentheses following the first usage of the term in the text, for example, polyacrylamide gel electrophoresis (PAGE) or catastrophic plate tectonics (CPT). Only the abbreviation need be used afterward. If numerous abbreviations are used, authors should consider providing a list of abbreviations. Also, because of the variable usage of the terms "microevolution" and "macroevolution," authors should clearly define how they are specifically using these terms. Use of the term "creationism" should be avoided. All figures and tables should be cited in the body of the text, and be numbered in the sequential order that they appear in the text (figures and tables are numbered separately with Arabic and Roman numerals, respectively).

5. Summary. A summary paragraph(s) is often useful for readers. The summary should provide the reader an overview of the material just presented, and often helps the reader to summarize the salient points and conclusions the author has made throughout the text.

6. References. Authors should take extra measures to be certain that all references cited within the text are documented in the reference section. These references should be formatted in the current *CRSQ* style. (When the *Quarterly* appears in the references multiple times, then an abbreviation to *CRSQ* is acceptable.) The examples below cover the most common types of references:

Robinson, D.A., and D.P. Cavanaugh. 1998. A quantitative approach to baraminology with examples from the catarrhine primates. *CRSQ* 34:196–208.

Lipman, E.A., B. Schuler, O. Bakajin, and W.A. Eaton. 2003. Single-molecule measurement of protein folding kinetics. *Science* 301:1233–1235.

Margulis, L. 1971a. The origin of plant and animal cells. *American Scientific* 59:230–235.

Margulis, L. 1971b. *Origin of Eukaryotic Cells*. Yale University Press, New Haven, CT.

Hitchcock, A.S. 1971. *Manual of Grasses of the United States*. Dover Publications, New York, NY.

Walker, T.B. 1994. A biblical geologic model. In Walsh, R.E. (editor), *Proceedings of the Third International Conference on Creationism* (technical symposium sessions), pp. 581–592. Creation Science Fellowship, Pittsburgh, PA.

7. Tables. All tables cited in the text should be individually placed in numerical order following the reference section, and not embedded in the text. Each table should have a header statement that serves as a title for that table (see a current issue of the *Quarterly* for specific examples). Use tabs, rather than multiple spaces, in aligning columns within a table. Tables should be composed with *14-point type* to insure proper appearance in the columns of the *CRSQ*.

8. Figures. All figures cited in the text should be individually placed in numerical order, and placed after the tables. Do not embed figures in the text. Each figure should contain a legend that provides sufficient description to enable the reader to understand the basic concepts of the figure without needing to refer to the text. Legends should be on a separate page from the figure. All figures and drawings should be of high quality (hand-drawn illustrations and lettering should be professionally done). Images are to be a minimum resolution of 300 dpi at 100% size. Patterns, not shading, should be used to distinguish areas within graphs or other figures. Unacceptable illustrations will result in rejection of the manuscript. Authors are also strongly encouraged to submit an electronic version (.cdr, .cpt, .gif, .jpg, and .tif formats) of all figures in individual files that are separate from the electronic file containing the text and tables.

Special Sections

Letters to the Editor:

Submission of letters regarding topics relevant to the Society or creation science is encouraged. Submission of letters commenting upon articles published in the *Quarterly* will be published two issues after the article's original publication date. Authors will be given an opportunity for a concurrent response. No further letters referring to a specific *Quarterly* article will be published.

Editor's Forum:

Occasionally, the editor will invite individuals to submit differing opinions on specific topics relevant to the *Quarterly*. Each author will have opportunity to present a position paper (2000 words), and one response (1000 words) to the differing position paper. In all matters, the editor will have final and complete editorial control. Topics for these forums will be solely at the editor's discretion, but suggestions of topics are welcome.

Book Reviews:

All book reviews should be submitted to the book review editor, who will determine the acceptability of each submitted review. Book reviews should be limited to 1000 words. Following the style of reviews printed in this issue, all book reviews should contain the following information: book title, author, publisher, publication date, number of pages, and retail cost. Reviews should endeavor to present the salient points of the book that are relevant to the issues of creation/evolution. Typically, such points are accompanied by the reviewer's analysis of the book's content, clarity, and relevance to the creation issue.

Author Copies:

CRSQ policy is that authors get 10 free copies of the issue containing their article, regardless of the number of co-authors. These free copies must be pre-ordered before the issue goes to press.

Creation Research Society Membership/Subscription Application and Renewal Form

The membership/subscription categories are defined below:

1. **Voting Member** .....Those having at least an earned master's degree in a recognized area of science.
2. **Sustaining Member** .....Those without an advanced degree in science, but who are interested in and support the work of the Society.
3. **Student Member** .....Those who are enrolled full time in high schools, undergraduate colleges, or postgraduate science programs (e.g., MS, PhD, MD, and DVM). Those holding post-doctoral positions are not eligible. A graduate student with a MS degree may request voting member status while enrolled as a student member.
4. **Senior Member** .....Voting or sustaining members who are age 65 or older.
5. **Life Member** .....A special category for voting and sustaining members, entitling them to a lifetime membership in the Society.
6. **Subscriber** .....Libraries, churches, schools, etc., and individuals who do not subscribe to the Statement of Belief.

All members (categories 1–5 above) must subscribe to the Statement of Belief as defined on the next page.

Please complete the lower portion of this form and mail it with payment to CRS Membership Secretary, 1 W. Firestorm Way #145, Glendale, AZ 85306, or fax for credit card payment to (928) 636-1153. Applications may also be completed online at creationresearch.org.

✂ ----------

This is a ❑ new ❑ renewal application for the subscription year beginning Summer ❑ 2021 ❑ _____. *(Please type or print legibly.)*

Name _____ Address _____

City _____ State _____ Postal/Zip code _____ Country _____

Phone (optional) _____ Email _____

Degree _____ Field _____

Year granted _____ Institution _____

Presently associated with _____

I have read and subscribe to the CRS Statement of Belief. Signature _____

For foreign orders, including Canadian, payment must be made in U.S. dollars by a check drawn on a U.S. bank, international money order, or credit card. *Please do not send cash.*

Indicate applicable category ⬇	*Indicate payment* ⬇			
	Paper**			
❑ Voting ❑ Sustaining	USA	Canada Mexico	Other countries	**Paper-less**‡
❑ Regular [per year]	❑ $43	❑ $63	❑ $80	❑ $33
❑ Senior [per year]	❑ $38	❑ $58	❑ $75	❑ $28
❑ Life member	❑ $500	❑ $500	❑ $500	❑ $500
❑ Student* [per year]	❑ $38	❑ $58	❑ $75	❑ $28
❑ Subscriber [per year]	❑ $46	❑ $66	❑ $83	❑ $36

* Student members are required to complete the bottom portion of this form.
NOTE: Student members may qualify for the *Future Leaders Sponsorship* program. See the CRS website at www.creationresearch.org for details.
** Rates for the paper option include postage for First Class Mail International

‡ **PAPERLESS option:** You may opt out of receiving paper copies of the CRS periodicals (*CRS Quarterly* and *Creation Matters*). By choosing this option you may register for access to the Premium Area of the website, where you may view or download electronic (PDF) versions of these publications. Of course, regular members and subscribers may also have access to the Premium Area. Only members, however, will have access to the Members Exclusive Area of the website.

Member/Subscriber	$_____ per year
	x _____ years
SUBTOTAL	$_____
Optional contribution	+ $_____
Life membership	+ $_____
TOTAL	$_____

❑ Visa ❑ MasterCard ❑ Discover
❑ American Express ❑ Check/money order
Card number _____
Expiration date (mo/yr) _____
Phone number (_____) _____
Signature _____

***Student Members* are required to complete the following:**

School or institution now attending _____

_____

Your current student status: ❑ high school; ❑ undergraduate; graduate program ❑ MS ❑ PhD; ❑ other _____

Year you expect to graduate or complete your degree _____

Major, if college or graduate student _____

Signature _____

Order Blank for Past Issues

Cost of complete volumes (per volume): .....members (all categories) – $18.00 + S/H
nonmembers and subscribers (libraries, schools, churches, etc.) – $25.00 + S/H

Cost of single issues (per issue):.....members (all categories) – $5.00 + S/H
nonmembers and subscribers (libraries, schools, churches, etc.) – $7.00 + S/H

	Number			
Volume	1	2	3	4
23	☐	☐	☐	☐
24	☐	☐	☐	☐
25	☐	☐	☐	☐
26	☐	☐	☐	☐
27	☐	☐	☐	☐
28	☐	☐	☐	☐
29	☐	☐	☐	☐
30	☐	☐	☐	☐
31	☐	☐	☐	☐
32	☐	☐	☐	☐
33	☐	☐	☐	☐
34	☐	☐	☐	☐

	Number			
Volume	1	2	3	4
35	☐	☐	☐	☐
36	☐	☐	☐	☐
37	☐	☐	☐	☐
38	☐	☐	☐	☐
39	☐	☐	☐	☐
40	☐	☐	☐	☐
41	☐	☐	☐	☐
42	☐	☐	☐	☐
43	☐	☐	☐	☐
44	☐	☐	☐	☐
45	☐	☐	☐	☐
46	☐	☐	☐	☐

	Number			
Volume	1	2	3	4
47	☐	☐	☐	☐
48	☐	☐	☐	☐
49	☐	☐	☐	☐
50	☐	☐	☐	☐
51	☐	☐	☐	☐
52	☐	☐	☐	☐
53	☐	☐	☐	☐
54	☐	☐	☐	☐
55	☐	☐	☐	☐
56	☐	☐	☐	☐
57	☐	☐	☐	☐
58	☐	☐	☐	☐
59	☐			

Add 20% for postage (**for U.S. orders:** min. $6, max. $18; **for Canadian orders:** min. $10, no max.; **for other foreign orders:** min. $15, no max.) **Total enclosed:** $_____

Make check or money order payable to Creation Research Society. Please do not send cash. For foreign orders, including Canadian, please use a check in U.S. funds drawn on a U.S. bank, an international money order, or a credit card.

(Please type or print legibly)

Name _____ Address _____

City _____ State _____ Zip _____ Country _____

❑ Visa ❑ MasterCard ❑ Discover ❑ American Express Card number _____

Expiration date (mo/yr) _____ Signature _____

Mail to: Creation Research Society, 1 W. Firestorm Way #145, Glendale, AZ 85306, USA

Creation Research Society

History—The Creation Research Society was organized in 1963, with Dr. Walter E. Lammerts as first president and editor of a quarterly publication. Initially started as an informal committee of 10 scientists, it has grown rapidly, evidently filling a need for an association devoted to research and publication in the field of scientific creation, with a current membership of over 600 voting members (graduate degrees in science) and about 1000 non-voting members. The *Creation Research Society Quarterly* is a peer-reviewed technical journal. It has been gradually enlarged and modified, and is currently recognized as one of the outstanding publications in the field. In 1996 the *CRSQ* was joined by the newsletter *Creation Matters* as a source of information of interest to creationists.

Activities—The Society is a research and publication society, and also engages in various meetings and promotional activities. There is no affiliation with any other scientific or religious organizations. Its members conduct research on problems related to its purposes, and a research fund and research center are maintained to assist in such projects. Contributions to the research fund for these purposes are tax deductible. As part of its vigorous research and field study programs, the Society operates the Van Andel Creation Research Center in Glendale, Arizona.

Membership—Voting membership is limited to scientists who have at least an earned graduate degree in a natural or applied science and subscribe to the Statement of Belief. Sustaining membership is available for those who do not meet the academic criterion for voting membership, but do subscribe to the Statement of Belief.

Statement of Belief—Members of the Creation Research Society, which include research scientists representing various fields of scientific inquiry, are committed to full belief in the biblical record of creation and early history, and thus to a concept of dynamic special creation (as opposed to evolution) both of the universe and the earth with its complexity of living forms. We propose to re-evaluate science from this viewpoint, and since 1964 have published a quarterly of research articles in this field. *All members of the Society subscribe to the following statement of belief:*

1. The Bible is the written Word of God, and because it is inspired throughout, all its assertions are historically and scientifically true in all the original autographs. To the student of nature this means that the account of origins in Genesis is a factual presentation of simple historical truths.
2. All basic types of living things, including humans, were made by direct creative acts of God during the Creation Week described in Genesis. Whatever biological changes have occurred since Creation Week have accomplished only changes within the original created kinds.
3. The Great Flood described in Genesis, commonly referred to as the Noachian Flood, was a historical event worldwide in its extent and effect.
4. We are an organization of Christian men and women of science who accept Jesus Christ as our Lord and Savior. The act of the special creation of Adam and Eve as one man and woman and their subsequent fall into sin is the basis for our belief in the necessity of a Savior for all people. Therefore, salvation can come only through accepting Jesus Christ as our Savior.

iDINO II

Investigation of Dinosaur Intact Natural Osteo-tissue

A fragment of the *Triceratops* brow horn. Fragments, such as this one, still contain tissue and cells.

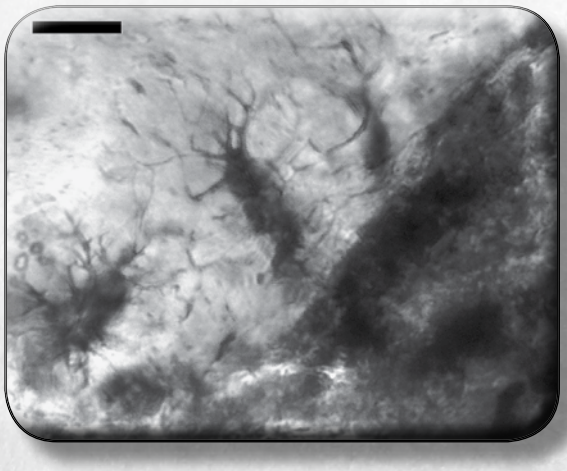

Microscopic examination of tissue extracted from a *Triceratops* horn reveals bone cells still present.

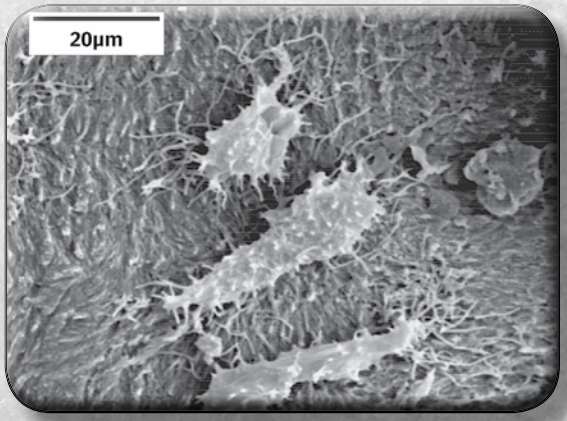

Electron microscope picture of intact bone cells still in tissue extracted from a *Triceratops* horn.

How can pliable, stretchable tissue survive inside dinosaur fossils for over 65 million years?

How can this tissue still contain intact cells and even dinosaur proteins?

How can this fragile biological material survive for so long?

The answer to these questions directly challenges the current, evolutionary-biased, geologic timescale.

The Creation Research Society began its iDINO research initiative for the purpose of studying soft tissue in dinosaur fossils. The first phase of the project detected pliable, unfossilized tissue in a brow horn of a *Triceratops*. Within this tissue were intact osteocytes (bone cells). Some results from the iDINO project have been published in a technical microscopy journal and presented at an international microscopy conference. The Spring 2015 issue of the *Creation Research Society Quarterly* also features a special report of the iDINO project. Plus, to further spread the important information about soft tissue, the Society is developing a video (Echoes of the Jurassic).

The **second phase** of the project (iDINO II) will look more extensively at the process of tissue preservation. Evolutionists have offered various theories of how this tissue could survive for millions of years. iDINO II will methodically investigate these preservation claims, assessing their plausibility.

The iDINO results have already provided a strong challenge to the evolutionary worldview. More extensive and detailed examination may provide even stronger evidence that the age of dinosaur fossils is far less than 65 million years. To this end, the Society continues to seek those willing to fund this project with either one-time gifts or monthly donations.

For more information contact us at (928) 636-1153 or crsvarc@crsvarc.com.

Also visit http://tinyurl.com/nphm2c4 for project updates and details.

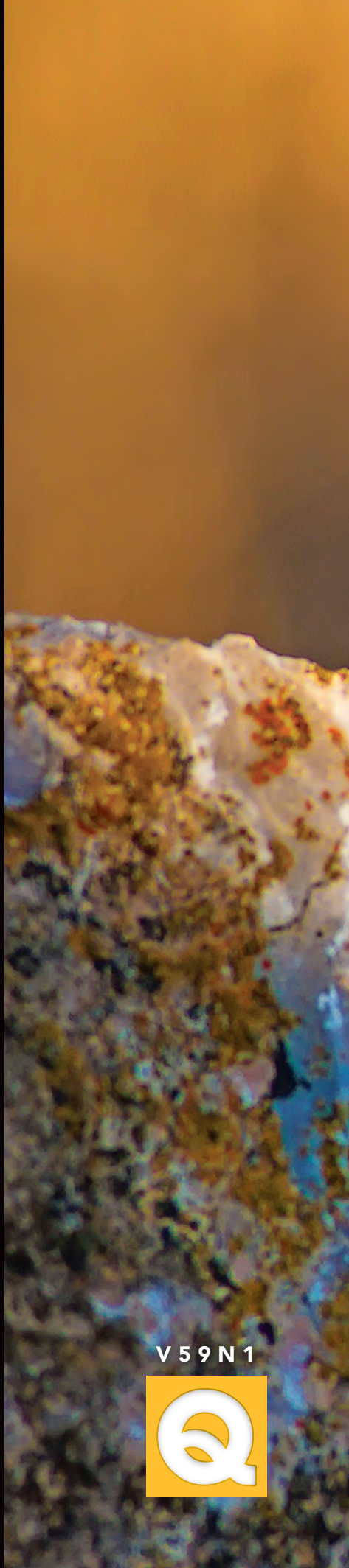

V59N1